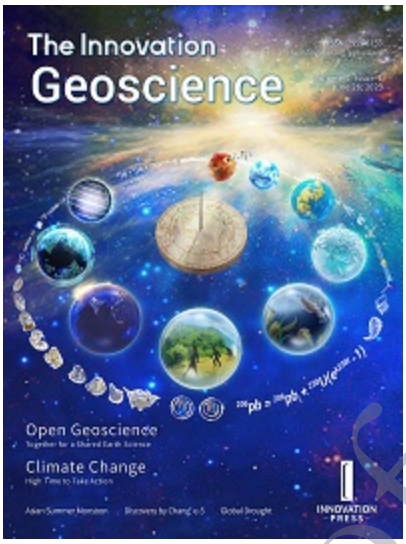

Seagrass restoration at the right time in the right site with right methods can generate persistent carbon benefits in China

Journal:	*The Innovation Geoscience*
Manuscript ID	XINNgeoscience-2025-0200.R2
Manuscript Type:	Article
Keywords:	carbon stock survey, driving factor, spatial distribution patterns, strategic restoration

Seagrass restoration at the right time in the right site with right methods can generate persistent carbon benefits in China

Hongzhen Wang,[1] Xinqi Li,[1] Yu Zang,[2] Jiayi Xin,[1] Song Xue,[2] Lei Liu,[1] Xuexi Tang,[1,*] Jun Chen[1,*]

[*]Correspondence: tangxx@ouc.edu.cn(X.T.); chenjun@ouc.edu.cn (J.C.)

GRAPHICAL ABSTRACT

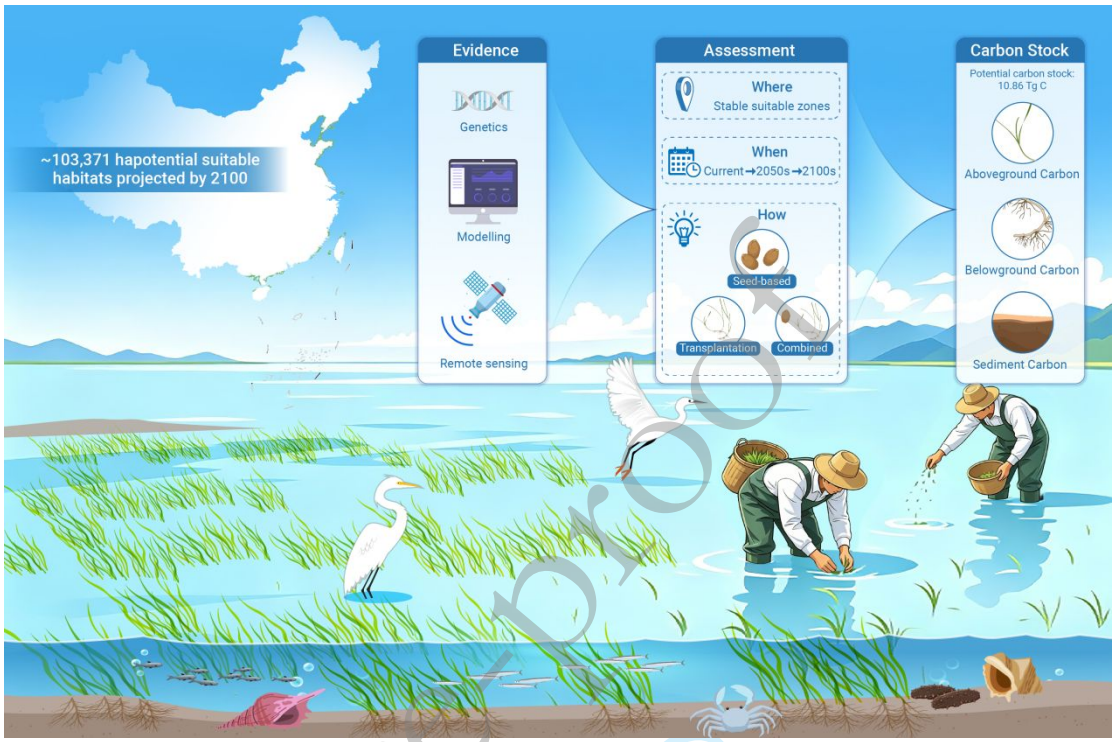

PUBLIC SUMMARY

- *Zostera japonica* beds have declined, and suitable habitats may contract under future climate change.
- Remote sensing and habitat modelling identify vulnerable areas and guide restoration planning.
- Site-specific strategies based on habitat, decline, and genetics improve restoration decisions.
- Linking restoration priorities with blue carbon assessment supports coastal conservation and management.

Key Words

strategic restoration/carbon stock survey/driving factors/spatial distribution patterns

Seagrass restoration at the right time in the right site with right methods can generate persistent carbon benefits in China

Hongzhen Wang,[1] Xinqi Li,[1] Yu Zang,[2] Jiayi Xin,[1] Song Xue,[2] Lei Liu,[1] Xuexi Tang,[1,*] Jun Chen[1,*]

1.MoE Key Laboratory of Evolution & Marine Biodiversity, College of Marine Life Sciences, Ocean University of China, Qingdao 266003, China.

2.Key Laboratory of Marine Eco-Environmental Science and Technology, First Institute of Oceanography, Ministry of Natural Resources, Qingdao 266061, China.

[*]Correspondence: tangxx@ouc.edu.cn(X.T.); chenjun@ouc.edu.cn (J.C.)

ABSTRACT

Zostera japonica beds have declined substantially along the coast of China, highlighting the need for targeted and effective restoration planning. This study develops a restoration roadmap that supports China's carbon neutrality goals by addressing three key questions: where restoration should occur, when it should be implemented, and which methods should be used. Field surveys, satellite remote sensing, genetic data, and species distribution modelling were integrated to identify restoration opportunities under current and future climate conditions. The results indicate that northern China, particularly the Bohai Sea region, contains the largest extent of suitable and persistent habitat, whereas several southern populations have experienced substantial bed degradation. A rule-based restoration decision framework combined seagrass bed decline and genetic diversity to recommend region-specific restoration strategies across the species range. The phased framework prioritizes areas suitable under current and 2050s conditions, particularly those projected to remain suitable by the 2100s, while treating areas becoming suitable mainly by the 2100s as long-term adaptive reserves. By the 2100s, approximately 103,371 ha of potential suitable habitat is projected, corresponding to an estimated potential carbon stock of 10.86 Tg C. These findings provide a spatially explicit framework for improving *Z. japonica* restoration planning and evaluating its potential long-term carbon benefits in China.

INTRODUCTION

Climate change poses substantial socioeconomic challenges for China, which has committed to advancing global climate change mitigation.[1] The principal driver of contemporary climate change is the accumulation of greenhouse gases (GHGs), largely resulting from the combustion of fossil fuels such as coal and oil.[2] Understanding the sources, sinks, and fate of GHGs is therefore essential for developing effective climate policies and mitigation measures. Quantifying global GHG budgets, particularly the carbon budget, has consequently become central to climate mitigation and sustainable ecosystem management.[3,4] Identifying and quantifying under-recognized carbon sinks has therefore emerged as a major challenge in global change research.

In China's national climate mitigation strategy, expanding forest area and enhancing terrestrial carbon sinks have been identified as important measures.[5-8] However, compared with many terrestrial ecosystems, some coastal blue carbon ecosystems can exhibit high carbon burial rates per unit area and retain carbon in sediments over long timescales.[9,10] Although ocean carbon research has traditionally emphasized pelagic carbon cycling, including plankton-mediated carbon uptake,[11] increasing attention has shifted toward vegetated coastal ecosystems, in which benthic macrophytes such as seagrass play a disproportionately important role.[12,13] Vegetated coastal ecosystems, including seagrass beds, occupy less than 0.2% of the global ocean surface but contribute substantially to organic carbon burial in marine sediments.[14,15] Globally, seagrass beds are estimated to sequester 48-112 $Tg \cdot C \cdot yr^{-1}$ and store several to tens of petagrams of carbon in their biomass and sediments.[14-16] In China, seagrass beds cover approximately 14,000-20,000 ha and contain an estimated 8.1-12.0 Tg·C, with an annual sequestration capacity of 0.12-0.18 $Tg \cdot C \cdot yr^{-1}$.[17-19] Together, these estimates highlight the under-recognized contribution of China's seagrass beds to coastal blue carbon storage and their potential relevance to carbon neutrality strategies.

However, seagrass ecosystems are declining rapidly because of climate change and human activities. Since 1880, at least 5,602 km^2 of documented seagrass meadow area has been lost globally.[20] Many assessments have focused primarily on documenting changes in bed area, whereas the environmental drivers of decline and the spatial priorities for restoration remain insufficiently resolved.[15,20] As seagrass ecosystems receive increasing attention within the global conservation agenda, it is essential to determine where and why these beds are declining and how their degradation can be reversed.

Substantial progress has been made in seagrass conservation and restoration in recent years.[21,22]

Nevertheless, restoration remains constrained by fragmented management, site-specific habitat degradation, limited species-specific guidance, and insufficient integration of ecological suitability with potential carbon benefits. The United Nations designated 1 March as World Seagrass Day to raise awareness of the ecological importance of seagrass ecosystems. China has also implemented numerous initiatives involving seagrass protection, restoration, and seed-based bed expansion.[17,18,23,24] Despite these efforts, several fundamental questions remain unresolved, including where seagrass restoration should be prioritized, which restoration methods are most appropriate, and when restoration should be implemented.

As a native intertidal species of the northwest Pacific coast, *Z. japonica* forms meadows that are the most widely distributed of all seagrass ecosystems in China.[25,26] However, this species has experienced substantial population declines under the combined pressures of chronic human disturbance and intensifying climatic extremes.[26-28] These pressures have caused widespread degradation of *Z. japonica* beds and raised concern about the long-term persistence of the species in its native habitats.[25,29,30] Consequently, changes in its distribution and condition can strongly influence the overall status and carbon storage capacity of China's seagrass resources. Previous studies have shown that *Z. japonica* beds contribute substantially to regional blue carbon stocks and help maintain carbon storage in shallow coastal ecosystems.[15,18] Given its ecological importance and extensive distribution, improving the conservation and restoration of *Z. japonica* is important for strengthening coastal ecosystem resilience and supporting China's marine carbon management goals.[17,18,31]

Here, we developed an illustrative restoration roadmap for *Z. japonica* in China by addressing three key questions: where to restore, how to restore, and when to restore. To determine where restoration should be prioritized, we used satellite remote sensing to quantify recent spatial changes in *Z. japonica* beds and combined species distribution modelling with habitat assessments under sea-level-rise scenarios to identify current and future potentially suitable areas. To determine how restoration should be implemented, we integrated bed decline, genetic diversity, and restoration practice into a rule-based decision framework for selecting among seed-based restoration, shoot transplantation, combined restoration, and protection or natural recovery. To determine when restoration should be prioritized, we compared current suitable areas with projected suitable areas under climate scenarios for the 2050s and 2100s and developed a phased restoration strategy. Finally, we combined projected suitable areas with field-based carbon stock estimates to evaluate the potential carbon stock associated with future

restoration opportunities. This framework provides a spatially explicit and method-oriented basis for *Z. japonica* restoration planning and coastal blue carbon management in China.

MATERIALS AND METHODS

Study area

The study area was defined by integrating multisource occurrence records of *Z. japonica* to provide a basis for spatial analysis. Occurrence records from peer-reviewed field studies were prioritized, and additional distribution points were obtained from GBIF (https://www.gbif.org) and OBIS (https://obis.org). All records were processed following standardized procedures for species distribution data that are widely applied in seagrass and coastal vegetation studies.[32] The procedure included removing duplicate coordinates, excluding records with spatial uncertainty greater than 1 km, evaluating the ecological plausibility of each record using published habitat descriptions, and verifying its geographic location using high-resolution satellite imagery. After applying these criteria, 37 reliable occurrence points were retained, 17 of which were located in Chinese coastal waters (Table S1). This workflow is consistent with established approaches in seagrass mapping and blue carbon research.[13]

To delineate the spatial extent of the regional analyses, we combined historical occurrence records, ecological literature describing the habitat requirements of *Z. japonica*, and multiyear satellite imagery spanning 2014 to 2022. Field surveys conducted in 2023 covered the major seagrass regions of the Bohai Sea, Yellow Sea, and northern South China Sea, representing the principal latitudinal distribution of *Z. japonica* within China. The species primarily occupies shallow littoral waters, generally less than 6 m deep and typically within 10 km of the coastline. To ensure that peripheral and potentially suitable coastal habitats were not excluded, a 20 km buffer was established along the Chinese coastline. This approach is consistent with commonly used practices in coastal habitat modelling and marine vegetation mapping. In addition to defining the operational extent of the regional analyses, we generated a global habitat suitability map using all 37 occurrence records to examine the broader spatial pattern of environmentally suitable areas under current conditions (Figure 1). We further analysed the centroid and directional shifts of suitable habitat within the northwestern Pacific region under current and future climate conditions (Figure 2). By contrast, all quantitative analyses conducted for Chinese coastal waters, including remote sensing extraction, habitat suitability assessment, and environmental factor analysis, were restricted to the defined 20 km coastal buffer. This distinction clarifies the relationship between the broad-scale suitability maps and the regional

analytical extent and avoids misinterpretation of model boundaries.[33]

All spatial analyses were performed in ArcGIS 10.4. These analyses included constructing the coastal buffer, extracting environmental variables, and generating spatial predictor layers for species distribution modelling. Climate-based projections were developed using environmental layers corresponding to the selected future climate scenarios. The integration of species occurrence records with environmental and climate variables followed the core methodological principles of species distribution modelling described in foundational studies.[34,35] To minimize multicollinearity among predictor variables, we adopted recommended procedures for ecological modelling.[36]

Construct *Z. japonica* index (*ZJI*)

The *Z. japonica* index (*ZJI*) was constructed by integrating field observations, historical records, and multitemporal remote sensing data in ArcGIS and Google Earth Engine. The methodological framework was adapted from the time-series spectral and phenological index developed for long-term monitoring of *Z. japonica* in the Yellow River Delta.[18]

First, identification of the potential distribution area. Time-series Landsat imagery, including Landsat 5 Thematic Mapper, Landsat 7 Enhanced Thematic Mapper Plus, and Landsat 8 Operational Land Imager surface reflectance products, was used to delineate the potential distribution area. The surface reflectance products were generated through atmospheric correction using the Landsat Ecosystem Disturbance Adaptive Processing System for Landsat 5 and 7 and the Landsat Surface Reflectance Code for Landsat 8. Poor-quality pixels affected by clouds, cirrus, cloud shadows, or snow were removed using the corresponding quality-assurance bands. This preprocessing workflow was consistent with established remote sensing methods for coastal wetland mapping.[18,37]

Second, calculation of spectral and phenological indices. For each valid pixel, three spectral indices were calculated following established definitions. The normalized difference vegetation index was calculated as:

$$NDVI = \frac{NIR-R}{NIR+R}$$

where NIR and R represent near-infrared and red reflectance, respectively.[38]

The modified normalized difference water index was computed as:

$$mNDWI = \frac{G - SWIR1}{G + SWIR1}$$

where G is green band reflectance and SWIR1 is shortwave infrared reflectance.[39]

The tasseled cap brightness index was calculated using sensor-specific Landsat transformation coefficients:[40]

$$TCBI = a_1 B + a_2 G + a_3 R + a_4 NIR + a_5 SWIR1 + a_6 SWIR2$$

where B, G, R, NIR, $SWIR1$, and $SWIR2$ represent blue, green, red, near-infrared, shortwave-infrared 1, and shortwave-infrared 2 reflectance, respectively,and a_1–a_6 are the corresponding sensor-specific coefficients.

The phenological characteristics of *Z. japonica* were represented using the maximum NDVI during the growing period and the mean NDVI during the senescence period. Based on long-term observations of *Z. japonica*, the growing period was defined as day of year 150–250 and the senescence period as day of year 260–330. For each analysis period, the maximum NDVI composite was generated, and the corresponding mNDWI and TCBI values were extracted from the date on which NDVI reached its maximum. Mean NDVI during the senescence period was also calculated for each pixel.

Third, construction of *ZJI*. The *Z. japonica* index was formulated by integrating spectral and phenological features that distinguish *Z. japonica* from other intertidal vegetation types such as *Spartina alterniflora*, *Suaeda salsa* and tidal flats. The index was defined as:

$$ZJI = \begin{cases} NoData & (mNDWI_{VImax} \le 0) \\ \frac{2NDVI_{max} - SeNDVI_{mean}}{TCBI_{VImax}} & (mNDWI_{VImax} > 0) \end{cases}$$

where $NDVI_{max}$ is the maximum NDVI during the growing period, $SeNDVI_{mean}$ is the mean NDVI during the senescence period, and $mNDWI_{VImax}$ and $TCBI_{VImax}$ are the mNDWI and TCBI values corresponding to the date of maximum NDVI. Pixels with $mNDWI_{VImax} \le 0$ were assigned NoData because this condition was used to exclude higher intertidal vegetation, particularly *S. alterniflora*, and other non-target cover types. These pixels were masked in subsequent classification.

Fourth, separability analysis. To evaluate the discriminatory ability of the individual spectral variables and *ZJI*, a separability index was calculated. The index incorporates both interclass differences and intraclass variability and was calculated as:[41]

$$SI_{zo} = \frac{|\mu_z - \mu_o|}{1.96 \times (\sigma_z + \sigma_o)}$$

where μ_z and μ_o denote the mean index values of *Z. japonica* and the other class and σ_z and σ_o denote the corresponding standard deviations.

Fifth, automated extraction using multilevel Otsu segmentation. For each analysis period, the *ZJI* image within the potential distribution area was classified using a multilevel Otsu thresholding algorithm implemented in Google Earth Engine. The algorithm divided the *ZJI* histogram into three classes by identifying two thresholds that maximized the between-class variance. The class with *ZJI* values greater than the upper threshold was classified as *Z. japonica*, whereas the remaining classes were classified as non-*Z. japonica*. Thresholds were determined independently for each analysis period to account for temporal and regional variation in spectral conditions.

Finally, accuracy assessment and validation. Stratified random validation samples were interpreted using field observations and contemporaneous or near-contemporaneous high-resolution Gaofen, WorldView, and SPOT imagery. Classification performance was evaluated using confusion matrices, from which producer's accuracy, user's accuracy, overall accuracy, and the kappa coefficient were calculated. As an additional external comparison, *ZJI*-derived maps were overlaid with publicly available seagrass distribution records from the CEARAC Web-GIS platform. Because CEARAC coverage is incomplete for the Chinese coast and is not consistently species specific, these records were used only to examine spatial correspondence in areas with confirmed seagrass occurrence and were not treated as a comprehensive species-level accuracy dataset.

Species distribution models

To predict the current and future habitat suitability of *Z. japonica*, we constructed species distribution models using MaxEnt. Model calibration and optimization were performed with the ENMeval package,[42] following established procedures for presence-only ecological niche modelling.[34,35] Two key parameters were tuned: the regularization multiplier and feature class. The regularization multiplier ranged from 0.5 to 5.0 at intervals of 0.5, resulting in ten candidate values. MaxEnt supports five feature types, including linear, quadratic, hinge, product, and threshold features. Eight feature-class combinations were evaluated: L, LQ, H, LQH, LQHP, LQHPT, HPT, and QPT. These settings generated 80 candidate parameter combinations, which were evaluated using the small-sample corrected Akaike information criterion implemented in

ENMeval. Additional metrics, including the omission rate at the 10% training-presence threshold and the difference between training and test AUC, were used to assess model complexity and potential overfitting.

After model selection, the optimal configuration consisted of a regularization multiplier of 3.5 and the LQHPT feature class. The maximum number of background points and model iterations were both set to 10,000. Model performance was evaluated using the area under the receiver operating characteristic curve, which is widely used for presence-only species distribution models.[34] AUC values range from 0 to 1, with values below 0.7 indicating low discriminatory ability, values between 0.7 and 0.9 indicating moderate discriminatory ability, and values above 0.9 indicating high discriminatory ability.

The final MaxEnt simulations produced continuous maps of relative habitat suitability for *Z. japonica*. The outputs were imported into ArcGIS for post-processing, and the mean suitability values from ten replicate runs were converted to raster format. Suitability values were classified into four categories: unsuitable, < 0.20; low suitability, 0.20 to < 0.50; moderate suitability, 0.50 to < 0.75; and high suitability, ≥ 0.75.

The Java-based MaxEnt software was used for all habitat suitability modelling, and 10,000 background points were sampled to represent the available environmental space. Predicted habitat suitability maps were converted into binary suitable and unsuitable grids using SDMtoolbox implemented in ArcGIS and the selected threshold-based conversion procedure.[43] Habitat dynamics under future scenarios were quantified by comparing current and future binary maps to identify areas of expansion, stability, contraction, and persistent unsuitability. Spatial pattern analysis was conducted using the centroid-shift tool in SDMtoolbox to estimate the geographic centers of suitable habitat and assess the direction and relative magnitude of projected shifts under future climate conditions. For the centroid analysis, only suitable raster cells within the northwestern Pacific region were included.

Sea level rise assessment of *Z. japonica*

Sea level rise data for regions containing *Z. japonica* populations were obtained from the Copernicus Marine Service. To evaluate the relationship between sea level change and long-term variation in seagrass bed area, we applied a generalized additive model, which is widely used to characterize nonlinear ecological responses to environmental gradients.[44,45]

A GAM was implemented to capture nonlinear relationships between sea level change and seagrass area dynamics:

$$Area_i = \beta_0 + f(SLR_i) + \varepsilon_i$$

where $Area_i$ represents the annual change in seagrass area at site i and SLR_i denotes the corresponding sea level anomaly. The smoothing function f was fitted using the mgcv package in R, which provides robust and flexible spline based estimation for ecological GAMs.[46]

The basis dimension k was set to three to avoid overfitting while capturing potential nonlinear patterns in the relationship between sea level rise and seagrass area change[44]. Model diagnostics included residual inspection, concurvity checks and evaluation of effective degrees of freedom following established GAM best practices.[45]

This modelling framework enabled the detection of nonlinear responses and potential thresholds in the sensitivity of *Z. japonica* to progressive sea level rise, complementing remote sensing derived seagrass dynamics documented in previous coastal vegetation studies.[47]

Projected habitat change based on MaxEnt and sea level rise

To evaluate future habitat changes of *Z. japonica* under sea level rise, we considered four representative climate scenarios for 2050 and 2100. Projected sea level increases were set to 0.3 and 0.6 m under RCP2.6, 0.4 and 0.8 m under RCP4.5, 0.5 and 1.0 m under RCP6.0, and 0.7 and 1.5 m under RCP8.5, respectively, with the 1.5 m projection representing an upper-range scenario consistent with recent assessments of accelerated sea level rise.[48,49] For each scenario, we estimated the extent of coastal areas subject to inundation and identified portions of the current intertidal zone that would shift to depths considered unsuitable for *Z. japonica*.

To delineate future water-depth conditions, elevation and bathymetric data were obtained from the General Bathymetric Chart of the Oceans GEBCO_2023 global grid (https://www.gebco.net), which has been widely used in regional and global assessments of coastal inundation and habitat exposure.[50,51] The GEBCO grid was resampled to a 1 m computational grid for spatial overlay and scenario analysis. Projected sea level increments were then added to the baseline elevation and bathymetric surface to generate scenario-specific layers representing future relative water-depth distributions along the Chinese coast. The effective spatial information of these layers remained constrained by the native resolution of

the GEBCO dataset.

The depth threshold for unsuitable seagrass habitat was determined by combining the generalized additive model results with published information on seagrass depth limits. A relative water depth of 1.5 m was selected as the critical threshold because *Z. japonica* bed area declined markedly near this level in the time-series analysis and because comparable shallow depth constraints have been reported for seagrasses in light-limited coastal environments.[52-54] Under each sea level rise scenario, grid cells with projected relative water depths shallower than 1.5 m were classified as potentially suitable in terms of depth, whereas cells exceeding this threshold were classified as unsuitable.

Binary habitat suitability maps derived from MaxEnt were then intersected with the depth-based suitability masks to quantify projected habitat dynamics under each scenario. Areas that remained suitable were classified as stable habitat, areas that shifted from unsuitable to suitable were classified as expansion zones, areas that shifted from suitable to unsuitable were classified as contraction zones, and areas that remained unsuitable were classified as persistently unsuitable. This combined approach linked climate-based habitat suitability projections with sea level rise exposure and was used to identify coastal regions where *Z. japonica* habitat may be vulnerable to future inundation.

Investigation and Assessment of Carbon Stock

The distribution of *Z. japonica* along the Chinese coast was divided into 11 principal regions. A total of 33 stations were established for sediment sampling, and 110 field plots were surveyed for seagrass biomass and environmental variables (Table S2 & Figure 3). Field surveys and sediment sampling were conducted in August 2023. A 10 m × 10 m survey area was established at each field plot, within which vegetation and environmental variables were assessed. During biomass sampling, all seagrass plants within the designated sampling quadrat were collected, rinsed carefully to remove sediment from the roots, and placed in labelled sample bags. Seagrass plants were separated into aboveground tissues, including leaves and leaf sheaths, and belowground tissues, including rhizomes and roots. Epiphytes were scraped from the leaf surfaces. Aboveground and belowground biomass samples were placed in separate labelled bags, and epiphytes were transferred to preweighed centrifuge tubes.

A handheld sediment corer (SD-1, Australia) was used to collect one sediment core to a

maximum depth of 1 m at each sediment-sampling station. Each core was sectioned and bagged in the field. Sediment from 0 to 50 cm was divided into five 10 cm intervals, whereas sediment from 50 to 100 cm was treated as a single interval, resulting in six depth intervals per core. When the full depth of 1 m could not be reached, the actual sampling depth was recorded. All plant and sediment samples were stored at −20°C and transported to the laboratory for analysis. Seagrass biomass samples were freeze-dried to constant mass, and their dry masses were recorded. The dried samples were ground, passed through a 100-mesh sieve, sealed in sample bags, and stored in a desiccator until analysis. Sediment samples were oven-dried at 60°C to constant mass. The dried sediments were homogenized using a ceramic mortar, passed through a 100-mesh sieve, sealed in sample bags, and stored in a desiccator until analysis. Organic carbon concentrations in seagrass tissues and epiphytes were measured using the nondispersive infrared absorption method, whereas sediment organic carbon concentrations were determined using the potassium dichromate oxidation method.

The total carbon stock of each seagrass bed consisted of plant carbon stock, including aboveground, belowground, and epiphytic carbon, and sediment carbon stock. Plant carbon stock was calculated as follows:

$$V_{\mathrm{Cstock}} = V_{\mathrm{Ca}} + V_{\mathrm{Cb}} + V_{\mathrm{Ce}}$$

where V_{Cstock} is the plant carbon stock, V_{Ca} is the biomass carbon stock in the above-ground fraction, V_{Cb} is the biomass carbon stock in the below-ground fraction, and V_{Ce} is the carbon stock in epiphytic organisms, all in megagrams of carbon (Mg C).

$$VC_a = \sum_{i=1}^{n} \omega_{\mathrm{C_{org},}i} \times M_{\mathrm{sp},i} \times \frac{S_i}{S_{\mathrm{sp},i}} \times 10^{-2}$$

$$VC_b = \sum_{i=1}^{n} \omega_{\mathrm{C_{orgb},}i} \times M_{\mathrm{spb},i} \times \frac{S_i}{S_{\mathrm{sp},i}} \times 10^{-2}$$

$$VC_e = \sum_{i=1}^{n} \omega_{\mathrm{C_{orge},}i} \times M_{\mathrm{spe},i} \times \frac{S_i}{S_{\mathrm{sp},i}} \times 10^{-2}$$

where $\omega_{Corg,i}$, $\omega_{Corgb,i}$ and $\omega_{Corge,i}$ are the mass fractions of plant above-ground fraction, plant below-ground fraction and epiphytic organisms' organic carbon in % for the ith seagrass partition sample, respectively. $M_{sp,i}$, $M_{spb,i}$ and $M_{spe,i}$ are the dry mass of above-ground plant parts, below-ground plant parts and epiphytic organisms in the ith seagrass compartment

sample, in g, respectively. $S_{sp,i}$: area of plant sample in the ith seagrass partition, in m^2; S_i: area of the ith seagrass partition, in ha.

$$S_{\mathrm{Cstock}} = \sum_{i=1}^{n} C_{\mathrm{col},i} \times S_i \times 100$$

$$C_{\mathrm{col},i} = \sum_{j=1}^{i} \omega_{C_{\mathrm{som},j}} \times \rho_j \times H_j$$

where S_{Cstock} is the sediment carbon stock in Mg C and $C_{col,i}$ is the organic carbon content of column samples at 100 cm or the actual depth of investigation in g/cm^2. S_i is the area of the ith seagrass partition in ha; $C_{\omega som,j}$ is the mass fraction of organic carbon in the jth layer of sediment in %. H_j is the thickness of the sediment in layer j in cm, the thickness of layers 1 to 5 are all 10 cm, and the thickness of layer 6 is the actual thickness of samples of 50 cm or more.

$$C_{\mathrm{stock}} = V_{\mathrm{Cstock}} + S_{\mathrm{Cstock}}$$

where C_{stock} is the total carbon stock in the seagrass bed ecosystem, V_{Cstock} is the plant carbon stock, and S_{Cstock} is the sediment carbon stock, all in Mg C.

Environment variables

To evaluate the relationships between environmental factors and the dynamics of *Z. japonica*, we examined variation in bed area, carbon stock, and habitat distribution across the study regions (Table S2). To analyse the influence of environmental variables on bed area, the maximum monthly bed area recorded at each site was used. A response ratio approach was applied to quantify the associations between environmental factors and bed area, following established methods used in ecological impact assessments.[55] Ten water quality variables were measured, including pH, water temperature, salinity, dissolved oxygen, total nitrogen, total phosphorus, total carbon, total organic carbon, dissolved inorganic carbon, and dissolved organic carbon. Additionally, mean annual temperature was obtained as a climatic variable.

To assess the relationships between environmental conditions and spatial habitat suitability, surface environmental layers were obtained from Bio-ORACLE, a widely used marine environmental database for species distribution modelling.[56,57] Environmental data representing the period from 2000 to 2014 were used to characterize current conditions. Future environmental layers were obtained for the 2050s and 2100s under the RCP2.6, RCP4.5, RCP6.0, and RCP8.5 scenarios. All layers were downloaded at a spatial resolution of 5 arc min,

converted to ASCII format, and processed in ArcGIS 10.4 for input into MaxEnt version 3.4.1. Percentage contribution and permutation importance were used to evaluate the relative importance of environmental variables in the MaxEnt model.

To minimize multicollinearity, pairwise Pearson correlation coefficients were calculated among the candidate environmental variables using ENMTools version 1.3. Variables with $|r| \geq 0.8$ were considered strongly collinear and were screened following established recommendations for species distribution modelling.[36] When two variables were strongly correlated, the variable with greater ecological relevance and model contribution was retained. Variance inflation factors were also calculated to further evaluate multicollinearity, and variables with VIF values below 10 were retained for model calibration.[58] After variable screening, nine environmental predictors were retained for the final MaxEnt model.

To evaluate the relationships between environmental variables and carbon stocks, we analysed sediment total nitrogen, total phosphorus, organic matter, pH, and sulfide concentrations, together with the corresponding seawater and oceanographic variables included in the structural equation models. Sediment total nitrogen was quantified using a combustion method with an elemental analyser, whereas total phosphorus was measured using the Olsen extraction method. Sediment organic matter was determined using the Walkley–Black dichromate oxidation procedure, and pH was measured using a calibrated digital pH meter. These analytical procedures followed established methods used in coastal blue carbon and sediment biogeochemical assessments.[59,60]

Literature Search and Screening

Our analysis involved a systematic literature search and screening process to identify seagrass restoration methods in relation to genetic diversity and the extent of bed area reduction. The search was conducted following the PRISMA framework. We searched the Web of Science Core Collection and China National Knowledge Infrastructure databases using predefined keyword combinations. The search terms included “seagrass restoration”, “eelgrass restoration”, “*Zostera japonica*”, “genetic diversity”, “heterozygosity”, “allelic richness”, “seagrass decline”, “area reduction”, “habitat loss”, “seed broadcasting”, “seed-based restoration”, “shoot transplanting”, “transplantation”, and “restoration method”. A total of 79 potentially relevant records were initially identified.

The screening process consisted of four steps. First, potentially relevant records were identified through database searches using the predefined search terms. Second, duplicate records and clearly irrelevant studies were removed. Third, titles and abstracts were screened to retain studies related to seagrass restoration, genetic diversity, bed area reduction, habitat loss, or restoration methods. Fourth, the full texts of potentially eligible studies were assessed, and relevant data were extracted from studies that met the inclusion criteria. After title and abstract screening, 50 articles were retained for full-text assessment.

Studies were included if they met one or more of the following criteria: they reported genetic diversity indicators, such as the number of alleles, heterozygosity, or allelic richness, and/or quantified the extent of seagrass bed area reduction; they specified the restoration method used, including seed broadcasting, other seed-based approaches, shoot transplantation, or combined methods; they described previous habitat conditions and human or natural disturbances affecting the seagrass bed; and they provided sufficient geographic information for contextual interpretation. The Sustainable Wetlands Adaptation and Mitigation Program database was additionally consulted to inform the organization of coastal blue carbon assessment variables. It was not used as a bibliographic database or as a source of records in the literature-screening process.

Rule-based restoration decision framework

A rule-based decision framework was developed using studies that met all inclusion criteria during the literature-screening process. The framework was designed to support the selection of seagrass restoration strategies based on two ecological indicators: genetic diversity and the extent of bed area reduction. Rule-based decision frameworks have increasingly been used in restoration planning because they allow categorical ecological information to be linked transparently with management options.[15,61]

The extent of bed degradation was determined by comparing the mapped bed area during the baseline period of 2014-2015 with that during the most recent assessment period of 2022-2023. Populations that had lost 50% or more of their baseline bed area were classified as having high bed degradation, whereas those with an area reduction of less than 50% were classified as having limited bed degradation. The 50% cutoff was used as an operational threshold to distinguish populations that had lost at least half of their mapped bed extent from those retaining

a larger proportion of the baseline bed.

Genetic diversity status was evaluated using multiple population-genetic metrics rather than nucleotide diversity alone.[62] The proportion of polymorphic loci (Pi), expected heterozygosity (He), and nucleotide diversity (π) were used as the principal diversity indicators. Observed heterozygosity (Ho) was used as supplementary information on realized heterozygosity, whereas FIS was considered separately to assess heterozygote deficiency or excess and was not treated as a direct measure of genetic diversity.[63,64]

Because all populations belonged to the same species and were analyzed using the same genomic dataset and filtering criteria, each principal genetic metric was standardized relative to the maximum value observed among the 11 populations. A relative genetic diversity index was then calculated as:

$$Gi = \frac{1}{3}\left(\frac{Pi}{Pmax} + \frac{He,i}{He,max} + \frac{\pi i}{\pi max}\right)$$

where Pi, He,i, and πi represent the proportion of polymorphic loci, expected heterozygosity, and nucleotide diversity of population i, respectively, and the denominators represent the corresponding maximum values observed across all populations. Populations with $Gi \geq 0.75$ were classified as having relatively high genetic diversity, whereas populations with $Gi < 0.75$ were classified as having relatively low genetic diversity. This operational boundary reflected the clear separation between the southern high-diversity populations and the northern lower-diversity populations in the present dataset and was not regarded as a universal genetic threshold.

Restoration methods were subsequently assigned using the combination of structural decline and genetic diversity status. Sites with low-to-moderate area reduction and high genetic diversity were assigned to natural recovery combined with habitat protection. Sites with high area reduction but high genetic diversity were assigned to shoot-transplantation-based restoration, because the principal requirement was rapid reconstruction of meadow structure while retaining locally adapted genetic resources. Sites with low-to-moderate area reduction and low genetic diversity were assigned to seed-based restoration, with seeds collected from multiple parent plants and, where appropriate, multiple environmentally compatible donor patches to increase sexual recruitment and genetic variation. Sites with both high area reduction

and low genetic diversity were assigned to combined seed-and-shoot restoration, in which transplanted shoots were used to rapidly establish meadow structure and multi-parent seed supplementation was used to broaden the genetic base and reduce bottleneck risks.

These recommendations were treated as preliminary restoration options rather than fixed prescriptions. Final method selection also considered donor availability, habitat suitability, hydrodynamic and sediment conditions, causes of bed degradation, risks of genetic transfer, potential impacts on donor beds, and the feasibility of long-term monitoring and maintenance.

Genetic diversity data of *Z. japonica*

Whole-genome resequencing was conducted to characterize the genetic diversity of *Z. japonica* across 11 geographic populations along the Chinese coast. Leaf tissues were collected from representative individuals, and genomic DNA was extracted using standard plant DNA extraction protocols. Paired-end sequencing libraries were constructed and sequenced on the Illumina NovaSeq platform to generate genome-wide resequencing data, following approaches commonly used in recent seagrass population genomic studies.[65]

Raw sequencing reads were quality-filtered using fastp and aligned to the *Z. japonica* reference genome using the Burrows–Wheeler Aligner. Sequence alignments were processed, and high-confidence single-nucleotide polymorphisms were identified following the Genome Analysis Toolkit best-practice workflow. Variant sites were subsequently filtered according to sequencing depth, missing-data rate, minor allele frequency, and allelic state. All resequencing data have been deposited in the National Center for Biotechnology Information Sequence Read Archive under BioProject accession PRJNA1344808.

Genetic diversity indices, including observed heterozygosity, expected heterozygosity, allelic richness, and nucleotide diversity (π), were calculated using VCFtools and appropriate R packages for population-genetic analysis. These indices are widely used to characterize genetic variation in marine angiosperm populations.[66,67]

RESULTS

Where to restore: mapping the potential restoration opportunity

Predicted distribution and habitat suitability provide spatially explicit indications of where environmental conditions may support restoration under specified climate conditions, rather than direct estimates of restoration success. Using MaxEnt, we predicted the global distribution

of environmentally suitable areas for *Z. japonica* under current conditions and found that the largest and most continuous suitable areas were concentrated in the northwestern Pacific Ocean (Figure 1). Centroid analysis of the suitable area within the northwestern Pacific region further showed that its geographic center was located in Chinese coastal waters (Figure 2). This spatial pattern suggests that China represents an important regional focus for the conservation and restoration planning of *Z. japonica*.

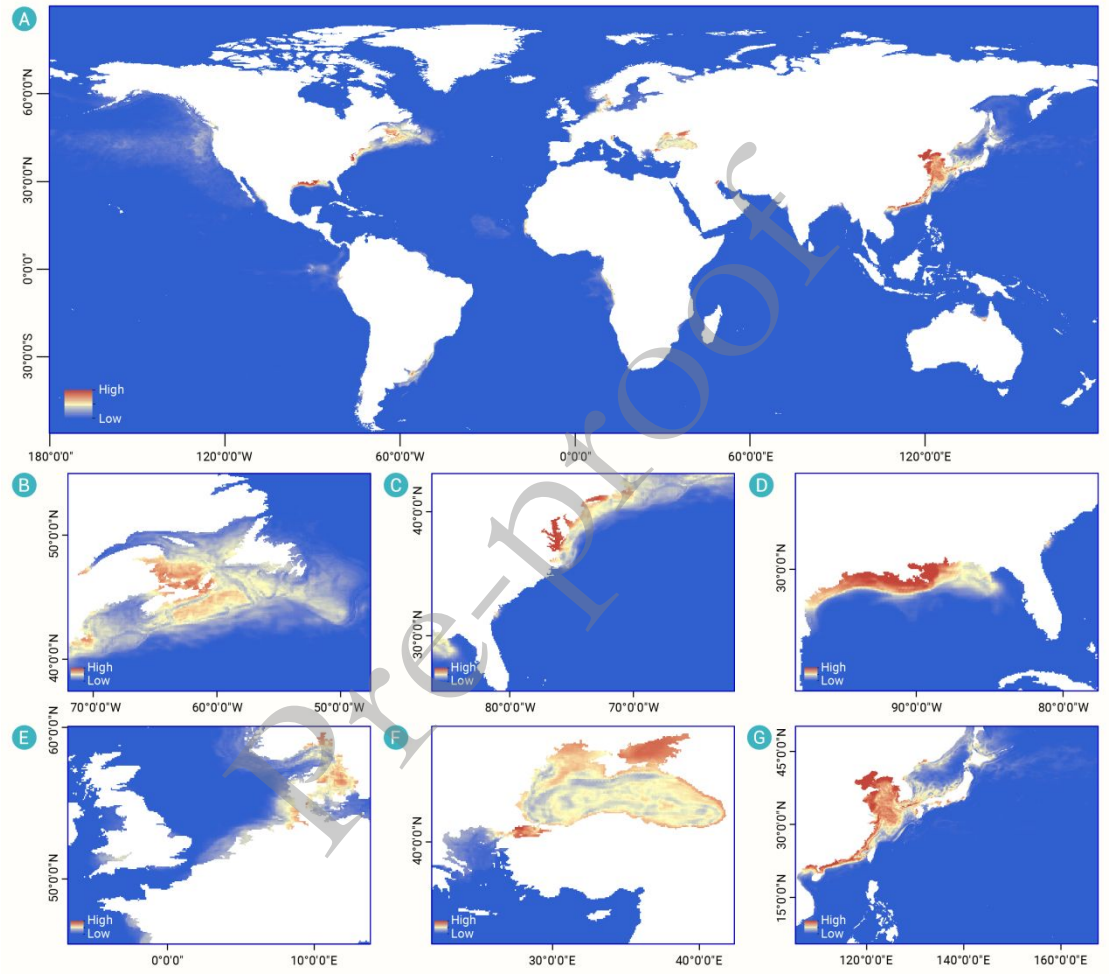

Figure 1. Predicted habitat suitability for *Z. japonica* under current environmental conditions (A) Global distribution of predicted habitat suitability. (B–G) Enlarged views of the major suitable regions in northeastern North America, the eastern coast of North America, the Gulf of Mexico, northern Europe, the Black Sea region, and East Asia, respectively. Colors from blue to red indicate increasing predicted habitat suitability from low to high.

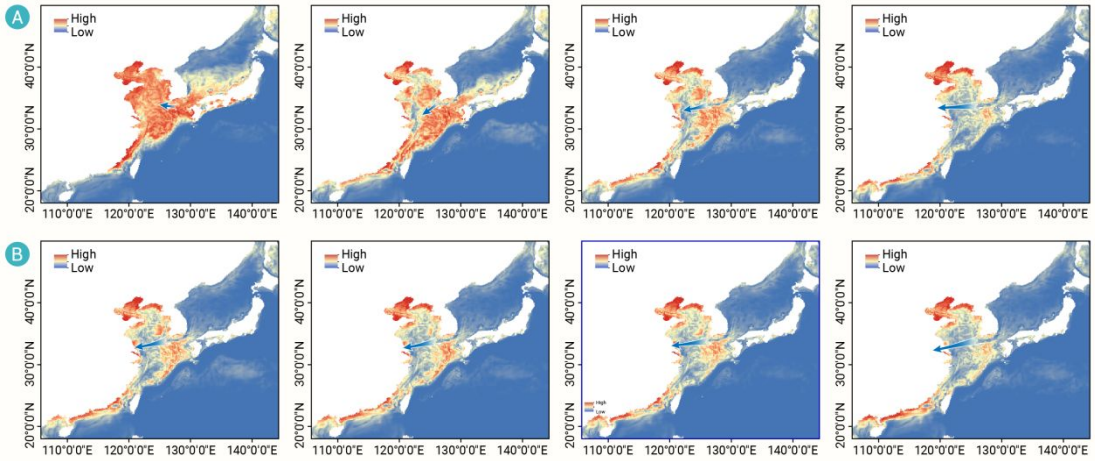

Figure 2. Projected shifts in the centroid of suitable habitat for *Z. japonica* under future climate scenarios within the northwestern Pacific region (A) Projected centroid shifts under RCP2.6, RCP4.5, RCP6.0, and RCP8.5 in the 2050s. (B) Projected centroid shifts under the same climate scenarios in the 2100s. Arrows indicate the direction and relative magnitude of projected changes in the geographic centroid of suitable habitat.

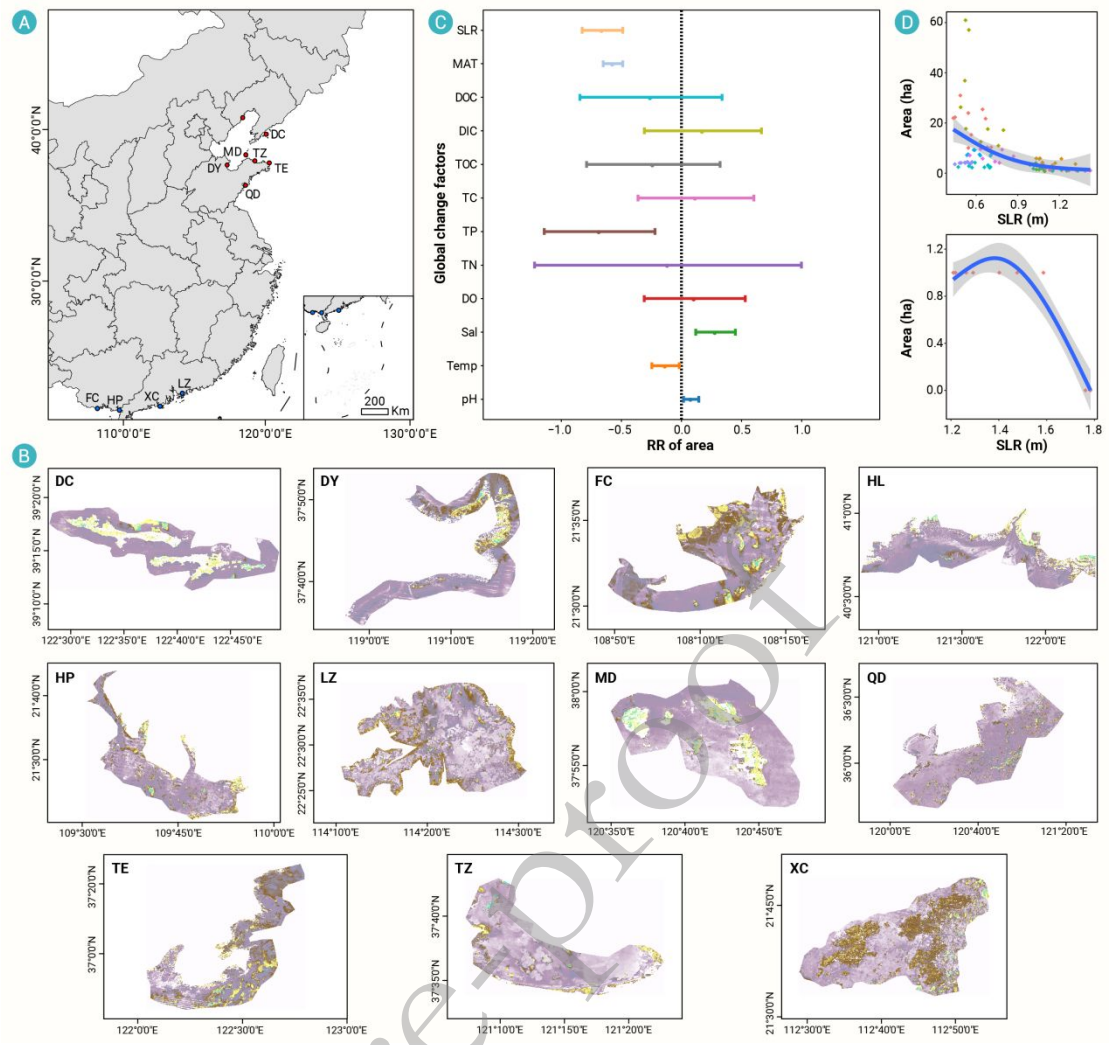

Figure 3. Spatial distribution and temporal changes of *Z. japonica* beds along the coast of China, excluding Taiwan Island (A) Locations of the 11 surveyed populations: QD, Huiquan Bay, Qingdao; TE, Swan Lake, Rongcheng; DY, Yellow River Delta, Dongying; HL, Xingcheng, Huludao; DC, Dachangshan Island, Dalian; MD, Miaodao Island, Yantai; TZ, Taozi Bay, Yantai; LZ, Lai Chi Wo, Hong Kong; XC, Xiachuan Island, Taishan; FC, Pearl Bay, Fangchenggang; and HP, Hepu, Beihai. The blue line indicates the coastline. (B) Spatial distribution and temporal changes in bed area and the *Z. japonica* index from 2014 to 2022 at the 11 study sites, green areas on the maps indicate pixels classified as *Z. japonica* beds based on the *ZJI*. In the temporal profiles, yellow and green lines indicate bed area and *ZJI*, respectively. (C) Response ratios of *Z. japonica* bed area to environmental variables across the study sites in 2023. (D) Generalized additive model showing the nonlinear relationship between sea level rise and *Z. japonica* bed area.

The 11 surveyed populations spanned the major distribution regions of Z. japonica along the Chinese coast, from the Bohai and Yellow seas to the northern South China Sea (Figure 3A). Remote sensing analyses revealed an overall decline in the mapped area of *Z. japonica* beds along the Chinese coast from 2014 to 2022, although the magnitude and temporal pattern of change varied among sites (Figure 3B). Greater losses were generally observed at sites in the South China Sea than at several northern sites. Response ratio analysis indicated that temperature and sea level rise were among the environmental variables most strongly associated with spatial variation in bed area (Figure 3C). The generalized additive model further identified a nonlinear relationship between sea level rise and bed area, with a marked decline occurring beyond approximately 0.9 m and bed area approaching low levels at approximately 1.5 m (Figure 3D).

MaxEnt projections of current habitat suitability within Chinese coastal waters identified three principal suitable regions: the coastal zone of the Liaodong Peninsula, the northwestern Bohai Sea, and selected coastal areas of the Shandong Peninsula, particularly its eastern and northeastern coasts and the Qingdao coastal region (Figure S1). These predicted suitable areas were generally consistent with the surveyed distribution of *Z. japonica* shown in Figure 3. Among the nine retained environmental predictors, mean sea surface temperature had the highest percentage contribution to the MaxEnt model, indicating its dominant contribution to model calibration. Mean surface current velocity had the highest permutation importance, indicating that model predictions were particularly sensitive to this variable. Minimum and mean sea surface salinity also contributed to model performance. Together, these results indicate that temperature, salinity, and current velocity were the principal environmental variables associated with the current predicted distribution of *Z. japonica* in Chinese coastal waters (Table S3).

When to restore: progressive restoration

Projected habitat changes under future sea level rise and climate scenarios provide a basis for prioritizing the timing of *Z. japonica* restoration. Our projections indicate progressive declines in both habitat suitability and the extent of suitable habitat under all future climate scenarios, with clear spatial differences among regions (Figure 4).

By the 2050s, both occurrence probability and suitable habitat extent are projected to decline

markedly in the northwestern Bohai Sea and the western coastal waters of the Liaodong Peninsula under the RCP4.5 and RCP8.5 scenarios, with some areas approaching local disappearance by the 2100s. In the coastal waters of the Shandong Peninsula and the eastern Liaodong Peninsula, suitable habitat is also projected to decline progressively from the 2050s to the 2100s under the same scenarios. Quantitatively, the suitable habitat of *Z. japonica* is projected to decrease by 56.76% under RCP4.5 and 57.35% under RCP8.5 by the 2050s. By the 2100s, the projected decline is 56.26% under RCP4.5 and 61.80% under RCP8.5 (Figure S2 & Table S4). In contrast, the potential for range expansion is very limited, with newly suitable habitat accounting for less than 2% under both scenarios in the 2050s and 2100s.

These projections support a progressive restoration strategy based on habitat persistence through time. Restoration should be prioritized in areas that are suitable under current conditions and remain suitable in the 2050s, particularly those also projected to remain suitable in the 2100s, because these areas represent relatively stable core restoration zones with greater potential for long-term persistence and sustained carbon storage. Areas projected to become suitable mainly by the 2100s should instead be regarded as long-term adaptive restoration reserves and incorporated into future monitoring and planning, rather than being treated as immediate restoration targets.

Under this framework, the total area projected to remain or become suitable for *Z. japonica* by the 2100s reaches 103,371 ha, depending on climate scenario and restoration planning assumptions (Figure 5). This projected area should be interpreted as a potential restoration opportunity space rather than as a direct estimate of realized restoration area.

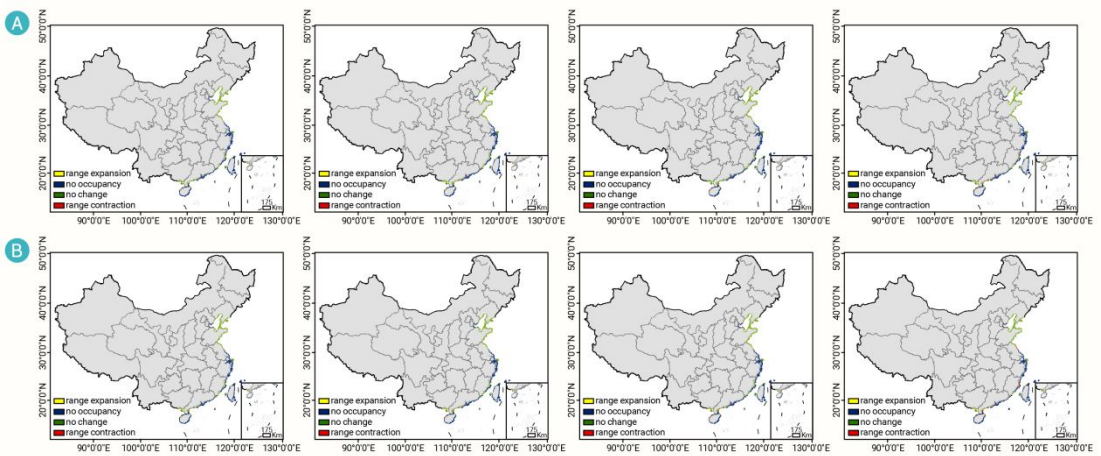

Figure 4. Spatial changes in suitable habitat for *Z. japonica* under future climate scenarios (A)

565 Spatial changes in suitable habitat under RCP2.6, RCP4.5, RCP6.0, and RCP8.5 in the 2050s. (B) Spatial
566 changes in suitable habitat under the same climate scenarios in the 2100s.

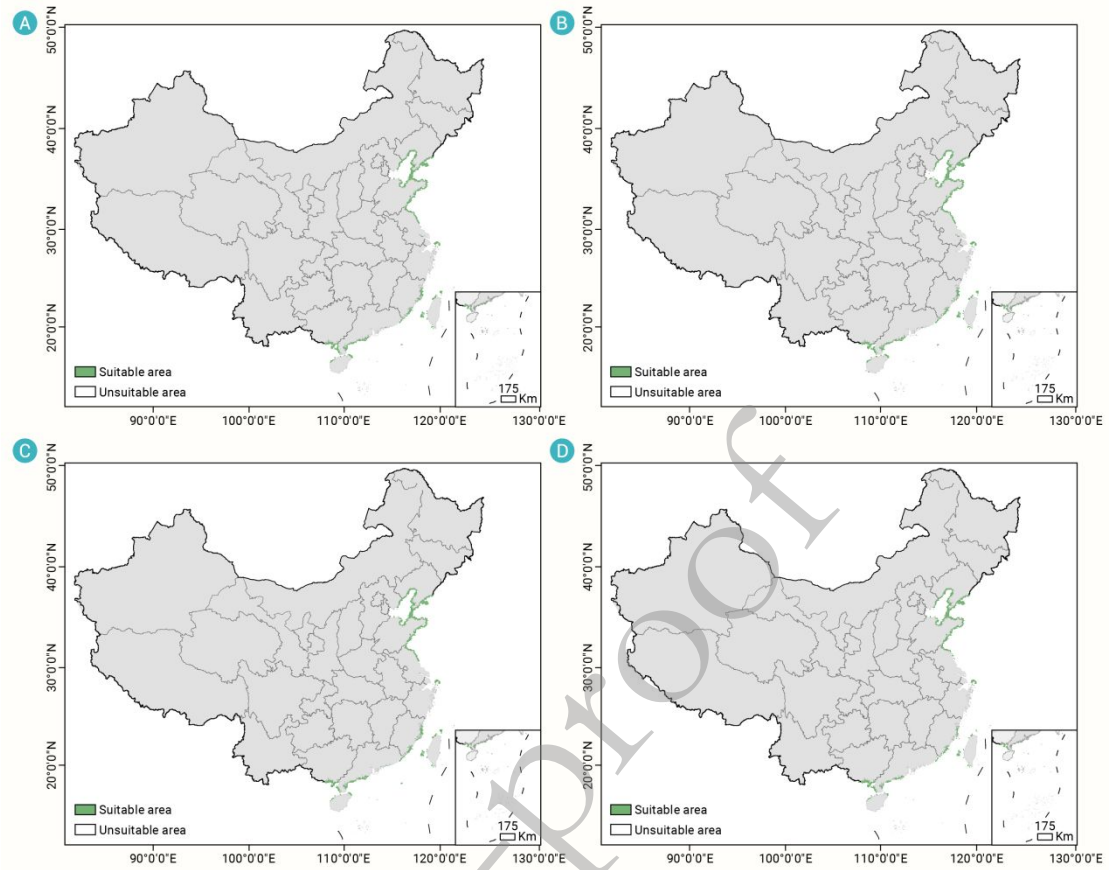

567

568 **Figure 5. Potential suitable and unsuitable areas for *Z. japonica* restoration in the 2100s under the**
569 **progressive restoration framework** (A) Projected suitable and unsuitable areas under RCP2.6. (B)
570 Projected suitable and unsuitable areas under RCP4.5. (C) Projected suitable and unsuitable areas under
571 RCP6.0. (D) Projected suitable and unsuitable areas under RCP8.5.

572 **With what methods to restore: selecting restoration approaches according to local**
573 **conditions**

574 Integrating genetic diversity, remote sensing observations, exposure to sea-level change, and
575 MaxEnt projections revealed marked spatial variation in the status of *Z. japonica* beds along
576 the Chinese coast. Populations in the Bohai Sea and Yellow Sea generally experienced lower
577 levels of bed degradation and were associated with the largest continuous areas projected to
578 remain suitable under current and future environmental conditions. In contrast, populations in
579 the South China Sea showed greater bed degradation and were associated with relatively limited
580 areas of persistent future suitability.

581 Genetic diversity and projected environmental suitability did not show the same spatial pattern.

Southern populations generally exhibited higher allelic richness and heterozygosity than northern populations, whereas the largest areas of projected future habitat suitability occurred in northern China. This spatial mismatch indicates that restoration planning should consider both the conservation value of genetically diverse populations and the long-term environmental suitability of candidate restoration sites.

Two principal active restoration approaches are used for *Z. japonica* along the Chinese coast: seed-based restoration and shoot transplantation, which may be applied separately or in combination with conservation-oriented management. We developed a rule-based regional recommendation framework primarily based on bed degradation and genetic diversity. For highly degraded populations with high genetic diversity, the framework prioritizes the use of local seeds and small-scale in situ transplantation while avoiding their use as major donor sources. For highly degraded populations with low genetic diversity, transplantation using material from genetically diverse donor populations is recommended, with supplementary use of local seeds where appropriate. For populations with relatively limited bed decline but low genetic diversity, local seed use, restricted donor supplementation, small-scale transplantation, and conservation-oriented management are recommended in combination. The resulting regional recommendations are summarized in Table S5. Final restoration decisions should additionally account for donor-material availability, local bed extent, potential impacts on donor beds, environmental compatibility, and the ecological and genetic risks associated with transferring material among differentiated populations.

Regional variation and environmental drivers of *Z. japonica* carbon stocks

Carbon stocks in *Z. japonica* beds varied considerably among the surveyed regions in China (Table S6). The highest total carbon stock values were recorded at DC, MD, TZ, and HL in the Bohai Sea region, whereas comparatively low values were recorded at HP in the South China Sea and QD in the Yellow Sea.

To examine the direct and indirect associations between environmental variables and different carbon pools, we fitted separate structural equation models for aboveground, belowground, and sediment carbon stocks using site-level mean values of the standardized variables. The three models showed acceptable overall fit, with comparative fit index and goodness-of-fit index values above 0.90 and standardized root mean square residual values below 0.07 (Figure 6).

For aboveground carbon stock, sea surface temperature was negatively associated with seawater dissolved oxygen and sediment pH, with standardized path coefficients of −0.74 and −0.47, respectively. In turn, dissolved oxygen and sediment pH showed positive direct associations with aboveground carbon stock, with standardized path coefficients of 0.46 and 0.70, respectively. These pathways indicate that the association between sea surface temperature and aboveground carbon stock was primarily indirect.

For belowground carbon stock, sediment-related variables showed comparatively stronger direct associations. Sediment pH had a positive path coefficient of 0.69, whereas sediment sulfides and sediment nitrogen showed positive but nonsignificant path coefficients of 0.25 and 0.23, respectively. For sediment carbon stock, sediment pH showed the strongest positive direct association, with a standardized path coefficient of 0.73. Sea surface temperature was negatively associated with sediment pH, indicating a potential indirect pathway linking temperature to sediment carbon stock.

Together, the models indicate that the three carbon pools were associated with partly distinct environmental pathways. Aboveground carbon stock was more closely related to seawater physicochemical conditions, whereas belowground carbon stock was more strongly associated with sediment properties. The sediment carbon stock model contained several nonsignificant pathways, suggesting that additional unmeasured factors may contribute to spatial variation in sediment carbon accumulation. These results highlight the compartment-specific environmental associations of carbon storage in *Z. japonica* beds.

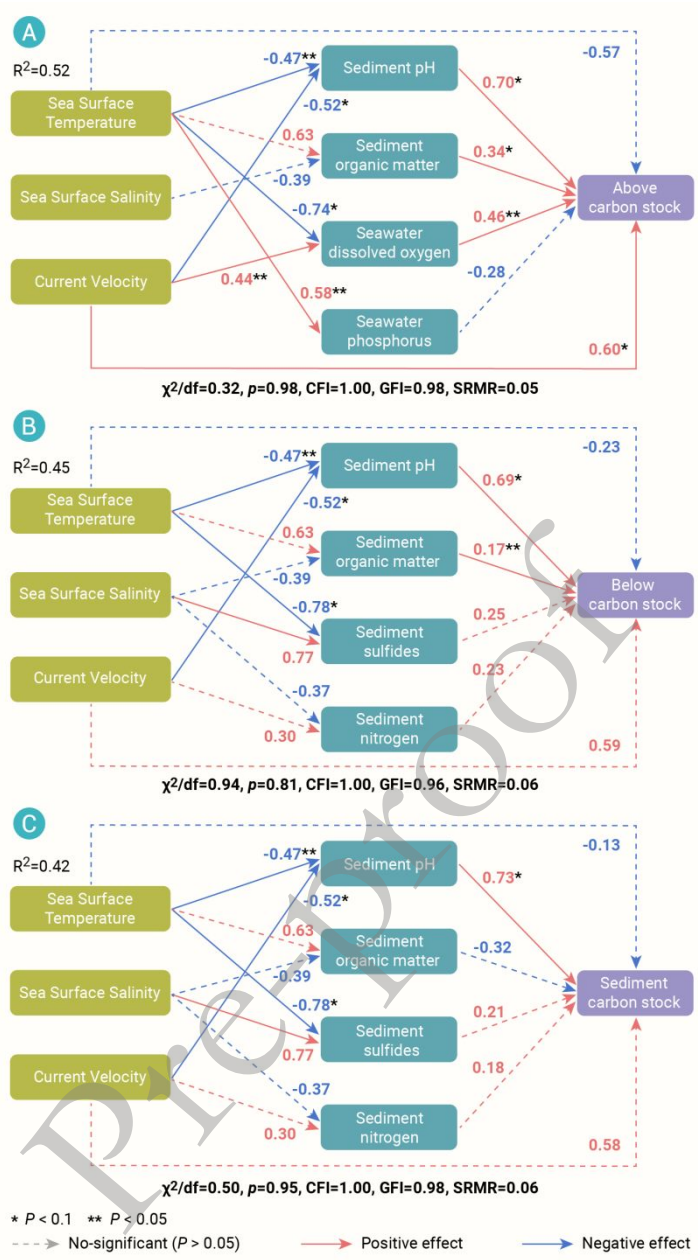

Figure 6. Structural equation models showing the environmental factors associated with carbon stocks in *Z. japonica* beds (A) Aboveground carbon stock, (B) belowground carbon stock, and (C) sediment carbon stock. Numbers adjacent to arrows indicate standardized path coefficients. Pink and blue arrows indicate positive and negative associations, respectively. Solid arrows indicate statistically significant paths, whereas dashed arrows indicate nonsignificant paths. Asterisks indicate the statistical significance of individual paths. R^2indicates the proportion of variance in each carbon stock component explained by the model. Model fit indices are shown below each panel.

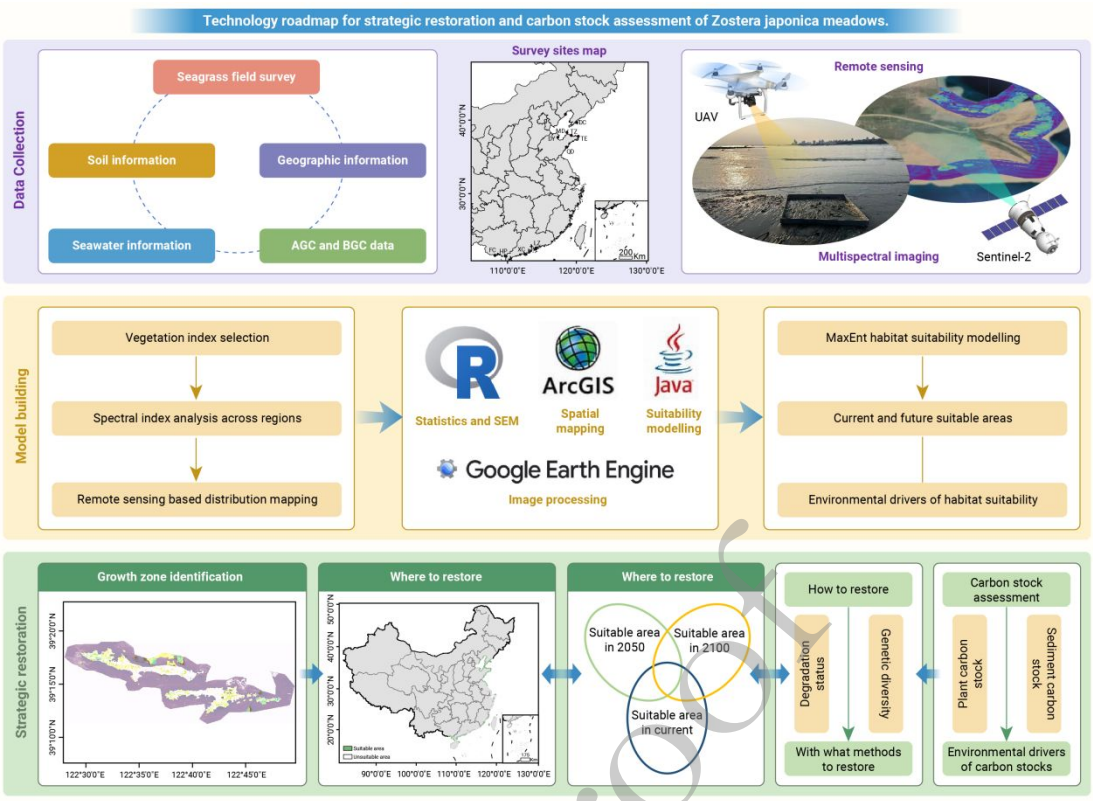

Figure 7. Technology roadmap for the strategic restoration of *Z. japonica* beds based on spatial modelling and carbon stock assessment The workflow integrates field data collection, remote sensing mapping, MaxEnt habitat suitability modelling, carbon stock assessment, and strategic restoration planning. Google Earth Engine, ArcGIS, Java based MaxEnt, and R were used for image processing, spatial mapping, habitat suitability prediction, and statistical analyses, respectively. Field derived carbon stock data were further used to support restoration planning and estimate the potential long term carbon benefits of future bed restoration.

DISCUSSION

The restoration of *Z. japonica* beds has the potential to enhance coastal carbon storage and contribute to China's carbon neutrality goals. By integrating habitat suitability modelling, remote sensing, field surveys, genetic information, and carbon stock assessments, this study provides a spatially explicit framework for determining where, when, and how restoration could be implemented along the Chinese coast.

We combined MaxEnt habitat suitability modelling with multitemporal remote sensing to identify potential priority areas for *Z. japonica* restoration. Under current and future climate scenarios, the Bohai Sea and Yellow Sea contained extensive areas of predicted suitable habitat, largely associated with favourable temperature, salinity, and hydrodynamic conditions. MaxEnt is widely used for species distribution modelling with presence-only data, and has been applied in marine species distribution and coastal habitat assessments,[34,35] including the identification of conservation and restoration priorities for seagrass ecosystems.[24] Nevertheless, predicted suitability represents the environmental potential for species occurrence rather than direct evidence of restoration success. Local substrate conditions, water quality, hydrodynamics, disturbance history, and propagule availability should therefore be evaluated before restoration is implemented.

Our temporal framework prioritizes areas predicted to remain suitable under current conditions and through the 2050s and 2100s as relatively stable core zones for restoration. Areas that are currently suitable but projected to become unsuitable should receive immediate conservation attention and may be appropriate only for short- to medium-term restoration where future risks can be managed. In contrast, areas projected to become suitable mainly by the 2100s should be regarded as potential adaptive reserves rather than immediate planting targets. This phased approach links present restoration opportunities with long-term environmental change and is consistent with restoration principles emphasizing appropriate timing, site selection, restoration scale, and adaptive management.[15,19,22,63]

Drawing on the literature synthesis and population genomic data, we developed a rule-based framework for selecting restoration methods according to bed degradation and genetic diversity[15]. Southern populations exhibited higher genetic diversity than northern populations, whereas northern China contained a larger extent of habitat projected to remain suitable under

future conditions. This spatial mismatch highlights the importance of considering both environmental suitability and evolutionary information in restoration planning. Southern populations represent important genetic resources and may provide candidate donor material for future assisted gene flow, but only after careful assessment of local adaptation, donor-bed impacts, genetic compatibility, and ecological risk. Northern regions, by contrast, provide extensive potential restoration space but may require greater attention to the conservation of locally adapted genetic resources. More generally, spatial differences between genetic diversity, population connectivity, and projected environmental suitability may arise from historical demographic processes, ocean-current-mediated dispersal, and climate-driven shifts in suitable habitat.[65,68-70]

This mismatch further highlights the importance of integrating evolutionary information with environmental projections. High-diversity southern populations represent valuable genetic resources that should be prioritized for conservation, because genetic variation can influence ecosystem resistance, recovery capacity, and long-term population persistence.[62,67,70] These populations may also inform future assisted gene flow, but the transfer of restoration material should proceed only after careful evaluation of local adaptation, donor availability, genetic compatibility, donor-population impacts, and ecological risk.[70-72] In contrast, northern regions provide extensive predicted suitable habitat for restoration. The framework distinguishes among seed-based restoration, shoot transplantation, combined approaches, and protection or natural recovery. Seed-based restoration may be appropriate where bed structure remains partly intact and suitable seed sources are available, provided that seeds are collected from environmentally compatible donor populations and impacts on donor beds are minimized[63,72]. Shoot transplantation may accelerate structural recovery in severely degraded beds when suitable donor material is available and disturbance pressures have been reduced.[15,63,73] A combined approach may be appropriate where both genetic diversity and bed area have declined substantially, although the relative contribution of seeds and transplanted shoots should be adjusted according to site conditions and donor-material availability.[63,73] Where genetic diversity remains high and area reduction is limited, protection, natural recovery, and continued monitoring should generally be prioritized.[15,16,64]

These recommendations should be treated as initial management options rather than fixed prescriptions because restoration outcomes also depend on sediment conditions, hydrodynamics, water quality, donor availability, restoration scale, and the causes of degradation. This approach aligns with restoration frameworks developed for seagrass and other coastal ecosystems, which emphasize context-dependent restoration based on environmental and biological conditions.[15,63,73] Previous studies have shown that restoration outcomes can be improved when methods are tailored to site conditions, including local environmental quality, historical population trends, restoration scale, and genetic variation.[21,62,63,72] Integrating these factors allows restoration planning to identify appropriate interventions and overcome limitations associated with reliance on a single method. Future work will benefit from combining genomic data with assessments of future vulnerability. Genome-level approaches can identify candidate adaptive genetic variation and improve the evaluation of population responses to environmental stress.[69-72] Integrating these approaches will improve the scientific basis of restoration planning and support the development of long-term strategies for *Z. japonica* conservation and recovery along the Chinese coast.

Carbon stocks in *Z. japonica* beds varied substantially among regions, with the highest values recorded at several sites in the Bohai Sea. Structural equation modelling was used to examine the environmental variables associated with these carbon stocks and indicated that different carbon pools were related to partly distinct environmental pathways. Aboveground carbon stock was associated with both water-column conditions and hydrodynamic variables, whereas belowground carbon stock was more closely associated with sediment physicochemical properties. Temperature may influence carbon stocks indirectly by altering oxygen availability and sediment chemical conditions, whereas hydrodynamic conditions may affect sediment stability, particle deposition, and organic matter retention[74,75]. However, the relatively high proportion of nonsignificant pathways in the sediment carbon model also suggests that additional factors, such as sediment grain size, sedimentation rate, organic matter sources, and historical carbon deposition, may contribute to sediment carbon accumulation[76]. Understanding these factors is important for developing restoration and management strategies that enhance coastal carbon storage and contribute to broader carbon-neutrality objectives[1,31,77,78].

Consistent with studies of mangrove carbon stocks, our results also emphasize the importance

of sediment conditions and temperature-related environmental processes in regulating coastal blue carbon storage.[59] However, the carbon benefits of restoration cannot be inferred from bed area alone. The projected suitable habitat represents a potential restoration opportunity space rather than a direct estimate of realized restoration area, and the associated carbon estimate represents potential carbon stock under the stated assumptions rather than guaranteed additional sequestration. Site-specific measurements of sediment properties, carbon stocks, and carbon accumulation rates will therefore be required to evaluate the realized carbon benefits of *Z. japonica* restoration.

Beyond carbon storage, restored seagrass beds can support biodiversity, improve water quality, stabilize sediments, and increase coastal resilience.[61,79,80] These co-benefits strengthen the rationale for incorporating seagrass restoration into broader coastal management and climate-mitigation strategies. Experiences from large-scale restoration programmes indicate that restoration success is improved by integrating spatial planning, context-specific method selection, appropriate restoration scale, and long-term monitoring.[15,63] Our framework extends these principles by linking habitat suitability, future environmental change, genetic information, restoration methods, and potential carbon benefits within a unified planning framework (Figure 7). However, field validation remains essential for translating projected habitat suitability and potential carbon benefits into successful restoration and long-term bed persistence.

Conclusion

The strategic restoration of *Z. japonica* beds offers a promising pathway for enhancing coastal carbon storage and supporting China's carbon neutrality goals. By integrating spatial modelling, field observations, genetic information, and carbon stock assessments, this study provides a practical framework for identifying priority restoration areas, selecting appropriate restoration methods, and evaluating potential ecological and carbon benefits. The framework emphasizes the importance of matching restoration timing and methods to local environmental conditions and population characteristics. Although our surveys covered most of the known distribution regions of *Z. japonica* in China, baseline information remains incomplete. Expanding long-term seagrass monitoring and carbon stock datasets will enable more robust assessments of restoration feasibility and the ecological and carbon benefits of seagrass beds.

References

[1] Liu Z., Deng Z., He G., et al. (2022). Challenges and opportunities for carbon neutrality in China. *Nat. Rev. Earth Environ.* **3**:141-155. DOI:10.1038/s43017-021-00244-x

[2] Houghton R. A. (2007). Balancing the global carbon budget. *Annu. Rev. Earth Planet. Sci.* **35**:313-347. DOI:10.1146/annurev.earth.35.031306.140057

[3] Luisetti T. (2021). Some countries donate blue carbon. *Nat. Clim. Change* **11**:647-648. DOI:10.1038/s41558-021-01103-9

[4] Duarte C. M., Agusti S., Barbier E., et al. (2020). Rebuilding marine life. *Nature* **580**:39-51. DOI:10.1038/s41586-020-2146-7

[5] Lu N., Tian H., Fu B., et al. (2022). Biophysical and economic constraints on China's natural climate solutions. *Nat. Clim. Change* **12**:847-853. DOI:10.1038/s41558-022-01432-3

[6] Lu F., Hu H., Sun W., et al. (2018). Effects of national ecological restoration projects on carbon sequestration in China from 2001 to 2010. *Proc. Natl. Acad. Sci. USA* **115**:4039-4044. DOI:10.1073/pnas.1700294115

[7] Yu Z., Ciais P., Piao S., et al. (2022). Forest expansion dominates China's land carbon sink since 1980. *Nat. Commun.* **13**:5374. DOI:10.1038/s41467-022-32961-2

[8] Piao S., He Y., Wang X., et al. (2022). Estimation of China's terrestrial ecosystem carbon sink: Methods, progress and prospects. *Sci. China Earth Sci.* **65**:641-651. DOI:10.1007/s11430-021-9892-6

[9] Nelleman C., Corcoran E., Duarte C. M., et al. (2008). Blue carbon: The role of healthy oceans in binding carbon (UNEP/FAO/UNESCO/IUCN/CSIC), pp:1-78. DOI:10.1590/S0100-06832008000200014.

[10] Macreadie P. I., Costa M. D. P., Atwood T. B., et al. (2021). Blue carbon as a natural climate solution. *Nat. Rev. Earth Environ.* **2**:826-839. DOI:10.1038/s43017-021-00224-1

[11] Falkowski P. G., Barber R. T. and Smetacek V. V. (1998). Biogeochemical controls and feedbacks on ocean primary production. *Science* **281**:200-207. DOI:10.1126/science.281.5374.200

[12] Duarte C. M. (1995). Submerged aquatic vegetation in relation to different nutrient regimes. *Ophelia* **41**:87-112. DOI:10.1080/00785236.1995.10422039

[13] Chefaoui R. M., Duarte C. M. and Serrao E. A. (2018). Dramatic loss of seagrass habitat under projected climate change in the Mediterranean Sea. *Global Change Biol.* **24**:4919-4928. DOI:10.1111/gcb.14401

[14] Duarte C. M., Kennedy H., Marbà N., et al. (2013). Assessing the capacity of seagrass meadows for carbon burial: Current limitations and future strategies. *Ocean Coast. Manage.* **83**:32-38. DOI:10.1016/j.ocecoaman.2011.09.001

[15] Orth R. J., Lefcheck J. S., McGlathery K. S., et al. (2020). Restoration of seagrass habitat leads to rapid recovery of coastal ecosystem services. *Sci. Adv.* **6**:eabc6434. DOI:10.1126/sciadv.abc6434

[16] Unsworth R. K. F., Cullen-Unsworth L. C., Jones B. L. H., et al. (2022). The planetary role of seagrass conservation. *Science* **377**:609-613. DOI:10.1126/science.abq6923

[17] Liu C., Liu G., Casazza M., et al. (2022). Current status and potential assessment of China's ocean carbon sinks. *Environ. Sci. Technol.* **56**:6584-6595. DOI:10.1021/acs.est.1c08106

[18] Zhou Q. Q., Ke Y. H., Wang X. Y., et al. (2022). Developing seagrass index for long term monitoring of seagrass bed: A case study in Yellow River Delta, China. *ISPRS J. Photogramm. Remote Sens.* **194**:286-301. DOI:10.1016/j.isprsjprs.2022.10.011

[19] Fourqurean J. W., Duarte C. M., Kennedy H., et al. (2012). Seagrass ecosystems as a globally significant carbon stock. *Nat. Geosci.* **5**:505-509. DOI:10.1038/ngeo1477

[20] Dunic J. C., Brown C. J., Connolly R. M., et al. (2021). Long-term declines and recovery of meadow area across the world's seagrass bioregions. *Global Change Biol.* **27**:4096-4109. DOI:10.1111/gcb.15684

[21] Orth R. J., Moore K. A., Marion S. R., et al. (2012). Seed addition facilitates eelgrass recovery in a coastal bay system. *Mar. Ecol. Prog. Ser.* **448**:177-195. DOI:10.3354/meps09522

[22] Waycott M., Duarte C. M., Carruthers T. J., et al. (2009). Accelerating loss of seagrasses across the globe threatens coastal ecosystems. *Proc. Natl. Acad. Sci. USA* **106**:12377-12381. DOI:10.1073/pnas.0905620106

[23] Huang Y.-H., Lee C.-L., Chung C.-Y., et al. (2015). Carbon budgets of multispecies seagrass beds at Dongsha Island in the South China Sea. *Mar. Environ. Res.* **106**:92-102. DOI:10.1016/j.marenvres.2015.03.004

[24] Hu W. J., Zhang D. A., Chen B., et al. (2021). Mapping the seagrass conservation and restoration priorities: Coupling habitat suitability and anthropogenic pressures. *Ecol. Indic.* **129**:107960. DOI:10.1016/j.ecolind.2021.107960

[25] Zhang X., Li Y. L., Kaldy J. E., et al. (2024). Population genetic patterns across the native and invasive range of a widely distributed seagrass: Phylogeographic structure, invasive history and conservation implications. *Divers. Distrib.* **30**:1-18. DOI:10.1111/ddi.13803

[26] Zhang X., Lin H., Song X., et al. (2019). A unique meadow of the marine angiosperm *Zostera japonica*, covering a large area in the turbid intertidal Yellow River Delta, China. *Sci. Total Environ.* **686**:118-130. DOI:10.1016/j.scitotenv.2019.05.320

[27] Huang X. P., Huang L. M., Li Y. H., et al. (2006). Main seagrass beds and threats to their habitats in the coastal sea of South China. *Chin. Sci. Bull.* **51**:136-142. DOI:10.1007/s11434-006-9136-5

[28] Yue S., Zhou Y., Xu S., et al. (2021). Can the non-native salt marsh halophyte Spartina alterniflora threaten native seagrass (*Zostera japonica*) habitats? a case study in the Yellow River Delta, China. *Front. Plant Sci.* **12**:643425. DOI:10.3389/fpls.2021.643425

[29] Hodoki Y., Ohbayashi K., Tanaka N., et al. (2013). Evaluation of Genetic Diversity in (Aschers. et Graebn.) for Seagrass Conservation in Brackish Lower Reaches of the Hii River System, Japan. *Estuaries Coasts* **36**:127-134. DOI:10.1007/s12237-012-9564-1

[30] Lee S., Ma S., Lim Y., et al. (2004). Genetic diversity and its implications in the conservation of endangered in Korea. *J. Plant Biol.* **47**:275-281. DOI:10.1007/Bf03030519

[31] Hepburn C., Qi Y., Stern N., et al. (2021). Towards carbon neutrality and China's 14th Five-Year Plan: Clean energy transition, sustainable urban development, and investment priorities. *Environ. Sci. Ecotechnol.* **8**:100130. DOI:10.1016/j.ese.2021.100130

[32] Short F. T. and Coles R. G. (2001). Global seagrass research methods (Elsevier), pp:1-473. DOI:10.1016/B978-0-444-50891-1.X5000-2.

[33] Hossain M. S., Bujang J. S., Zakaria M. H., et al. (2015). The application of remote sensing to seagrass ecosystems: an overview and future research prospects. *Int. J. Remote Sens.* **36**:61-114. DOI:10.1080/01431161.2014.990649

[34] Phillips S. J., Anderson R. P. and Schapire R. E. (2006). Maximum entropy modeling of species geographic distributions. *Ecol. Modell.* **190**:231-259. DOI:10.1016/j.ecolmodel.2005.03.026

[35] Elith J., Phillips S. J., Hastie T., et al. (2011). A statistical explanation of MaxEnt for ecologists. *Divers. Distrib.* **17**:43-57. DOI:10.1111/j.1472-4642.2010.00725.x

[36] Dormann C. F., Elith J., Bacher S., et al. (2013). Collinearity: a review of methods to deal with it and a simulation study evaluating their performance. *Ecography* **36**:27-46. DOI:10.1111/j.1600-0587.2012.07348.x

[37] Liang H., Wang L., Wang S., et al. (2023). Remote sensing detection of seagrass distribution in a marine lagoon (Swan Lake), China. *Opt. Express* **31**:27677-27695. DOI:10.1364/OE.498901

[38] Tucker C. J. (1979). Red and photographic infrared linear combinations for monitoring vegetation. *Remote Sens. Environ.* **8**:127-150. DOI:10.1016/0034-4257(79)90013-0

[39] Xu H. Q. (2006). Modification of normalised difference water index (NDWI) to enhance open water features in remotely sensed imagery. *Int. J. Remote Sens.* **27**:3025-3033. DOI:10.1080/01431160600589179

[40] Healey S. P., Cohen W. B., Yang Z. Q., et al. (2005). Comparison of tasseled cap-based landsat data structures for use in forest disturbance detection. *Remote Sens. Environ.* **97**:301-310. DOI:10.1016/j.rse.2005.05.009

[41] Somers B. and Asner G. P. (2013). Multi-temporal hyperspectral mixture analysis and feature selection for invasive species mapping in rainforests. *Remote Sens. Environ.* **136**:14-27. DOI:10.1016/j.rse.2013.04.006

[42] Muscarella R., Galante P. J., Soley-Guardia M., et al. (2014). ENMeval: An R package for conducting spatially independent evaluations and estimating optimal model complexity for MAXENT ecological niche models. *Methods Ecol. Evol.* **5**:1198-1205. DOI:10.1111/2041-210x.12261

[43] Brown J. L., Bennett J. R. and French C. M. (2017). SDMtoolbox 2.0: the next generation Python-based GIS toolkit for landscape genetic, biogeographic and species distribution model analyses. *PeerJ* **5**:e4095. DOI:10.7717/peerj.4095

[44] Wood S. N. (2017). Generalized additive models: an introduction with R (chapman and hall/CRC), pp:1-447. DOI:10.1201/9781315370279.

[45] Zuur A. F., Ieno E. N., Walker N. J., et al. (2009). Mixed effects models and extensions in ecology with R (Springer), pp:938–939. DOI:10.1111/j.1467-985X.2010.00663_9.x.

[46] Wood S. N. (2011). Fast stable restricted maximum likelihood and marginal likelihood estimation of semiparametric generalized linear models. *Journal of the Royal Statistical Society Series B-Statistical Methodology* **73**:3-36. DOI:10.1111/j.1467-9868.2010.00749.x

[47] Saunders M. I., Leon J., Phinn S. R., et al. (2013). Coastal retreat and improved water quality mitigate losses of seagrass from sea level rise. *Glob Chang Biol* **19**:2569-2583. DOI:10.1111/gcb.12218

[48] Stocker T. F., Qin D., Plattner G.-K., et al. (2014). IPCC, 2013: climate change 2013: the physical science basis. Contribution of working group I to the fifth assessment report of the intergovernmental panel on climate change (Cambridge University Press), pp:117-1308. DOI:10.1017/CBO9781107415324.

[49] Pörtner H.-O., Roberts D. C., Masson-Delmotte V., et al. (2019). The ocean and cryosphere in a changing climate. *IPCC special report on the ocean and cryosphere in a changing climate* **1155**:10-1017. DOI:10.1017/9781009157964

[50] Giribabu D., Hari R., Sharma J., et al. (2024). Performance assessment of GEBCO_2023 gridded bathymetric data in selected shallow waters of Indian ocean using the seafloor from ICESat-2 photons. *Mar. Geophys. Res.* **45**:1. DOI:10.1007/s11001-023-09534-z

[51] Nicholls R. J. and Cazenave A. (2010). Sea-level rise and its impact on coastal zones. *Science* **328**:1517-1520. DOI:10.1126/science.1185782

[52] Duarte C. M. (1991). Seagrass Depth Limits. *Aquat. Bot.* **40**:363-377. DOI:10.1016/0304-3770(91)90081-F

[53] Duarte C. M., Marbà N., Krause-Jensen D., et al. (2007). Testing the predictive power of seagrass depth limit models. *Estuaries Coasts* **30**:652-656. DOI:10.1007/Bf02841962

[54] Capistrant-Fossa K. A. and Dunton K. H. (2024). Rapid sea level rise causes loss of seagrass meadows. *Commun. Earth Environ.* **5**:87. DOI:10.1038/s43247-024-01236-7

[55] Lajeunesse M. J. (2015). Bias and correction for the log response ratio in ecological meta-analysis. *Ecology* **96**:2056-2063. DOI:10.1890/14-2402.1

[56] Assis J., Tyberghein L., Bosch S., et al. (2018). Bio-ORACLE v2. 0: Extending marine data layers for bioclimatic modelling. *Global Ecol. Biogeogr.* **27**:277-284. DOI:10.1111/geb.12693

[57] Tyberghein L., Verbruggen H., Pauly K., et al. (2012). Bio-ORACLE: a global environmental dataset for marine species distribution modelling. *Global Ecol. Biogeogr.* **21**:272-281. DOI:10.1111/J.1466-8238.2011.00656.X

[58] Wu N., Qu Y., Guse B., et al. (2018). Hydrological and environmental variables outperform spatial factors in structuring species, trait composition, and beta diversity of pelagic algae. *Ecol. Evol.* **8**:2947-2961. DOI:10.1002/ece3.3903

[59] Meng Y. C., Gou R. K., Bai J. K., et al. (2022). Spatial patterns and driving factors of carbon stocks in mangrove forests on Hainan Island, China. *Global Ecol. Biogeogr.* **31**:1692-1706. DOI:10.1111/geb.13549

[60] Rahmawati S., Hernawan U. E., McMahon K., et al. (2019). Blue carbon in seagrass ecosystem: guideline for the assessment of carbon stock and sequestration in Southeast Asia (UGM PRESS), pp:1-112.

[61] Saunders M. I., Doropoulos C., Bayraktarov E., et al. (2020). Bright Spots in Coastal Marine Ecosystem Restoration. *Curr. Biol.* **30**:R1500-R1510. DOI:10.1016/j.cub.2020.10.056

[62] Hughes A. R. and Stachowicz J. J. (2004). Genetic diversity enhances the resistance of a seagrass ecosystem to disturbance. *Proc. Natl. Acad. Sci. USA* **101**:8998-9002. DOI:10.1073/pnas.0402642101

[63] van Katwijk M. M., Thorhaug A., Marbà N., et al. (2016). Global analysis of seagrass restoration: the importance of large-scale planting. *J. Appl. Ecol.* **53**:567-578. DOI:10.1111/1365-2664.12562

[64] Duarte C. M., Apostolaki E. T., Serrano O., et al. (2025). Conserving seagrass ecosystems to meet global biodiversity and climate goals. *Nat. Rev. Biodivers.* **1**:150-165. DOI:10.1038/s44358-025-00028-x

[65] Yu L., Khachaturyan M., Matschiner M., et al. (2023). Ocean current patterns drive the worldwide colonization of eelgrass (*Zostera marina*). *Nat. Plants* **9**:1207-1220. DOI:10.1038/s41477-023-01464-3

[66] Reusch T. B. H. (2006). Does disturbance enhance genotypic diversity in clonal organisms? A field test in the marine angiosperm *Zostera marina*. *Mol. Ecol.* **15**:277-286. DOI:10.1111/j.1365-294X.2005.02779.x

[67] Jahnke M., Olsen J. L. and Procaccini G. (2015). A meta-analysis reveals a positive correlation between genetic diversity metrics and environmental status in the long-lived seagrass *Posidonia oceanica*. *Mol. Ecol.* **24**:2336-2348. DOI:10.3390/biology10111089

[68] Atwater D. Z., Ervine C. and Barney J. N. (2018). Climatic niche shifts are common in introduced plants. *Nat. Ecol. Evol.* **2**:34-43. DOI:10.1038/s41559-017-0396-z

[69] Jahnke M., Gullström M., Larsson J., et al. (2019). Population genetic structure and connectivity of the seagrass in the Western Indian Ocean is influenced by predominant ocean currents. *Ecol. Evol.* **9**:8953-8964. DOI:10.1002/ece3.5420

[70] Procaccini G., Olsen J. L. and Reusch T. B. H. (2007). Contribution of genetics and genomics to seagrass biology and conservation. *J. Exp. Mar. Biol. Ecol.* **350**:234-259. DOI:10.1016/j.jembe.2007.05.035

[71] van Oosterhout C., Supple M. A., Morales H. E., et al. (2025). Genome engineering in biodiversity conservation and restoration. *Nat. Rev. Biodivers.* **1**:543-555. DOI:10.1038/s44358-025-00065-6

[72] Thorogood R., Mustonen V., Aleixo A., et al. (2023). Understanding and applying biological resilience, from genes to ecosystems. *npj Biodivers.* **2**:16. DOI:10.1038/s44185-023-00022-6

[73] Pansini A., Berlino M., Mangano M. C., et al. (2025). Meta-analysis reveals the effectiveness and best practices for the iconic Mediterranean seagrass restoration. *Sci. Total Environ.* **976**:179325. DOI:10.1016/j.scitotenv.2025.179325

[74] Samper-Villarreal J., Lovelock C. E., Saunders M. I., et al. (2016). Organic carbon in seagrass sediments is influenced by seagrass canopy complexity, turbidity, wave height, and water depth. *Limnol. Oceanogr.* **61**:938-952. DOI:10.1002/lno.10262

[75] Röhr M. E., Holmer M., Baum J. K., et al. (2018). Blue carbon storage capacity of temperate eelgrass (*Zostera marina*) meadows. *Global Biogeochem. Cycles* **32**:1457-1475. DOI:10.1029/2018GB005941

[76] Krause J. R., Cameron C., Arias-Ortiz A., et al. (2025). Global seagrass carbon stock variability and emissions from seagrass loss. *Nat. Commun.* **16**:3798. DOI:10.1038/s41467-025-59204-4

[77] Zhu J.-J. and Yan B. (2022). Blue carbon sink function and carbon neutrality potential of mangroves (Elsevier), pp:153438. DOI:10.1016/j.scitotenv.2022.153438.

[78] Zhang D., Zhao Y. and Wu J. (2023). Assessment of carbon balance attribution and carbon storage potential in China's terrestrial ecosystem. *Resour. Conserv. Recycl.* **189**:106748. DOI:10.1016/j.resconrec.2022.106748

[79] Lovelock C. E. and Reef R. (2020). Variable Impacts of Climate Change on Blue Carbon. *One Earth* **3**:195-211. DOI:10.1016/j.oneear.2020.07.010

[80] Wang F., Sanders C. J., Santos I. R., et al. (2021). Global blue carbon accumulation in tidal wetlands increases with climate change. *Natl. Sci. Rev.* **8**:nwaa296. DOI:10.1093/nsr/nwaa296

FUNDING AND ACKNOWLEDGMENTS

This research was funded by the National Natural Science Foundation of China (42206117), the Natural Science Foundation of Shandong Province (ZR2024QD017), the NSFC-Shandong Joint Fund (U1806213), and the National Key R&D Program of China (2019YFD0901204). The funders had no role in study design, data collection and analysis, decision to publish, or preparation of the manuscript.

AUTHOR CONTRIBUTIONS

H. W. contributed to the conceptualization, methodology, software, formal analysis, and writing (original draft) of the manuscript. J. C., and X. T. contributed to the conceptualization, methodology, funding acquisition, supervision, and review & editing of the manuscript. X. L., Y. Z., J. X., S. X., and L. L. contributed to the conceptualization and review & editing of the manuscript. All authors contributed to the manuscript and approved the final version.

DECLARATION OF INTERESTS

The authors declare that there are no conflicts of interest.

DATA AND CODE AVAILABILITY

The data that support the findings of this study are available from the corresponding author upon reasonable request

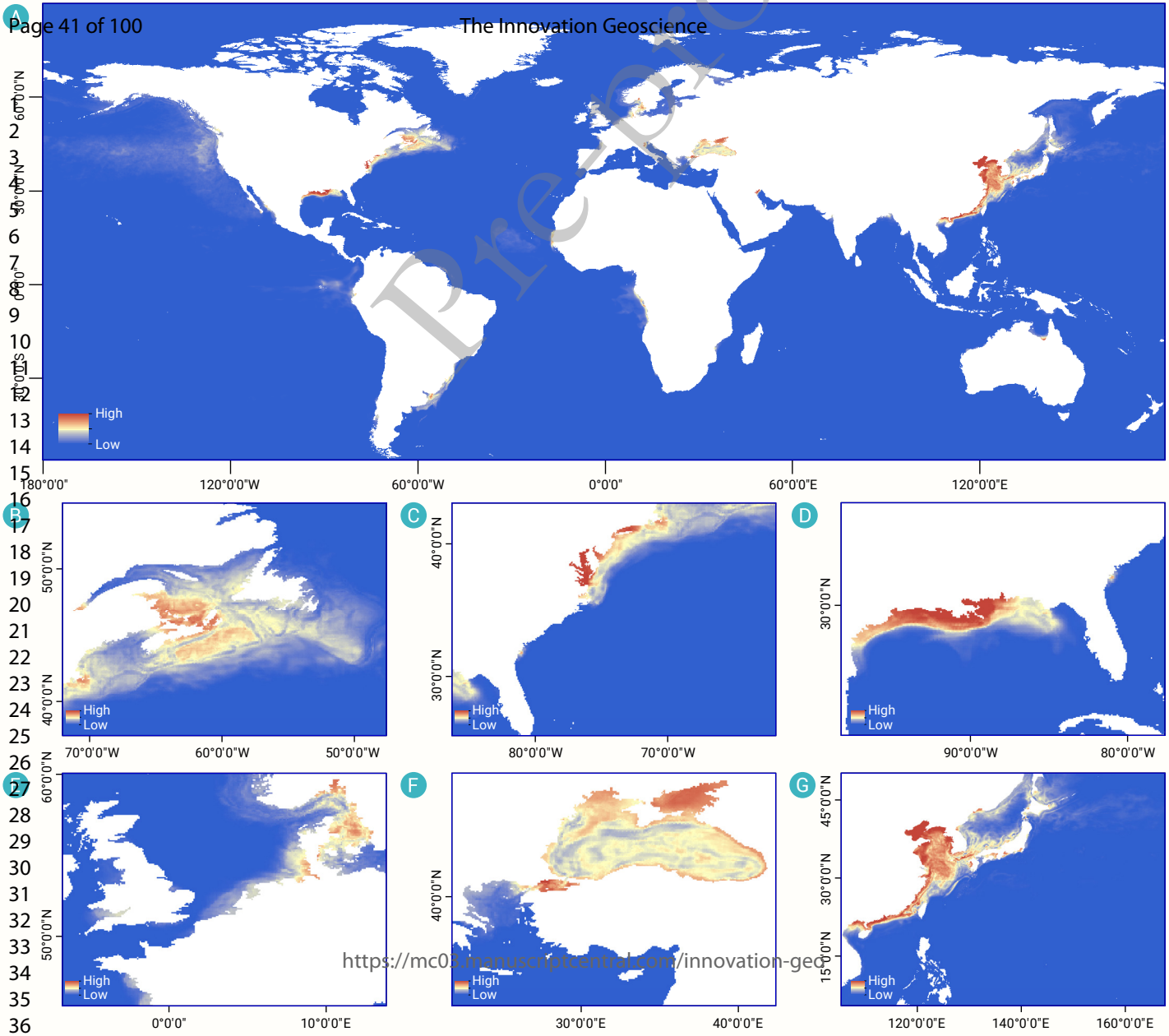

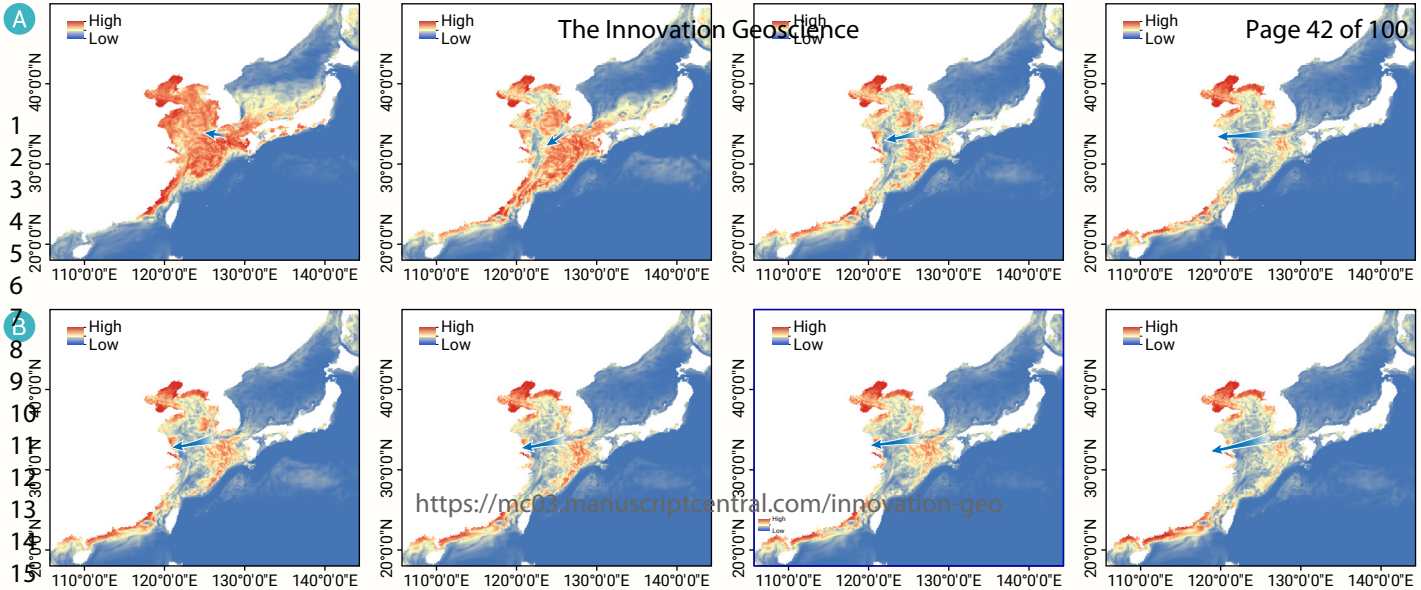

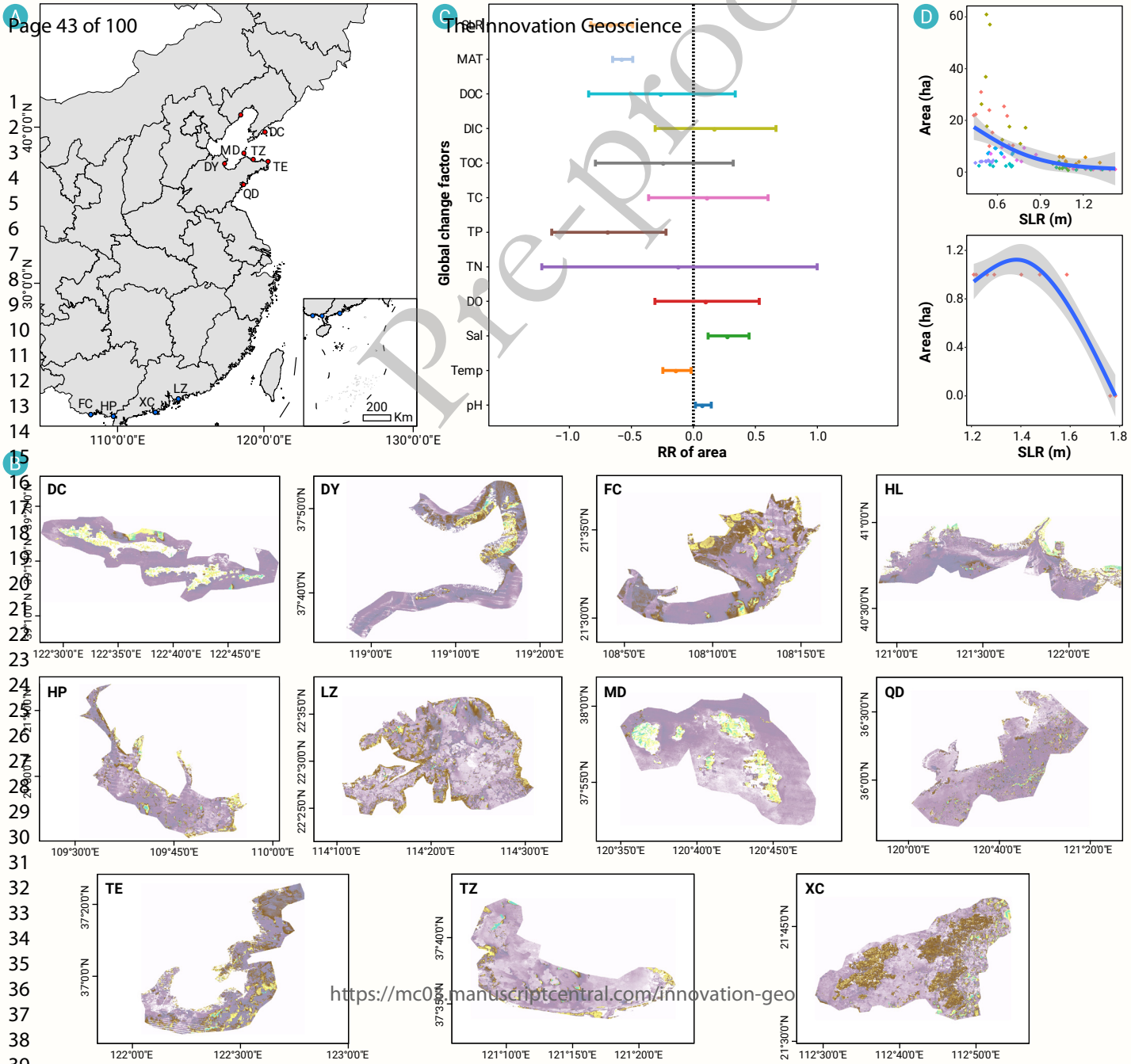

A

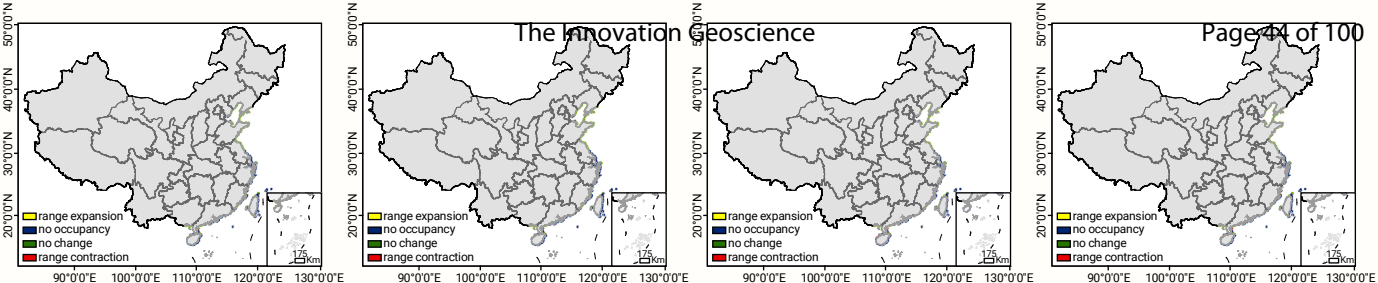

B

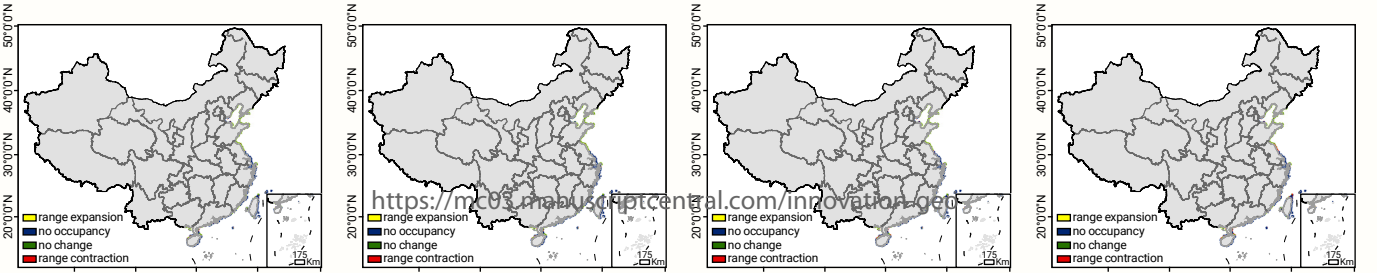

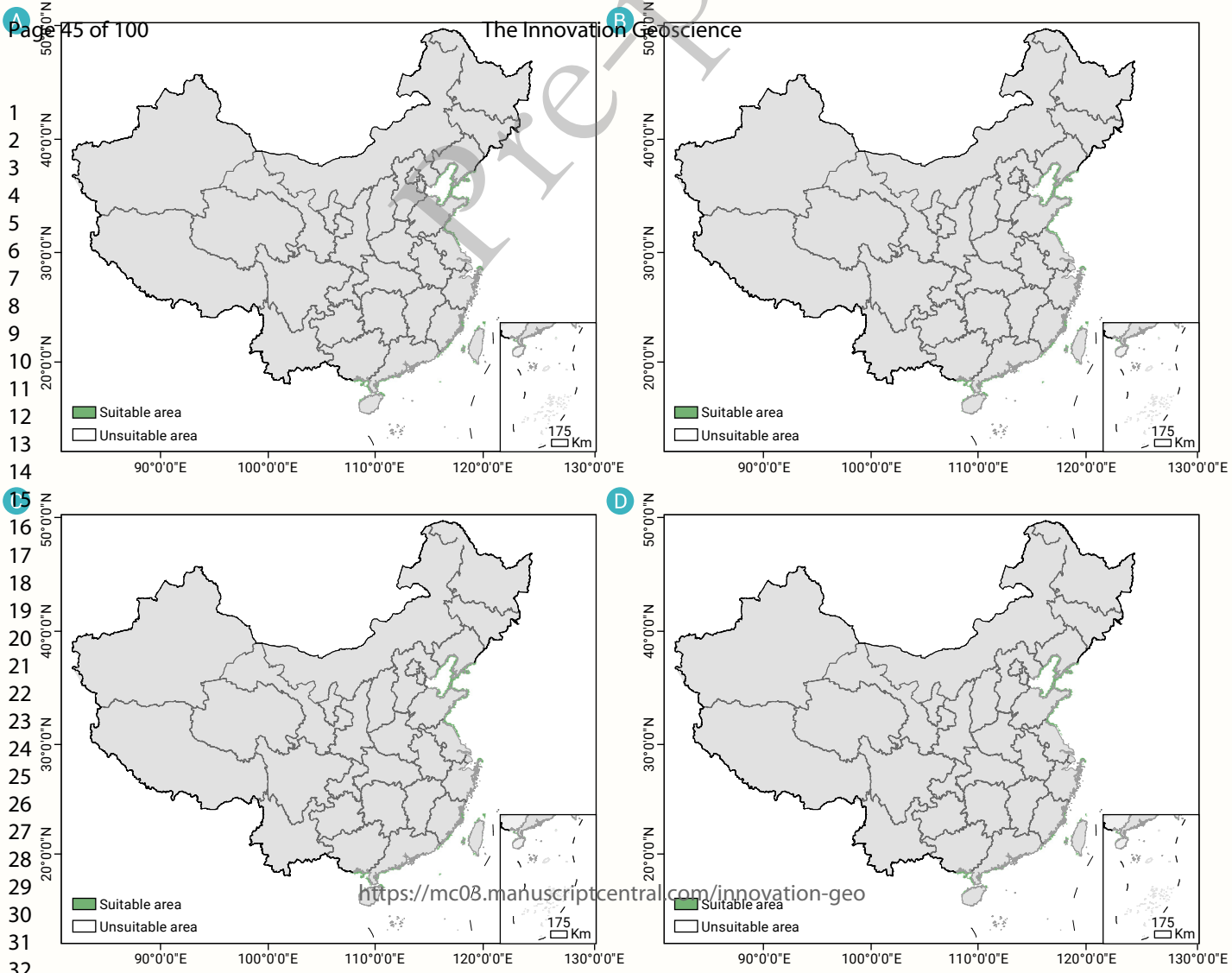

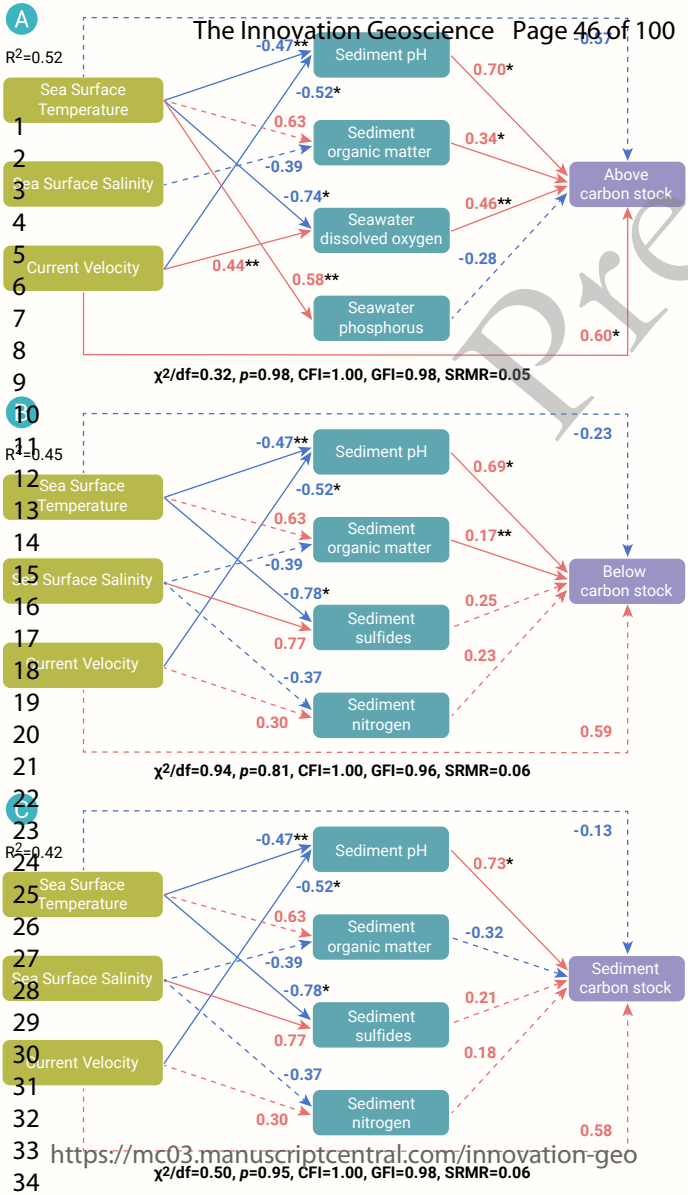

* $P < 0.1$ ** $P < 0.05$

No-significant ($P > 0.05$) Positive effect Negative effect

Data Collection

Seagrass field survey

Soil information

Geographic information

Seawater information

AGC and BGC data

Survey sites map

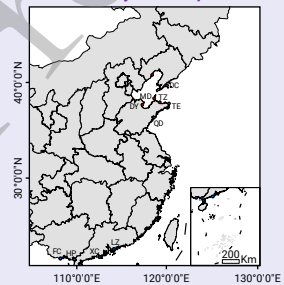

Remote sensing

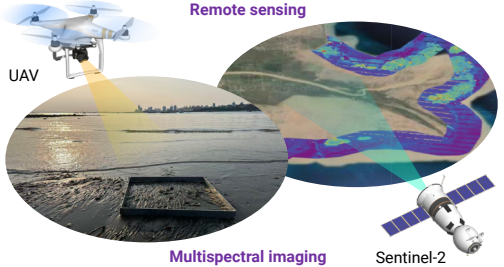

Model building

Vegetation index selection

Spectral index analysis across regions

Remote sensing based distribution mapping

Statistics and SEM

ArcGIS

Spatial mapping

Java

Suitability modelling

Google Earth Engine

Image processing

MaxEnt habitat suitability modelling

Current and future suitable areas

Environmental drivers of habitat suitability

Spatial assessment

Growth zone identification

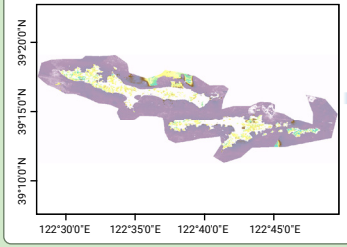

Where to restore

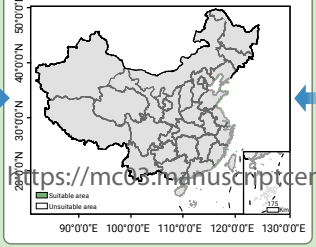

Where to restore

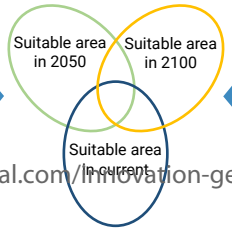

How to restore

Degradation status

Genetic diversity

With what methods to restore

Carbon stock assessment

Plant carbon stock

Sediment carbon stock

Environmental drivers of carbon stocks

Author Response

Manuscript ID: XINNgeoscience-2025-0200.R1
Title: *Seagrass restoration at the right time in the right site with right methods can generate persistent carbon benefits in China*

Dear Prof. Cheng and Editorial Team,

Thank you very much for your careful evaluation of our revised manuscript and for informing us that the peer-review process is approaching completion. We sincerely appreciate the positive assessment from Reviewer 1 and the Editorial Board, as well as the opportunity to further improve the presentation of our work prior to the final decision.

In accordance with the editorial requirements, we have carefully reviewed the manuscript and the Final File Checklist and have further checked the manuscript formatting, figures, tables, supplementary materials, references, and associated submission files. We will actively cooperate with the editors and artists during the figure-improvement process and will make all necessary revisions to ensure that the figures and tables meet the journal's publication and promotional standards.

We have also carefully reviewed the Publication License Agreement and the instructions regarding the Article Processing Charge. The required documents and final manuscript files will be completed and submitted through the ScholarOne system in accordance with the journal's instructions. Any redundant files will be removed before final submission.

Response to Reviewer 1

Comment:
Given that the author has replied and corrected the relevant issues, I have no reason not to accept this paper.

Response:
We sincerely thank the reviewer for carefully evaluating our revised manuscript and for recognizing the revisions that we made in response to the previous comments. The reviewer's constructive suggestions substantially improved the scientific clarity, methodological description, and overall presentation of the manuscript. We greatly appreciate the reviewer's positive recommendation.

Response to the Editorial Board

Comment:
After figure polishment, this paper can be accepted.

Response:
We sincerely thank the Editorial Board for the positive evaluation of our manuscript. We have carefully reviewed the figures and will work closely with the editorial team and artists to further improve their visual quality, consistency, readability, and suitability for publication and promotion. We

will fully incorporate the recommended figure-polishing revisions into the final version of the manuscript.

We are grateful to the Editor-in-Chief, Editorial Board, reviewers, project editor, and journal staff for their time, careful assessment, and valuable guidance throughout the review process. We greatly appreciate the opportunity to publish our work in *The Innovation Geoscience* and will ensure that all final requirements are addressed carefully and promptly.

Sincerely,

Hongzhen Wang
on behalf of all authors

Table S1. Sampling information of *Z. japonica* populations

	Code	Country	Location	Latitude
1	QD	China	Huiquan Bay, Qingdao	36°03'05"N, 120°20'17"E
2	TE	China	Swan Lake, Rongcheng	37°21'01"N, 122°34'46"E
3	DY	China	Yellow River Delta, Donying	37°43'09"N, 119°09'49"E
4	HL	China	Xingcheng, Huludao	40°24'13"N, 120°36'17"E
5	DC	China	Dachangshan Island, Dalian	39°14'01"N, 122°31'15"E
6	MD	China	Miaodao Island, Yantai	37°56′00″N, 120°40′50″E
7	TZ	China	Taozi Bay, Yantai	37°35′02″N, 121°19′47″E
8	Yon	South Korea	Yongbuk, Koje Island, Busan	35°26'58"N, 128°35'45"E
9	Oha	Japan	Ohashi River, Shimane	34°48'04"N, 133°06'45"E
10	Sar	Japan	Saroma Lake, Abashiri, Hokaido	44°04'08"N, 144°11'38"E
11	Not	Japan	Notoro Lake, Abashiri, Hokaido	44°05'59"N, 143°52'12"E
12	Onn	Japan	Onneto Lake, Nemuro, Hokaido	43°15'47"N, 145°29'28"E
13	Kat	Japan	Katsura-jima Island, Miyagi	38°20'08"N, 141°05'14"E
14	Tok	Japan	Tokyo Bay, Tokyo	35°18'46"N, 139°48'49"E
15	Ago	Japan	Ago Bay, Mie	34°18'03"N, 136°50'50"E
16	Birch	America	Birch Bay, WA	48°54'07"N, 122°46'26"W
17	Padi	America	Padilla, WA	48°28'50"N, 122°28'37"W
18	Willa	America	Willapa Bay, WA	46°43'40"N, 123°57'06"W
19	Neta	America	Netarts Bay, OR	45°24'37"N, 123°56'07"W
20	Yaqu	America	Yaquina Bay, OR	44°34'51"N, 123°59'41"W
21	Coos	America	Coos Bay, OR	43°18'53"N, 124°19'09"W
22	Humb	America	Humboldt Bay, CA	40°51'29"N, 124°09'27"W
23	Nan	Japan	Nanao bay, Noto Penisula, Japan	37°12'11"N, 136°54'24"E
24	Yul	South Korea	Yulpo, Koje Island, Busan	34°46'04"N, 128°35'45"E
25	Hir	Japan	Jigozen, Hiroshima bay, Japan	34°20'02"N, 132°19'15"E
26	Lid	Japan	Lida Bay, Noto Penisula, Japan	37°25'59"N, 137°15'30"E
27	Oki	Japan	Okinawa Island, Japan	26°20'51"N, 127°53'07"E
28	WJR	China	Wujiang River, Kinmen Island,	24°25'36"N, 118°18'34"E
29	XSW	China	Xiangshan Wetland, Taiwan Island	24°46'38"N, 120°54'45"E
30	GMW	China	Gaomei Wetland, Taiwan Island	24°18'57"N, 120°32'38"E
31	WDP	China	Wude Port, Penghu Island	23°31'43"N, 119°35'48"E
32	JQ	China	Jiangmei and Qitou, Penghu Island	23°38'57"N, 119°36'16"E
33	LZ	China	Laichiwo, Hongkong	22°03'21"N, 114°16'10"E
34	XC	China	Xiachuan Island, Taishan	21°39'22"N, 112°45'48"E
35	FC	China	Perl Bay, Fangchenggang	21°35'52"N, 108°12'46"E
36	HP	China	Hepu, Beihai	21°28′40″N, 109°42′50″E
37	BGI	China	Beigang Island, Haikou	20°00'54"N, 110°33'45"E

Data	Time
Sea Surface Temperature (SST)	2015-2022
Sea surface salinity (SSS)	2015-2022
Precipitation	2015-2022
Chlorophyll a concentration	2015-2022
SST max/mean/min	2050
SSS max/mean/min	2050
Currents velocity max/mean/min	2050
SST max/mean/min	2100
SSS max/mean/min	2100
Currents velocity max/mean/min	2100
SST	2023-08
SSS	2023-08
Currents velocity	2023-08
Soil pH	2023-08
Seawater dissolved oxygen	2023-08
Soil sulfides	2023-08
Soil organic matter content	2023-08
Seawater phosphorus content	2023-08
Seawater nitrogen content	2023-08

Table S2. Data source

Source	Application
HYCOM: Hybrid Coordinate Ocean Model, Water Temperature and Salinity | Earth Engine Data Catalog | Google for Developers GSMaP Operational: Global Satellite Mapping of Precipitation - V6 | Earth Engine Data Catalog | Google for Developers Ocean Color SMI: Standard Mapped Image MODIS Aqua Data | Earth Engine Data Catalog | Google for Developers	Effects of environmental factors on changes in seagrass meadow area
Bio-ORACLE : Marine data layers for ecological modelling	Effects of environmental factors on changes in spatial distribution
HYCOM: Hybrid Coordinate Ocean Model, Water Temperature and Salinity | Earth Engine Data Catalog | Google for Developers HYCOM: Hybrid Coordinate Ocean Model, Water Velocity | Earth Engine Data Catalog | Google for Developers self-measurement self-measurement self-measurement self-measurement self-measurement self-measurement	Effects of environmental factors on changes in seagrass carbon stock

Table S3. Degree to which each environmental variable contributes to the MAXENT model

Variable	Percent contribution	Permutation importance
mean SST	38.8	7.3
min SSS	15.1	7.3
mean surface current velocity	12.7	32.7
mean SSS	12.4	16.3
max SST	9.2	1.4
min SST	5	5.7
min surface current velocity	3	6.3
max SSS	2.3	16.3
max surface current velocity	1.5	6.6

Table S4. Distribution Changes of *Z. japonic*

name	2050 RCP26	2050 RCP45	2050 RCP60	2050 RCP85
range expansion	438.9445183	987.6251661	1316.833555	768.152907
no occupancy (absence in both)	131683.3555	131134.6748	130805.4664	131354.1471
no change (presence in both)	105017.476	103590.9063	103151.9618	102383.8089
range contraction	4718.653572	6145.223256	6584.167774	7352.320681

a changes

2100 RCP26	2100 RCP45	2100 RCP60	2100 RCP 85
438.9445183	1207.097425	877.8890366	219.4722591
131683.3555	130915.2026	131244.411	131902.8277
104139.587	104578.5315	100518.2947	92178.34884
5596.542608	5157.59809	9217.834884	17557.78073

Region	Degree of reduction in area	π	Pi	He
FC	Low	0.21015	70.07212	0.19565
HP	High	0.19759	65.66114	0.18411
XC	High	0.20299	66.99615	0.18771
LZ	High	0.19934	64.81833	0.18547
QD	High	0.05341	17.6047	0.04946
DY	High	0.09467	31.92494	0.08867
TE	Low	0.09204	32.21143	0.08636
TZ	Low	0.08276	23.81164	0.07587
MD	Low	0.09296	30.20932	0.08724
HL	Low	0.08296	23.7141	0.07759
DC	Low	0.09557	31.82898	0.08856

Table S5

Ho	Fis
0.26022	-0.11807
0.25026	-0.1212
0.253	-0.1151
0.25439	-0.12539
0.06599	-0.02734
0.11859	-0.05315
0.11756	-0.05638
0.11279	-0.06024
0.12336	-0.06572
0.12265	-0.08032
0.11922	-0.05183

5. Recommended Restoration Methods for Specific Areas

Recommended methods
Natural recovery combined with habitat protection
Plant transplantation-based restoration
Natural recovery combined with habitat protection
Plant transplantation-based restoration
Seed-based restoration
Combined seed-and-shoot restoration
Seed-based restoration
Combined seed-and-shoot restoration
Seed-based restoration
Combined seed-and-shoot restoration
Combined seed-and-shoot restoration

Recommended reasons
FC retains the highest genetic diversity among all surveyed populations, while its area reduction is moderate. Priority should therefore be given to protecting remnant patches, controlling local stressors, maintaining
Despite an area loss of more than 80%, HP retains high genetic diversity. Local, genetically diverse and environmentally compatible shoots can therefore be used to rapidly rebuild meadow structure, provided that the
XC retains high genetic diversity and has shown slight recent area recovery. Protection of existing patches, maintenance of habitat connectivity, and reduction of human disturbance should precede any active
LZ has experienced substantial area decline but still retains high genetic diversity. Local shoots collected from multiple remnant patches can be used to rebuild meadow structure while preserving locally adapted genetic
QD shows the lowest genetic diversity among the surveyed populations, although its area decline is moderate. Multi-parent seed supplementation is recommended to increase genetic variation and sexual recruitment
DY has experienced the greatest proportional area loss and also exhibits relatively low genetic diversity. Shoots are needed to rapidly reconstruct meadow structure, while seeds from multiple genetically compatible
The meadow area in TE has remained generally stable, but genetic diversity is relatively low. Small-scale, multi-parent seed supplementation should be used to improve genetic variation while conserving the existing
TZ has experienced substantial and continuing area decline together with low genetic diversity. Shoot transplantation alone could reproduce the existing genetic bottleneck; therefore, structural transplantation
MD has experienced relatively limited total decline and has recently shown clear area recovery, but its genetic diversity remains low. Seed supplementation around meadow margins and between fragmented patches is
HL has lost approximately 80% of its historical meadow area and retains relatively low genetic diversity. Shoots should be used to establish stable patches, while repeated multi-parent seed addition should increase genetic
DC has lost approximately half of its historical area and exhibits relatively low genetic diversity, although recent recovery has occurred. Small-scale combined restoration trials should be conducted first, using compatible

Table S6. Distribution of *Z. japonica* carbon stocks among

Region	AGC	BGC	BGC soil part	TC
HL	1	0.41	122	123.41
DC	2.2	0.73	143	145.93
MD	1.7	0.68	137	139.38
TZ	0.7	0.47	130	131.17
DY	0.6	0.16	90	90.76
TE	0.92	0.25	110	111.17
QD	1.1	0.2	60	61.3
LZ	1.4	0.19	92	93.59
XC	1.3	0.58	104	105.88
FC	1.6	0.41	100	102.01
HP	0.6	0.21	50	50.81

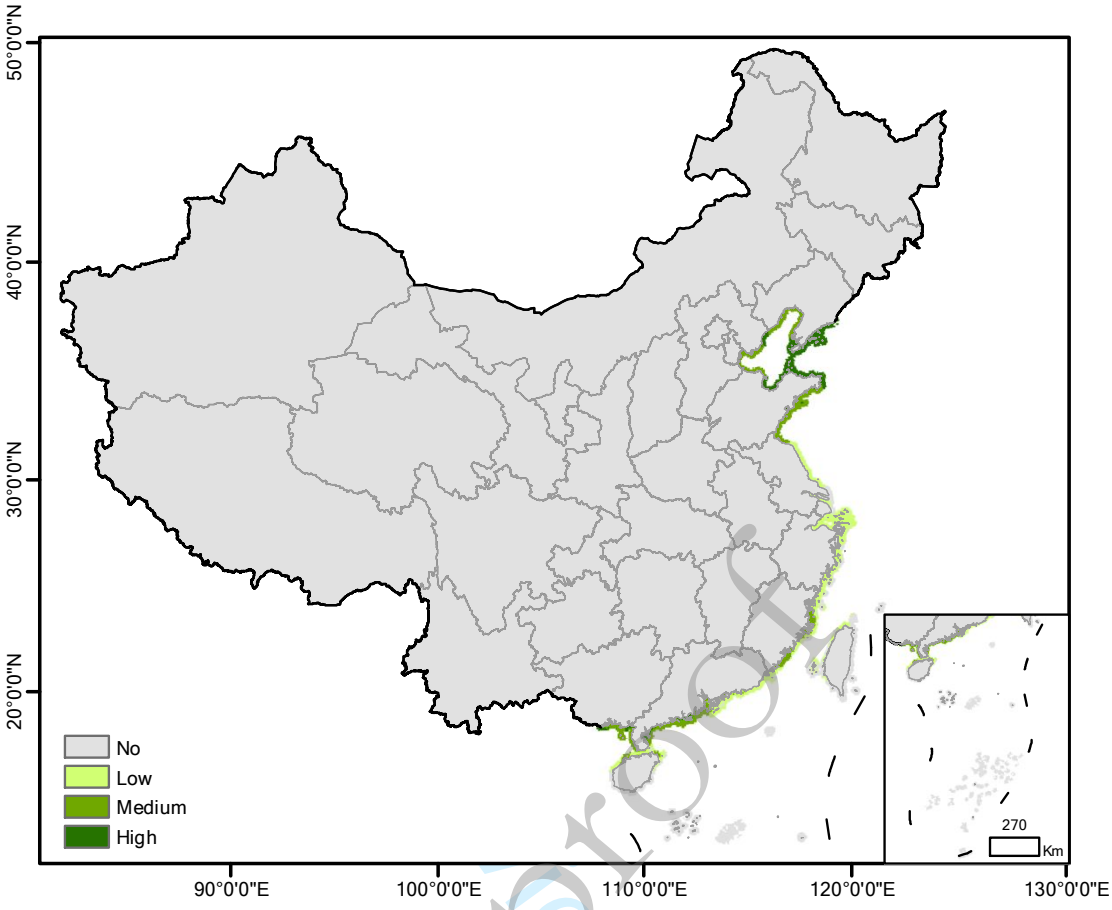

Figure S1. The current potential distribution and suitable/unsuitable habitat of *Z. japonica*

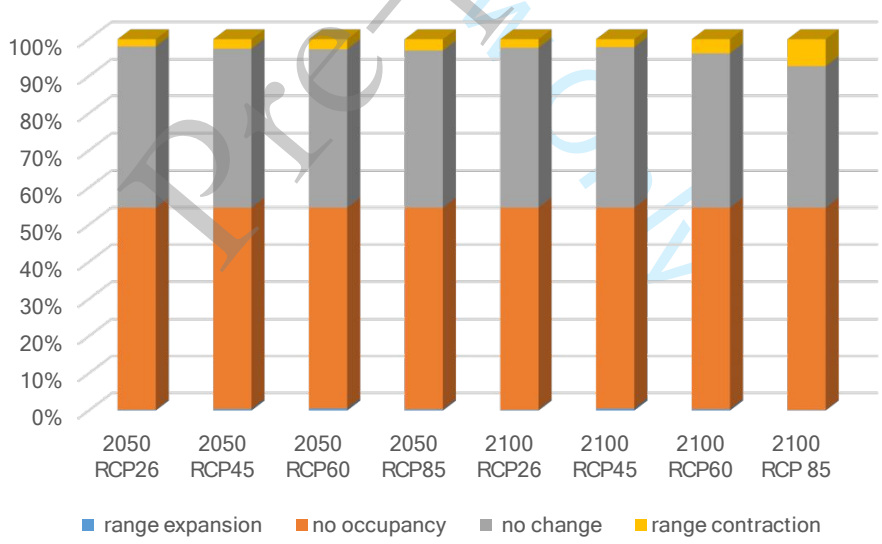

Figure S2. The current potential distribution and suitable/unsuitable habitat of *Z. japonica*

Seagrass restoration at the right time in the right site with right methods can generate persistent carbon benefits in China

Hongzhen Wang,[1] Xinqi Li,[1] Yu Zang,[2] Jiayi Xin,[1] Song Xue,[2] Lei Liu,[1] Xuexi Tang,[1,*] Jun Chen[1,*]

[*]Correspondence: tangxx@ouc.edu.cn(X.T.); chenjun@ouc.edu.cn (J.C.)

GRAPHICAL ABSTRACT

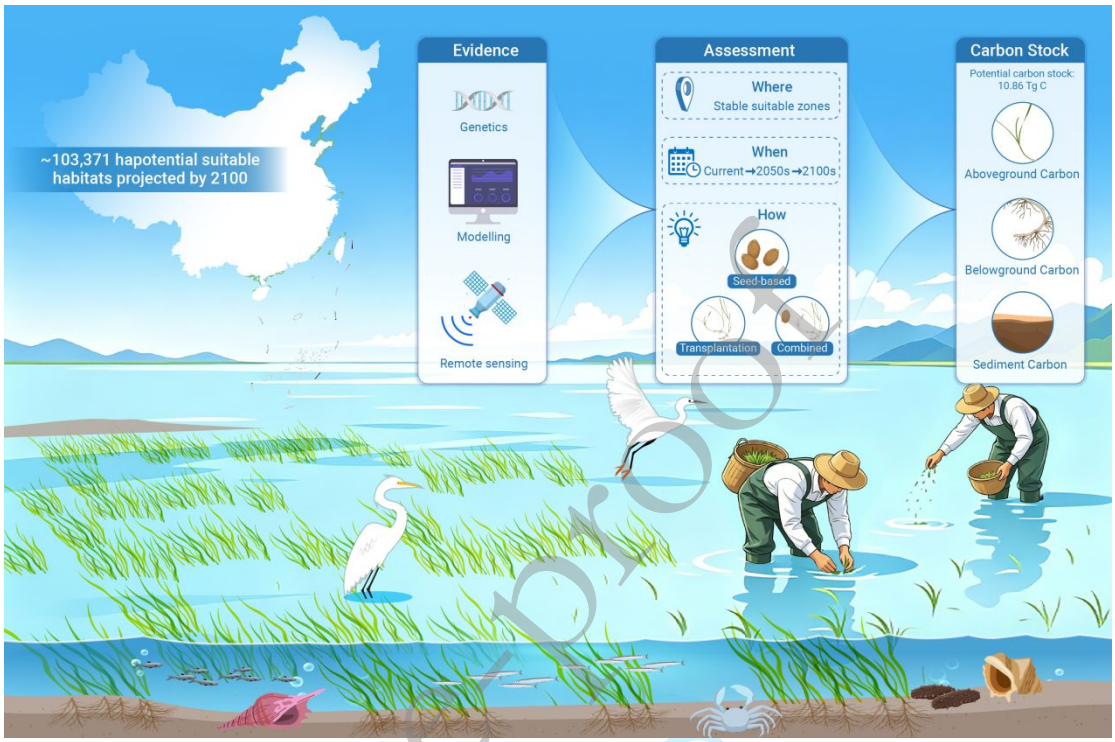

PUBLIC SUMMARY

- *Zostera japonica* beds have declined, and suitable habitats may contract under future climate change.
- Remote sensing and habitat modelling identify vulnerable areas and guide restoration planning.
- Site-specific strategies based on habitat, decline, and genetics improve restoration decisions.
- Linking restoration priorities with blue carbon assessment supports coastal conservation and management.

Key Words

strategic restoration/carbon stock survey/driving factors/spatial distribution patterns

Seagrass restoration at the right time in the right site with right methods can generate persistent carbon benefits in China

Hongzhen Wang,[1] Xinqi Li,[1] Yu Zang,[2] Jiayi Xin,[1] Song Xue,[2] Lei Liu,[1] Xuexi Tang,[1,*] Jun Chen[1,*]

1.MoE Key Laboratory of Evolution & Marine Biodiversity, College of Marine Life Sciences, Ocean University of China, Qingdao 266003, China.

2.Key Laboratory of Marine Eco-Environmental Science and Technology, First Institute of Oceanography, Ministry of Natural Resources, Qingdao 266061, China.

[*]Correspondence: tangxx@ouc.edu.cn(X.T.); chenjun@ouc.edu.cn (J.C.)

ABSTRACT

Zostera japonica beds have declined substantially along the coast of China, highlighting the need for targeted and effective restoration planning. This study develops a restoration roadmap that supports China's carbon neutrality goals by addressing three key questions: where restoration should occur, when it should be implemented, and which methods should be used. Field surveys, satellite remote sensing, genetic data, and species distribution modelling were integrated to identify restoration opportunities under current and future climate conditions. The results indicate that northern China, particularly the Bohai Sea region, contains the largest extent of suitable and persistent habitat, whereas several southern populations have experienced substantial bed degradation. A rule-based restoration decision framework combined seagrass bed decline and genetic diversity to recommend region-specific restoration strategies across the species range. The phased framework prioritizes areas suitable under current and 2050s conditions, particularly those projected to remain suitable by the 2100s, while treating areas becoming suitable mainly by the 2100s as long-term adaptive reserves. By the 2100s, approximately 103,371 ha of potential suitable habitat is projected, corresponding to an estimated potential carbon stock of 10.86 Tg C. These findings provide a spatially explicit framework for improving *Z. japonica* restoration planning and evaluating its potential long-term carbon benefits in China.

INTRODUCTION

Climate change poses substantial socioeconomic challenges for China, which has committed to advancing global climate change mitigation.[1] The principal driver of contemporary climate change is the accumulation of greenhouse gases (GHGs), largely resulting from the combustion of fossil fuels such as coal and oil.[2] Understanding the sources, sinks, and fate of GHGs is therefore essential for developing effective climate policies and mitigation measures. Quantifying global GHG budgets, particularly the carbon budget, has consequently become central to climate mitigation and sustainable ecosystem management.[3,4] Identifying and quantifying under-recognized carbon sinks has therefore emerged as a major challenge in global change research.

In China's national climate mitigation strategy, expanding forest area and enhancing terrestrial carbon sinks have been identified as important measures.[5-8] However, compared with many terrestrial ecosystems, some coastal blue carbon ecosystems can exhibit high carbon burial rates per unit area and retain carbon in sediments over long timescales.[9,10] Although ocean carbon research has traditionally emphasized pelagic carbon cycling, including plankton-mediated carbon uptake,[11] increasing attention has shifted toward vegetated coastal ecosystems, in which benthic macrophytes such as seagrass play a disproportionately important role.[12,13] Vegetated coastal ecosystems, including seagrass beds, occupy less than 0.2% of the global ocean surface but contribute substantially to organic carbon burial in marine sediments.[14,15] Globally, seagrass beds are estimated to sequester 48-112 $Tg \cdot C \cdot yr^{-1}$ and store several to tens of petagrams of carbon in their biomass and sediments.[14-16] In China, seagrass beds cover approximately 14,000-20,000 ha and contain an estimated 8.1-12.0 $Tg \cdot C$, with an annual sequestration capacity of 0.12-0.18 $Tg \cdot C \cdot yr^{-1}$.[17-19] Together, these estimates highlight the under-recognized contribution of China's seagrass beds to coastal blue carbon storage and their potential relevance to carbon neutrality strategies.

However, seagrass ecosystems are declining rapidly because of climate change and human activities. Since 1880, at least 5,602 km^2 of documented seagrass meadow area has been lost globally.[20] Many assessments have focused primarily on documenting changes in bed area, whereas the environmental drivers of decline and the spatial priorities for restoration remain insufficiently resolved.[15,20] As seagrass ecosystems receive increasing attention within the global conservation agenda, it is essential to determine where and why these beds are declining and how their degradation can be reversed.

Substantial progress has been made in seagrass conservation and restoration in recent years.[21,22]

Nevertheless, restoration remains constrained by fragmented management, site-specific habitat degradation, limited species-specific guidance, and insufficient integration of ecological suitability with potential carbon benefits. The United Nations designated 1 March as World Seagrass Day to raise awareness of the ecological importance of seagrass ecosystems. China has also implemented numerous initiatives involving seagrass protection, restoration, and seed-based bed expansion.[17,18,23,24] Despite these efforts, several fundamental questions remain unresolved, including where seagrass restoration should be prioritized, which restoration methods are most appropriate, and when restoration should be implemented.

As a native intertidal species of the northwest Pacific coast, *Z. japonica* forms meadows that are the most widely distributed of all seagrass ecosystems in China.[25,26] However, this species has experienced substantial population declines under the combined pressures of chronic human disturbance and intensifying climatic extremes.[26-28] These pressures have caused widespread degradation of *Z. japonica* beds and raised concern about the long-term persistence of the species in its native habitats.[25,29,30] Consequently, changes in its distribution and condition can strongly influence the overall status and carbon storage capacity of China's seagrass resources. Previous studies have shown that *Z. japonica* beds contribute substantially to regional blue carbon stocks and help maintain carbon storage in shallow coastal ecosystems.[15,18] Given its ecological importance and extensive distribution, improving the conservation and restoration of *Z. japonica* is important for strengthening coastal ecosystem resilience and supporting China's marine carbon management goals.[17,18,31]

Here, we developed an illustrative restoration roadmap for *Z. japonica* in China by addressing three key questions: where to restore, how to restore, and when to restore. To determine where restoration should be prioritized, we used satellite remote sensing to quantify recent spatial changes in *Z. japonica* beds and combined species distribution modelling with habitat assessments under sea-level-rise scenarios to identify current and future potentially suitable areas. To determine how restoration should be implemented, we integrated bed decline, genetic diversity, and restoration practice into a rule-based decision framework for selecting among seed-based restoration, shoot transplantation, combined restoration, and protection or natural recovery. To determine when restoration should be prioritized, we compared current suitable areas with projected suitable areas under climate scenarios for the 2050s and 2100s and developed a phased restoration strategy. Finally, we combined projected suitable areas with field-based carbon stock estimates to evaluate the potential carbon stock associated with future

restoration opportunities. This framework provides a spatially explicit and method-oriented basis for *Z. japonica* restoration planning and coastal blue carbon management in China.

MATERIALS AND METHODS

Study area

The study area was defined by integrating multisource occurrence records of *Z. japonica* to provide a basis for spatial analysis. Occurrence records from peer-reviewed field studies were prioritized, and additional distribution points were obtained from GBIF (https://www.gbif.org) and OBIS (https://obis.org). All records were processed following standardized procedures for species distribution data that are widely applied in seagrass and coastal vegetation studies.[32] The procedure included removing duplicate coordinates, excluding records with spatial uncertainty greater than 1 km, evaluating the ecological plausibility of each record using published habitat descriptions, and verifying its geographic location using high-resolution satellite imagery. After applying these criteria, 37 reliable occurrence points were retained, 17 of which were located in Chinese coastal waters (Table S1). This workflow is consistent with established approaches in seagrass mapping and blue carbon research.[13]

To delineate the spatial extent of the regional analyses, we combined historical occurrence records, ecological literature describing the habitat requirements of *Z. japonica*, and multiyear satellite imagery spanning 2014 to 2022. Field surveys conducted in 2023 covered the major seagrass regions of the Bohai Sea, Yellow Sea, and northern South China Sea, representing the principal latitudinal distribution of *Z. japonica* within China. The species primarily occupies shallow littoral waters, generally less than 6 m deep and typically within 10 km of the coastline. To ensure that peripheral and potentially suitable coastal habitats were not excluded, a 20 km buffer was established along the Chinese coastline. This approach is consistent with commonly used practices in coastal habitat modelling and marine vegetation mapping. In addition to defining the operational extent of the regional analyses, we generated a global habitat suitability map using all 37 occurrence records to examine the broader spatial pattern of environmentally suitable areas under current conditions (Figure 1). We further analysed the centroid and directional shifts of suitable habitat within the northwestern Pacific region under current and future climate conditions (Figure 2). By contrast, all quantitative analyses conducted for Chinese coastal waters, including remote sensing extraction, habitat suitability assessment, and environmental factor analysis, were restricted to the defined 20 km coastal buffer. This distinction clarifies the relationship between the broad-scale suitability maps and the regional

analytical extent and avoids misinterpretation of model boundaries.[33]

All spatial analyses were performed in ArcGIS 10.4. These analyses included constructing the coastal buffer, extracting environmental variables, and generating spatial predictor layers for species distribution modelling. Climate-based projections were developed using environmental layers corresponding to the selected future climate scenarios. The integration of species occurrence records with environmental and climate variables followed the core methodological principles of species distribution modelling described in foundational studies.[34,35] To minimize multicollinearity among predictor variables, we adopted recommended procedures for ecological modelling.[36]

Construct *Z. japonica* index (*ZJI*)

The *Z. japonica* index (*ZJI*) was constructed by integrating field observations, historical records, and multitemporal remote sensing data in ArcGIS and Google Earth Engine. The methodological framework was adapted from the time-series spectral and phenological index developed for long-term monitoring of *Z. japonica* in the Yellow River Delta.[18]

First, identification of the potential distribution area. Time-series Landsat imagery, including Landsat 5 Thematic Mapper, Landsat 7 Enhanced Thematic Mapper Plus, and Landsat 8 Operational Land Imager surface reflectance products, was used to delineate the potential distribution area. The surface reflectance products were generated through atmospheric correction using the Landsat Ecosystem Disturbance Adaptive Processing System for Landsat 5 and 7 and the Landsat Surface Reflectance Code for Landsat 8. Poor-quality pixels affected by clouds, cirrus, cloud shadows, or snow were removed using the corresponding quality-assurance bands. This preprocessing workflow was consistent with established remote sensing methods for coastal wetland mapping.[18,37]

Second, calculation of spectral and phenological indices. For each valid pixel, three spectral indices were calculated following established definitions. The normalized difference vegetation index was calculated as:

$$NDVI = \frac{NIR - R}{NIR + R}$$

where NIR and R represent near-infrared and red reflectance, respectively.[38]

The modified normalized difference water index was computed as:

$$mNDWI = \frac{G - SWIR1}{G + SWIR1}$$

where G is green band reflectance and SWIR1 is shortwave infrared reflectance.[39]

The tasseled cap brightness index was calculated using sensor-specific Landsat transformation coefficients:[40]

$$TCBI = a_1 B + a_2 G + a_3 R + a_4 NIR + a_5 SWIR1 + a_6 SWIR2$$

where B, G, R, NIR, $SWIR1$, and $SWIR2$ represent blue, green, red, near-infrared, shortwave-infrared 1, and shortwave-infrared 2 reflectance, respectively,and a_1–a_6 are the corresponding sensor-specific coefficients.

The phenological characteristics of *Z. japonica* were represented using the maximum NDVI during the growing period and the mean NDVI during the senescence period. Based on long-term observations of *Z. japonica*, the growing period was defined as day of year 150–250 and the senescence period as day of year 260–330. For each analysis period, the maximum NDVI composite was generated, and the corresponding mNDWI and TCBI values were extracted from the date on which NDVI reached its maximum. Mean NDVI during the senescence period was also calculated for each pixel.

Third, construction of *ZJI*. The *Z. japonica* index was formulated by integrating spectral and phenological features that distinguish *Z. japonica* from other intertidal vegetation types such as *Spartina alterniflora*, *Suaeda salsa* and tidal flats. The index was defined as:

$$ZJI = \begin{cases} NoData & (mNDWI_{VImax} \le 0) \\ \frac{2NDVI_{max} - SeNDVI_{mean}}{TCBI_{VImax}} & (mNDWI_{VImax} > 0) \end{cases}$$

where $NDVI_{max}$ is the maximum NDVI during the growing period, $SeNDVI_{mean}$ is the mean NDVI during the senescence period, and $mNDWI_{VImax}$ and $TCBI_{VImax}$ are the mNDWI and TCBI values corresponding to the date of maximum NDVI. Pixels with $mNDWI_{VImax} \le 0$ were assigned NoData because this condition was used to exclude higher intertidal vegetation, particularly *S. alterniflora*, and other non-target cover types. These pixels were masked in subsequent classification.

Fourth, separability analysis. To evaluate the discriminatory ability of the individual spectral variables and *ZJI*, a separability index was calculated. The index incorporates both interclass differences and intraclass variability and was calculated as:[41]

$$SI_{zo} = \frac{|\mu_z - \mu_o|}{1.96 \times (\sigma_z + \sigma_o)}$$

where μ_z and μ_o denote the mean index values of *Z. japonica* and the other class and σ_z and σ_o denote the corresponding standard deviations.

Fifth, automated extraction using multilevel Otsu segmentation. For each analysis period, the *ZJI* image within the potential distribution area was classified using a multilevel Otsu thresholding algorithm implemented in Google Earth Engine. The algorithm divided the *ZJI* histogram into three classes by identifying two thresholds that maximized the between-class variance. The class with *ZJI* values greater than the upper threshold was classified as *Z. japonica*, whereas the remaining classes were classified as non-*Z. japonica*. Thresholds were determined independently for each analysis period to account for temporal and regional variation in spectral conditions.

Finally, accuracy assessment and validation. Stratified random validation samples were interpreted using field observations and contemporaneous or near-contemporaneous high-resolution Gaofen, WorldView, and SPOT imagery. Classification performance was evaluated using confusion matrices, from which producer's accuracy, user's accuracy, overall accuracy, and the kappa coefficient were calculated. As an additional external comparison, *ZJI*-derived maps were overlaid with publicly available seagrass distribution records from the CEARAC Web-GIS platform. Because CEARAC coverage is incomplete for the Chinese coast and is not consistently species specific, these records were used only to examine spatial correspondence in areas with confirmed seagrass occurrence and were not treated as a comprehensive species-level accuracy dataset.

Species distribution models

To predict the current and future habitat suitability of *Z. japonica*, we constructed species distribution models using MaxEnt. Model calibration and optimization were performed with the ENMeval package,[42] following established procedures for presence-only ecological niche modelling.[34,35] Two key parameters were tuned: the regularization multiplier and feature class. The regularization multiplier ranged from 0.5 to 5.0 at intervals of 0.5, resulting in ten candidate values. MaxEnt supports five feature types, including linear, quadratic, hinge, product, and threshold features. Eight feature-class combinations were evaluated: L, LQ, H, LQH, LQHP, LQHPT, HPT, and QPT. These settings generated 80 candidate parameter combinations, which were evaluated using the small-sample corrected Akaike information criterion implemented in

ENMeval. Additional metrics, including the omission rate at the 10% training-presence threshold and the difference between training and test AUC, were used to assess model complexity and potential overfitting.

After model selection, the optimal configuration consisted of a regularization multiplier of 3.5 and the LQHPT feature class. The maximum number of background points and model iterations were both set to 10,000. Model performance was evaluated using the area under the receiver operating characteristic curve, which is widely used for presence-only species distribution models.[34] AUC values range from 0 to 1, with values below 0.7 indicating low discriminatory ability, values between 0.7 and 0.9 indicating moderate discriminatory ability, and values above 0.9 indicating high discriminatory ability.

The final MaxEnt simulations produced continuous maps of relative habitat suitability for *Z. japonica*. The outputs were imported into ArcGIS for post-processing, and the mean suitability values from ten replicate runs were converted to raster format. Suitability values were classified into four categories: unsuitable, < 0.20; low suitability, 0.20 to < 0.50; moderate suitability, 0.50 to < 0.75; and high suitability, ≥ 0.75.

The Java-based MaxEnt software was used for all habitat suitability modelling, and 10,000 background points were sampled to represent the available environmental space. Predicted habitat suitability maps were converted into binary suitable and unsuitable grids using SDMtoolbox implemented in ArcGIS and the selected threshold-based conversion procedure.[43] Habitat dynamics under future scenarios were quantified by comparing current and future binary maps to identify areas of expansion, stability, contraction, and persistent unsuitability. Spatial pattern analysis was conducted using the centroid-shift tool in SDMtoolbox to estimate the geographic centers of suitable habitat and assess the direction and relative magnitude of projected shifts under future climate conditions. For the centroid analysis, only suitable raster cells within the northwestern Pacific region were included.

Sea level rise assessment of *Z. japonica*

Sea level rise data for regions containing *Z. japonica* populations were obtained from the Copernicus Marine Service. To evaluate the relationship between sea level change and long-term variation in seagrass bed area, we applied a generalized additive model, which is widely used to characterize nonlinear ecological responses to environmental gradients.[44,45]

A GAM was implemented to capture nonlinear relationships between sea level change and seagrass area dynamics:

$$Area_i = \beta_0 + f(SLR_i) + \varepsilon_i$$

where $Area_i$ represents the annual change in seagrass area at site i and SLR_i denotes the corresponding sea level anomaly. The smoothing function f was fitted using the mgcv package in R, which provides robust and flexible spline based estimation for ecological GAMs.[46]

The basis dimension k was set to three to avoid overfitting while capturing potential nonlinear patterns in the relationship between sea level rise and seagrass area change[44]. Model diagnostics included residual inspection, concurvity checks and evaluation of effective degrees of freedom following established GAM best practices.[45]

This modelling framework enabled the detection of nonlinear responses and potential thresholds in the sensitivity of *Z. japonica* to progressive sea level rise, complementing remote sensing derived seagrass dynamics documented in previous coastal vegetation studies.[47]

Projected habitat change based on MaxEnt and sea level rise

To evaluate future habitat changes of *Z. japonica* under sea level rise, we considered four representative climate scenarios for 2050 and 2100. Projected sea level increases were set to 0.3 and 0.6 m under RCP2.6, 0.4 and 0.8 m under RCP4.5, 0.5 and 1.0 m under RCP6.0, and 0.7 and 1.5 m under RCP8.5, respectively, with the 1.5 m projection representing an upper-range scenario consistent with recent assessments of accelerated sea level rise.[48,49] For each scenario, we estimated the extent of coastal areas subject to inundation and identified portions of the current intertidal zone that would shift to depths considered unsuitable for *Z. japonica*.

To delineate future water-depth conditions, elevation and bathymetric data were obtained from the General Bathymetric Chart of the Oceans GEBCO_2023 global grid (https://www.gebco.net), which has been widely used in regional and global assessments of coastal inundation and habitat exposure.[50,51] The GEBCO grid was resampled to a 1 m computational grid for spatial overlay and scenario analysis. Projected sea level increments were then added to the baseline elevation and bathymetric surface to generate scenario-specific layers representing future relative water-depth distributions along the Chinese coast. The effective spatial information of these layers remained constrained by the native resolution of

the GEBCO dataset.

The depth threshold for unsuitable seagrass habitat was determined by combining the generalized additive model results with published information on seagrass depth limits. A relative water depth of 1.5 m was selected as the critical threshold because *Z. japonica* bed area declined markedly near this level in the time-series analysis and because comparable shallow depth constraints have been reported for seagrasses in light-limited coastal environments.[52-54] Under each sea level rise scenario, grid cells with projected relative water depths shallower than 1.5 m were classified as potentially suitable in terms of depth, whereas cells exceeding this threshold were classified as unsuitable.

Binary habitat suitability maps derived from MaxEnt were then intersected with the depth-based suitability masks to quantify projected habitat dynamics under each scenario. Areas that remained suitable were classified as stable habitat, areas that shifted from unsuitable to suitable were classified as expansion zones, areas that shifted from suitable to unsuitable were classified as contraction zones, and areas that remained unsuitable were classified as persistently unsuitable. This combined approach linked climate-based habitat suitability projections with sea level rise exposure and was used to identify coastal regions where *Z. japonica* habitat may be vulnerable to future inundation.

Investigation and Assessment of Carbon Stock

The distribution of *Z. japonica* along the Chinese coast was divided into 11 principal regions. A total of 33 stations were established for sediment sampling, and 110 field plots were surveyed for seagrass biomass and environmental variables (Table S2 & Figure 3). Field surveys and sediment sampling were conducted in August 2023. A 10 m × 10 m survey area was established at each field plot, within which vegetation and environmental variables were assessed. During biomass sampling, all seagrass plants within the designated sampling quadrat were collected, rinsed carefully to remove sediment from the roots, and placed in labelled sample bags. Seagrass plants were separated into aboveground tissues, including leaves and leaf sheaths, and belowground tissues, including rhizomes and roots. Epiphytes were scraped from the leaf surfaces. Aboveground and belowground biomass samples were placed in separate labelled bags, and epiphytes were transferred to preweighed centrifuge tubes.

A handheld sediment corer (SD-1, Australia) was used to collect one sediment core to a

maximum depth of 1 m at each sediment-sampling station. Each core was sectioned and bagged in the field. Sediment from 0 to 50 cm was divided into five 10 cm intervals, whereas sediment from 50 to 100 cm was treated as a single interval, resulting in six depth intervals per core. When the full depth of 1 m could not be reached, the actual sampling depth was recorded. All plant and sediment samples were stored at −20°C and transported to the laboratory for analysis. Seagrass biomass samples were freeze-dried to constant mass, and their dry masses were recorded. The dried samples were ground, passed through a 100-mesh sieve, sealed in sample bags, and stored in a desiccator until analysis. Sediment samples were oven-dried at 60°C to constant mass. The dried sediments were homogenized using a ceramic mortar, passed through a 100-mesh sieve, sealed in sample bags, and stored in a desiccator until analysis. Organic carbon concentrations in seagrass tissues and epiphytes were measured using the nondispersive infrared absorption method, whereas sediment organic carbon concentrations were determined using the potassium dichromate oxidation method.

The total carbon stock of each seagrass bed consisted of plant carbon stock, including aboveground, belowground, and epiphytic carbon, and sediment carbon stock. Plant carbon stock was calculated as follows:

$$V_{\mathrm{Cstock}} = V_{\mathrm{Ca}} + V_{\mathrm{Cb}} + V_{\mathrm{Ce}}$$

where V_{Cstock} is the plant carbon stock, V_{Ca} is the biomass carbon stock in the above-ground fraction, V_{Cb} is the biomass carbon stock in the below-ground fraction, and V_{Ce} is the carbon stock in epiphytic organisms, all in megagrams of carbon (Mg C).

$$VC_a = \sum_{i=1}^{n} \omega_{\mathrm{C_{org},}i} \times M_{\mathrm{sp},i} \times \frac{S_i}{S_{\mathrm{sp},i}} \times 10^{-2}$$

$$VC_b = \sum_{i=1}^{n} \omega_{\mathrm{C_{orgb},}i} \times M_{\mathrm{spb},i} \times \frac{S_i}{S_{\mathrm{sp},i}} \times 10^{-2}$$

$$VC_e = \sum_{i=1}^{n} \omega_{\mathrm{C_{orge},}i} \times M_{\mathrm{spe},i} \times \frac{S_i}{S_{\mathrm{sp},i}} \times 10^{-2}$$

where $\omega_{Corg,i}$, $\omega_{Corgb,i}$ and $\omega_{Corge,i}$ are the mass fractions of plant above-ground fraction, plant below-ground fraction and epiphytic organisms' organic carbon in % for the ith seagrass partition sample, respectively. $M_{sp,i}$, $M_{spb,i}$ and $M_{spe,i}$ are the dry mass of above-ground plant parts, below-ground plant parts and epiphytic organisms in the ith seagrass compartment

sample, in g, respectively. $S_{sp,i}$: area of plant sample in the ith seagrass partition, in m^2; S_i: area of the ith seagrass partition, in ha.

$$S_{\mathrm{Cstock}} = \sum_{i=1}^{n} C_{\mathrm{col},i} \times S_i \times 100$$

$$C_{\mathrm{col},i} = \sum_{j=1}^{i} \omega_{C_{\mathrm{som},j}} \times \rho_j \times H_j$$

where S_{Cstock} is the sediment carbon stock in Mg C and $C_{col,i}$ is the organic carbon content of column samples at 100 cm or the actual depth of investigation in g/cm^2. S_i is the area of the ith seagrass partition in ha; $C_{\omega som,j}$ is the mass fraction of organic carbon in the jth layer of sediment in %. H_j is the thickness of the sediment in layer j in cm, the thickness of layers 1 to 5 are all 10 cm, and the thickness of layer 6 is the actual thickness of samples of 50 cm or more.

$$C_{\mathrm{stock}} = V_{\mathrm{Cstock}} + S_{\mathrm{Cstock}}$$

where C_{stock} is the total carbon stock in the seagrass bed ecosystem, V_{Cstock} is the plant carbon stock, and S_{Cstock} is the sediment carbon stock, all in Mg C.

Environment variables

To evaluate the relationships between environmental factors and the dynamics of *Z. japonica*, we examined variation in bed area, carbon stock, and habitat distribution across the study regions (Table S2). To analyse the influence of environmental variables on bed area, the maximum monthly bed area recorded at each site was used. A response ratio approach was applied to quantify the associations between environmental factors and bed area, following established methods used in ecological impact assessments.[55] Ten water quality variables were measured, including pH, water temperature, salinity, dissolved oxygen, total nitrogen, total phosphorus, total carbon, total organic carbon, dissolved inorganic carbon, and dissolved organic carbon. Additionally, mean annual temperature was obtained as a climatic variable.

To assess the relationships between environmental conditions and spatial habitat suitability, surface environmental layers were obtained from Bio-ORACLE, a widely used marine environmental database for species distribution modelling.[56,57] Environmental data representing the period from 2000 to 2014 were used to characterize current conditions. Future environmental layers were obtained for the 2050s and 2100s under the RCP2.6, RCP4.5, RCP6.0, and RCP8.5 scenarios. All layers were downloaded at a spatial resolution of 5 arc min,

converted to ASCII format, and processed in ArcGIS 10.4 for input into MaxEnt version 3.4.1. Percentage contribution and permutation importance were used to evaluate the relative importance of environmental variables in the MaxEnt model.

To minimize multicollinearity, pairwise Pearson correlation coefficients were calculated among the candidate environmental variables using ENMTools version 1.3. Variables with $|r| \geq 0.8$ were considered strongly collinear and were screened following established recommendations for species distribution modelling.[36] When two variables were strongly correlated, the variable with greater ecological relevance and model contribution was retained. Variance inflation factors were also calculated to further evaluate multicollinearity, and variables with VIF values below 10 were retained for model calibration.[58] After variable screening, nine environmental predictors were retained for the final MaxEnt model.

To evaluate the relationships between environmental variables and carbon stocks, we analysed sediment total nitrogen, total phosphorus, organic matter, pH, and sulfide concentrations, together with the corresponding seawater and oceanographic variables included in the structural equation models. Sediment total nitrogen was quantified using a combustion method with an elemental analyser, whereas total phosphorus was measured using the Olsen extraction method. Sediment organic matter was determined using the Walkley–Black dichromate oxidation procedure, and pH was measured using a calibrated digital pH meter. These analytical procedures followed established methods used in coastal blue carbon and sediment biogeochemical assessments.[59,60]

Literature Search and Screening

Our analysis involved a systematic literature search and screening process to identify seagrass restoration methods in relation to genetic diversity and the extent of bed area reduction. The search was conducted following the PRISMA framework. We searched the Web of Science Core Collection and China National Knowledge Infrastructure databases using predefined keyword combinations. The search terms included “seagrass restoration”, “eelgrass restoration”, “*Zostera japonica*”, “genetic diversity”, “heterozygosity”, “allelic richness”, “seagrass decline”, “area reduction”, “habitat loss”, “seed broadcasting”, “seed-based restoration”, “shoot transplanting”, “transplantation”, and “restoration method”. A total of 79 potentially relevant records were initially identified.

The screening process consisted of four steps. First, potentially relevant records were identified through database searches using the predefined search terms. Second, duplicate records and clearly irrelevant studies were removed. Third, titles and abstracts were screened to retain studies related to seagrass restoration, genetic diversity, bed area reduction, habitat loss, or restoration methods. Fourth, the full texts of potentially eligible studies were assessed, and relevant data were extracted from studies that met the inclusion criteria. After title and abstract screening, 50 articles were retained for full-text assessment.

Studies were included if they met one or more of the following criteria: they reported genetic diversity indicators, such as the number of alleles, heterozygosity, or allelic richness, and/or quantified the extent of seagrass bed area reduction; they specified the restoration method used, including seed broadcasting, other seed-based approaches, shoot transplantation, or combined methods; they described previous habitat conditions and human or natural disturbances affecting the seagrass bed; and they provided sufficient geographic information for contextual interpretation. The Sustainable Wetlands Adaptation and Mitigation Program database was additionally consulted to inform the organization of coastal blue carbon assessment variables. It was not used as a bibliographic database or as a source of records in the literature-screening process.

Rule-based restoration decision framework

A rule-based decision framework was developed using studies that met all inclusion criteria during the literature-screening process. The framework was designed to support the selection of seagrass restoration strategies based on two ecological indicators: genetic diversity and the extent of bed area reduction. Rule-based decision frameworks have increasingly been used in restoration planning because they allow categorical ecological information to be linked transparently with management options.[15,61]

The extent of bed degradation was determined by comparing the mapped bed area during the baseline period of 2014-2015 with that during the most recent assessment period of 2022-2023. Populations that had lost 50% or more of their baseline bed area were classified as having high bed degradation, whereas those with an area reduction of less than 50% were classified as having limited bed degradation. The 50% cutoff was used as an operational threshold to distinguish populations that had lost at least half of their mapped bed extent from those retaining

a larger proportion of the baseline bed.

Genetic diversity status was evaluated using multiple population-genetic metrics rather than nucleotide diversity alone.[62] The proportion of polymorphic loci (Pi), expected heterozygosity (He), and nucleotide diversity (π) were used as the principal diversity indicators. Observed heterozygosity (Ho) was used as supplementary information on realized heterozygosity, whereas FIS was considered separately to assess heterozygote deficiency or excess and was not treated as a direct measure of genetic diversity.[63,64]

Because all populations belonged to the same species and were analyzed using the same genomic dataset and filtering criteria, each principal genetic metric was standardized relative to the maximum value observed among the 11 populations. A relative genetic diversity index was then calculated as:

$$Gi = \frac{1}{3}\left(\frac{Pi}{Pmax} + \frac{He,i}{He,max} + \frac{\pi i}{\pi max}\right)$$

where Pi, He,i, and πi represent the proportion of polymorphic loci, expected heterozygosity, and nucleotide diversity of population i, respectively, and the denominators represent the corresponding maximum values observed across all populations. Populations with $Gi \geq 0.75$ were classified as having relatively high genetic diversity, whereas populations with $Gi < 0.75$ were classified as having relatively low genetic diversity. This operational boundary reflected the clear separation between the southern high-diversity populations and the northern lower-diversity populations in the present dataset and was not regarded as a universal genetic threshold.

Restoration methods were subsequently assigned using the combination of structural decline and genetic diversity status. Sites with low-to-moderate area reduction and high genetic diversity were assigned to natural recovery combined with habitat protection. Sites with high area reduction but high genetic diversity were assigned to shoot-transplantation-based restoration, because the principal requirement was rapid reconstruction of meadow structure while retaining locally adapted genetic resources. Sites with low-to-moderate area reduction and low genetic diversity were assigned to seed-based restoration, with seeds collected from multiple parent plants and, where appropriate, multiple environmentally compatible donor patches to increase sexual recruitment and genetic variation. Sites with both high area reduction

and low genetic diversity were assigned to combined seed-and-shoot restoration, in which transplanted shoots were used to rapidly establish meadow structure and multi-parent seed supplementation was used to broaden the genetic base and reduce bottleneck risks.

These recommendations were treated as preliminary restoration options rather than fixed prescriptions. Final method selection also considered donor availability, habitat suitability, hydrodynamic and sediment conditions, causes of bed degradation, risks of genetic transfer, potential impacts on donor beds, and the feasibility of long-term monitoring and maintenance.

Genetic diversity data of *Z. japonica*

Whole-genome resequencing was conducted to characterize the genetic diversity of *Z. japonica* across 11 geographic populations along the Chinese coast. Leaf tissues were collected from representative individuals, and genomic DNA was extracted using standard plant DNA extraction protocols. Paired-end sequencing libraries were constructed and sequenced on the Illumina NovaSeq platform to generate genome-wide resequencing data, following approaches commonly used in recent seagrass population genomic studies.[65]

Raw sequencing reads were quality-filtered using fastp and aligned to the *Z. japonica* reference genome using the Burrows–Wheeler Aligner. Sequence alignments were processed, and high-confidence single-nucleotide polymorphisms were identified following the Genome Analysis Toolkit best-practice workflow. Variant sites were subsequently filtered according to sequencing depth, missing-data rate, minor allele frequency, and allelic state. All resequencing data have been deposited in the National Center for Biotechnology Information Sequence Read Archive under BioProject accession PRJNA1344808.

Genetic diversity indices, including observed heterozygosity, expected heterozygosity, allelic richness, and nucleotide diversity (π), were calculated using VCFtools and appropriate R packages for population-genetic analysis. These indices are widely used to characterize genetic variation in marine angiosperm populations.[66,67]

RESULTS

Where to restore: mapping the potential restoration opportunity

Predicted distribution and habitat suitability provide spatially explicit indications of where environmental conditions may support restoration under specified climate conditions, rather than direct estimates of restoration success. Using MaxEnt, we predicted the global distribution

of environmentally suitable areas for *Z. japonica* under current conditions and found that the largest and most continuous suitable areas were concentrated in the northwestern Pacific Ocean (Figure 1). Centroid analysis of the suitable area within the northwestern Pacific region further showed that its geographic center was located in Chinese coastal waters (Figure 2). This spatial pattern suggests that China represents an important regional focus for the conservation and restoration planning of *Z. japonica*.

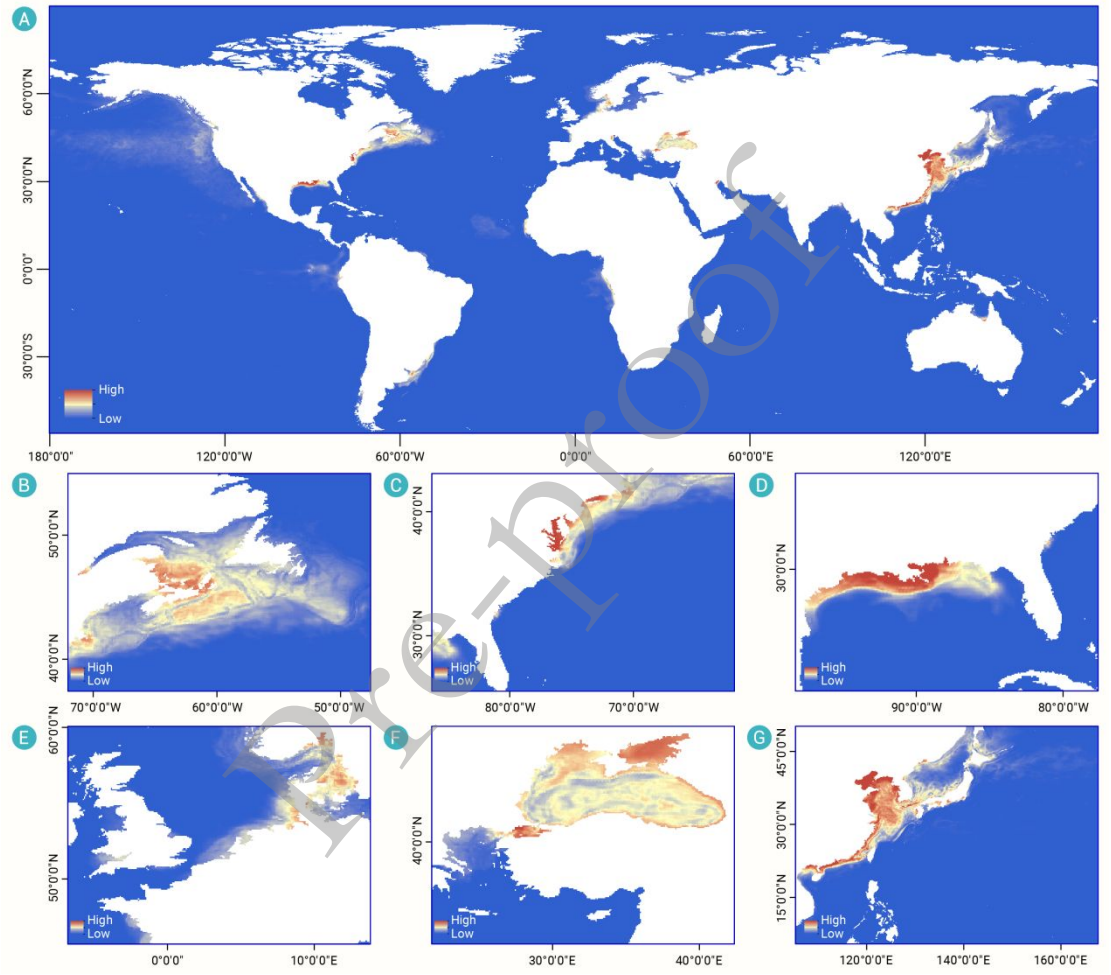

Figure 1. Predicted habitat suitability for *Z. japonica* under current environmental conditions (A) Global distribution of predicted habitat suitability. (B–G) Enlarged views of the major suitable regions in northeastern North America, the eastern coast of North America, the Gulf of Mexico, northern Europe, the Black Sea region, and East Asia, respectively. Colors from blue to red indicate increasing predicted habitat suitability from low to high.

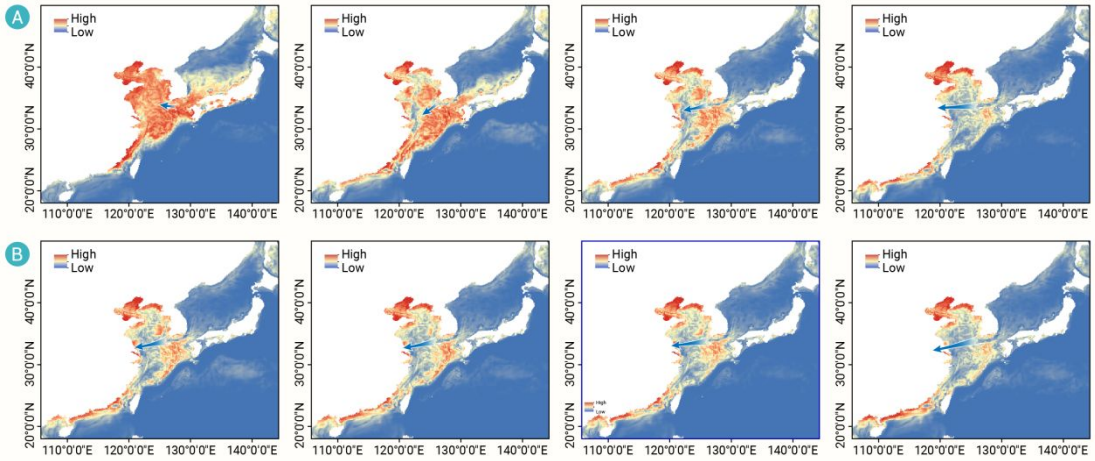

Figure 2. Projected shifts in the centroid of suitable habitat for *Z. japonica* under future climate scenarios within the northwestern Pacific region (A) Projected centroid shifts under RCP2.6, RCP4.5, RCP6.0, and RCP8.5 in the 2050s. (B) Projected centroid shifts under the same climate scenarios in the 2100s. Arrows indicate the direction and relative magnitude of projected changes in the geographic centroid of suitable habitat.

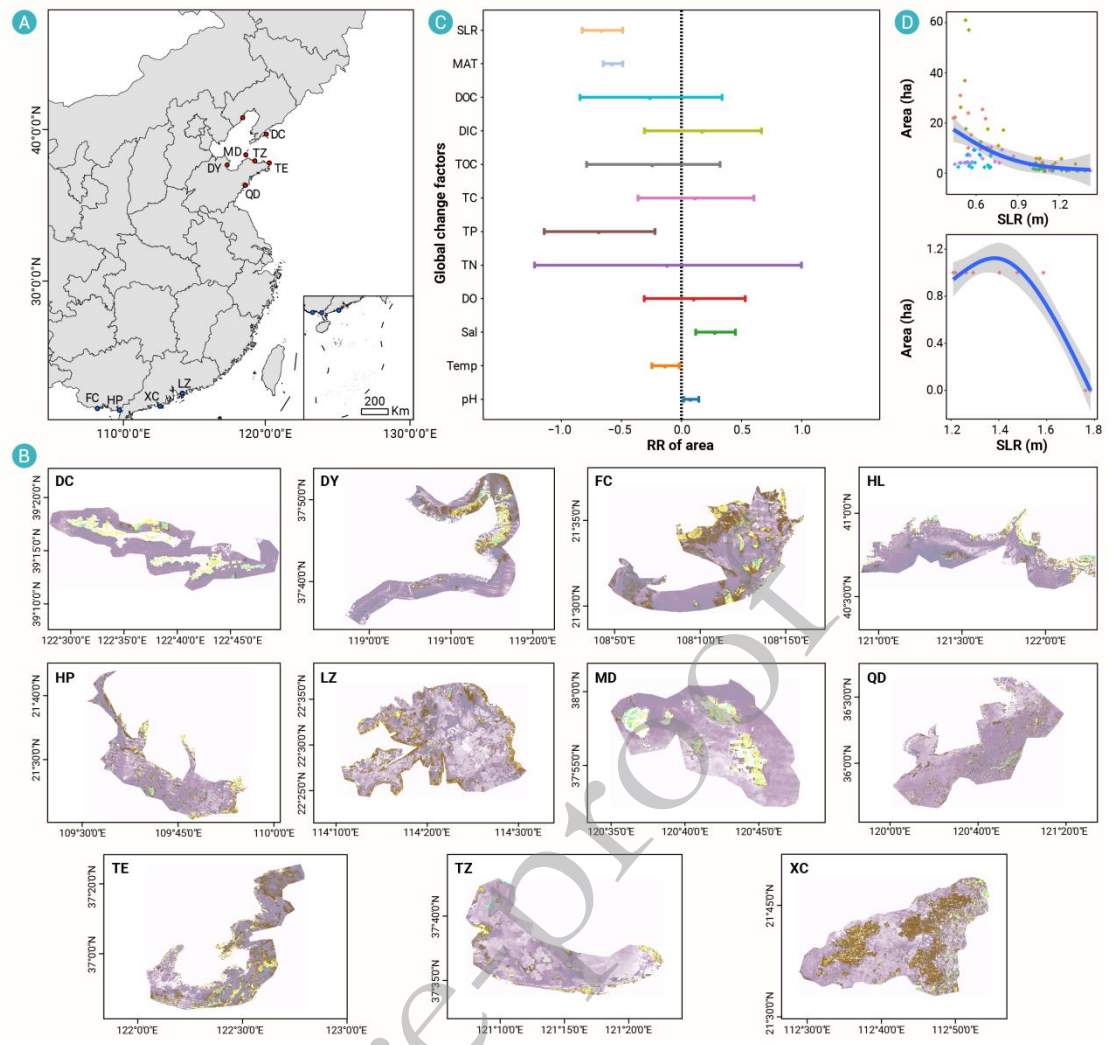

Figure 3. Spatial distribution and temporal changes of *Z. japonica* beds along the coast of China, excluding Taiwan Island (A) Locations of the 11 surveyed populations: QD, Huiquan Bay, Qingdao; TE, Swan Lake, Rongcheng; DY, Yellow River Delta, Dongying; HL, Xingcheng, Huludao; DC, Dachangshan Island, Dalian; MD, Miaodao Island, Yantai; TZ, Taozi Bay, Yantai; LZ, Lai Chi Wo, Hong Kong; XC, Xiachuan Island, Taishan; FC, Pearl Bay, Fangchenggang; and HP, Hepu, Beihai. The blue line indicates the coastline. (B) Spatial distribution and temporal changes in bed area and the *Z. japonica* index from 2014 to 2022 at the 11 study sites, green areas on the maps indicate pixels classified as *Z. japonica* beds based on the *ZJI*. In the temporal profiles, yellow and green lines indicate bed area and *ZJI*, respectively. (C) Response ratios of *Z. japonica* bed area to environmental variables across the study sites in 2023. (D) Generalized additive model showing the nonlinear relationship between sea level rise and *Z. japonica* bed area.

The 11 surveyed populations spanned the major distribution regions of Z. japonica along the Chinese coast, from the Bohai and Yellow seas to the northern South China Sea (Figure 3A). Remote sensing analyses revealed an overall decline in the mapped area of *Z. japonica* beds along the Chinese coast from 2014 to 2022, although the magnitude and temporal pattern of change varied among sites (Figure 3B). Greater losses were generally observed at sites in the South China Sea than at several northern sites. Response ratio analysis indicated that temperature and sea level rise were among the environmental variables most strongly associated with spatial variation in bed area (Figure 3C). The generalized additive model further identified a nonlinear relationship between sea level rise and bed area, with a marked decline occurring beyond approximately 0.9 m and bed area approaching low levels at approximately 1.5 m (Figure 3D).

MaxEnt projections of current habitat suitability within Chinese coastal waters identified three principal suitable regions: the coastal zone of the Liaodong Peninsula, the northwestern Bohai Sea, and selected coastal areas of the Shandong Peninsula, particularly its eastern and northeastern coasts and the Qingdao coastal region (Figure S1). These predicted suitable areas were generally consistent with the surveyed distribution of *Z. japonica* shown in Figure 3. Among the nine retained environmental predictors, mean sea surface temperature had the highest percentage contribution to the MaxEnt model, indicating its dominant contribution to model calibration. Mean surface current velocity had the highest permutation importance, indicating that model predictions were particularly sensitive to this variable. Minimum and mean sea surface salinity also contributed to model performance. Together, these results indicate that temperature, salinity, and current velocity were the principal environmental variables associated with the current predicted distribution of *Z. japonica* in Chinese coastal waters (Table S3).

When to restore: progressive restoration

Projected habitat changes under future sea level rise and climate scenarios provide a basis for prioritizing the timing of *Z. japonica* restoration. Our projections indicate progressive declines in both habitat suitability and the extent of suitable habitat under all future climate scenarios, with clear spatial differences among regions (Figure 4).

By the 2050s, both occurrence probability and suitable habitat extent are projected to decline

markedly in the northwestern Bohai Sea and the western coastal waters of the Liaodong Peninsula under the RCP4.5 and RCP8.5 scenarios, with some areas approaching local disappearance by the 2100s. In the coastal waters of the Shandong Peninsula and the eastern Liaodong Peninsula, suitable habitat is also projected to decline progressively from the 2050s to the 2100s under the same scenarios. Quantitatively, the suitable habitat of *Z. japonica* is projected to decrease by 56.76% under RCP4.5 and 57.35% under RCP8.5 by the 2050s. By the 2100s, the projected decline is 56.26% under RCP4.5 and 61.80% under RCP8.5 (Figure S2 & Table S4). In contrast, the potential for range expansion is very limited, with newly suitable habitat accounting for less than 2% under both scenarios in the 2050s and 2100s.

These projections support a progressive restoration strategy based on habitat persistence through time. Restoration should be prioritized in areas that are suitable under current conditions and remain suitable in the 2050s, particularly those also projected to remain suitable in the 2100s, because these areas represent relatively stable core restoration zones with greater potential for long-term persistence and sustained carbon storage. Areas projected to become suitable mainly by the 2100s should instead be regarded as long-term adaptive restoration reserves and incorporated into future monitoring and planning, rather than being treated as immediate restoration targets.

Under this framework, the total area projected to remain or become suitable for *Z. japonica* by the 2100s reaches 103,371 ha, depending on climate scenario and restoration planning assumptions (Figure 5). This projected area should be interpreted as a potential restoration opportunity space rather than as a direct estimate of realized restoration area.

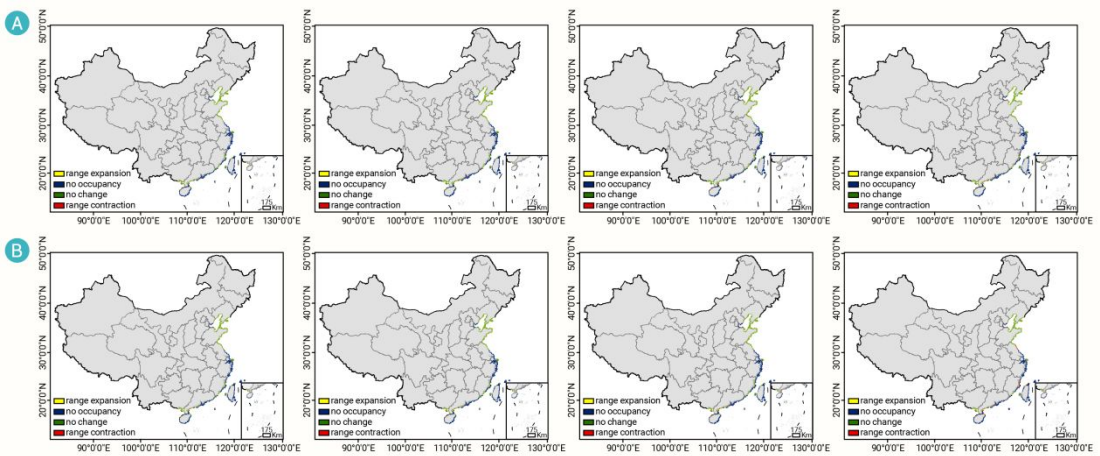

Figure 4. Spatial changes in suitable habitat for *Z. japonica* under future climate scenarios (A)

Spatial changes in suitable habitat under RCP2.6, RCP4.5, RCP6.0, and RCP8.5 in the 2050s. (B) Spatial changes in suitable habitat under the same climate scenarios in the 2100s.

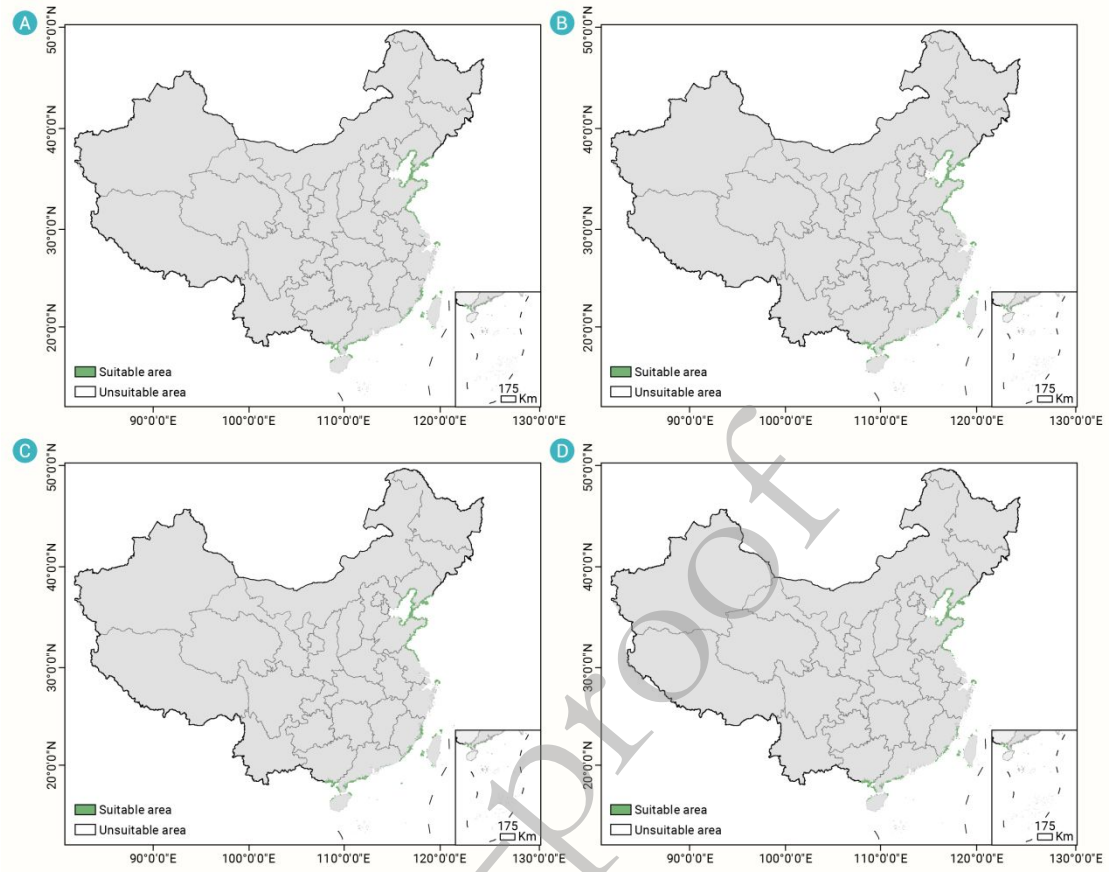

Figure 5. Potential suitable and unsuitable areas for *Z. japonica* restoration in the 2100s under the progressive restoration framework (A) Projected suitable and unsuitable areas under RCP2.6. (B) Projected suitable and unsuitable areas under RCP4.5. (C) Projected suitable and unsuitable areas under RCP6.0. (D) Projected suitable and unsuitable areas under RCP8.5.

With what methods to restore: selecting restoration approaches according to local conditions

Integrating genetic diversity, remote sensing observations, exposure to sea-level change, and MaxEnt projections revealed marked spatial variation in the status of *Z. japonica* beds along the Chinese coast. Populations in the Bohai Sea and Yellow Sea generally experienced lower levels of bed degradation and were associated with the largest continuous areas projected to remain suitable under current and future environmental conditions. In contrast, populations in the South China Sea showed greater bed degradation and were associated with relatively limited areas of persistent future suitability.

Genetic diversity and projected environmental suitability did not show the same spatial pattern.

Southern populations generally exhibited higher allelic richness and heterozygosity than northern populations, whereas the largest areas of projected future habitat suitability occurred in northern China. This spatial mismatch indicates that restoration planning should consider both the conservation value of genetically diverse populations and the long-term environmental suitability of candidate restoration sites.

Two principal active restoration approaches are used for *Z. japonica* along the Chinese coast: seed-based restoration and shoot transplantation, which may be applied separately or in combination with conservation-oriented management. We developed a rule-based regional recommendation framework primarily based on bed degradation and genetic diversity. For highly degraded populations with high genetic diversity, the framework prioritizes the use of local seeds and small-scale in situ transplantation while avoiding their use as major donor sources. For highly degraded populations with low genetic diversity, transplantation using material from genetically diverse donor populations is recommended, with supplementary use of local seeds where appropriate. For populations with relatively limited bed decline but low genetic diversity, local seed use, restricted donor supplementation, small-scale transplantation, and conservation-oriented management are recommended in combination. The resulting regional recommendations are summarized in Table S5. Final restoration decisions should additionally account for donor-material availability, local bed extent, potential impacts on donor beds, environmental compatibility, and the ecological and genetic risks associated with transferring material among differentiated populations.

Regional variation and environmental drivers of *Z. japonica* carbon stocks

Carbon stocks in *Z. japonica* beds varied considerably among the surveyed regions in China (Table S6). The highest total carbon stock values were recorded at DC, MD, TZ, and HL in the Bohai Sea region, whereas comparatively low values were recorded at HP in the South China Sea and QD in the Yellow Sea.

To examine the direct and indirect associations between environmental variables and different carbon pools, we fitted separate structural equation models for aboveground, belowground, and sediment carbon stocks using site-level mean values of the standardized variables. The three models showed acceptable overall fit, with comparative fit index and goodness-of-fit index values above 0.90 and standardized root mean square residual values below 0.07 (Figure 6).

For aboveground carbon stock, sea surface temperature was negatively associated with seawater dissolved oxygen and sediment pH, with standardized path coefficients of −0.74 and −0.47, respectively. In turn, dissolved oxygen and sediment pH showed positive direct associations with aboveground carbon stock, with standardized path coefficients of 0.46 and 0.70, respectively. These pathways indicate that the association between sea surface temperature and aboveground carbon stock was primarily indirect.

For belowground carbon stock, sediment-related variables showed comparatively stronger direct associations. Sediment pH had a positive path coefficient of 0.69, whereas sediment sulfides and sediment nitrogen showed positive but nonsignificant path coefficients of 0.25 and 0.23, respectively. For sediment carbon stock, sediment pH showed the strongest positive direct association, with a standardized path coefficient of 0.73. Sea surface temperature was negatively associated with sediment pH, indicating a potential indirect pathway linking temperature to sediment carbon stock.

Together, the models indicate that the three carbon pools were associated with partly distinct environmental pathways. Aboveground carbon stock was more closely related to seawater physicochemical conditions, whereas belowground carbon stock was more strongly associated with sediment properties. The sediment carbon stock model contained several nonsignificant pathways, suggesting that additional unmeasured factors may contribute to spatial variation in sediment carbon accumulation. These results highlight the compartment-specific environmental associations of carbon storage in *Z. japonica* beds.

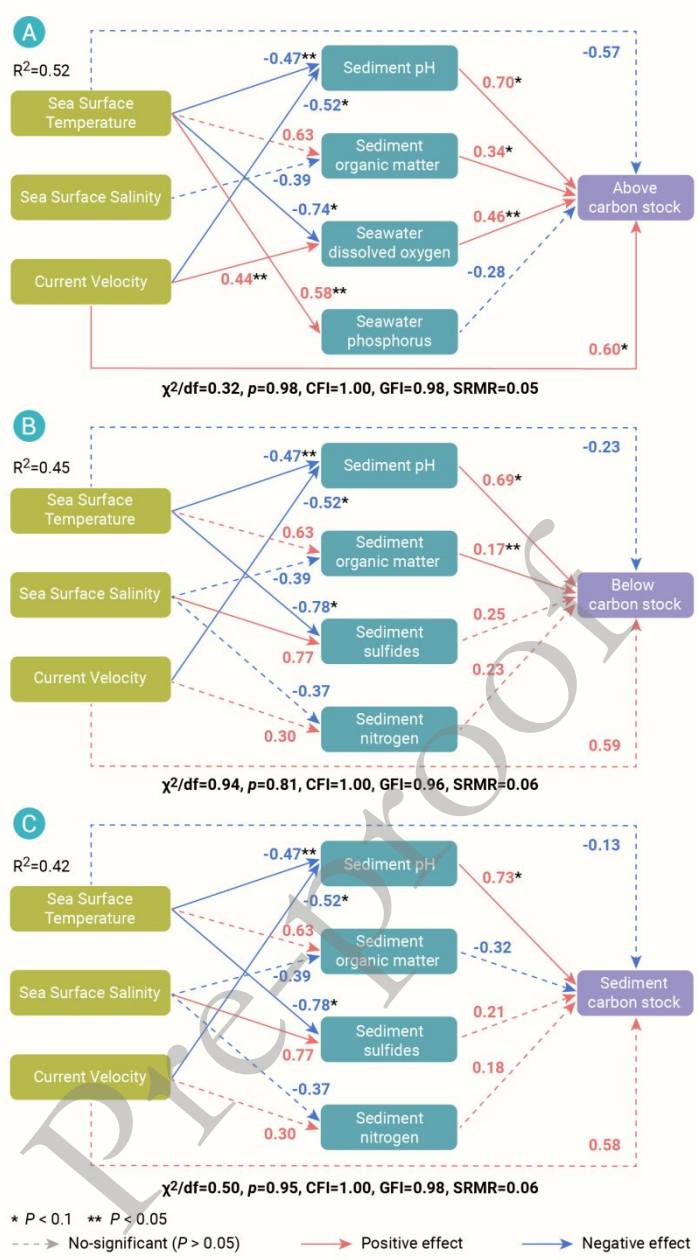

Figure 6. Structural equation models showing the environmental factors associated with carbon stocks in *Z. japonica* beds (A) Aboveground carbon stock, (B) belowground carbon stock, and (C) sediment carbon stock. Numbers adjacent to arrows indicate standardized path coefficients. Pink and blue arrows indicate positive and negative associations, respectively. Solid arrows indicate statistically significant paths, whereas dashed arrows indicate nonsignificant paths. Asterisks indicate the statistical significance of individual paths. R^2indicates the proportion of variance in each carbon stock component explained by the model. Model fit indices are shown below each panel.

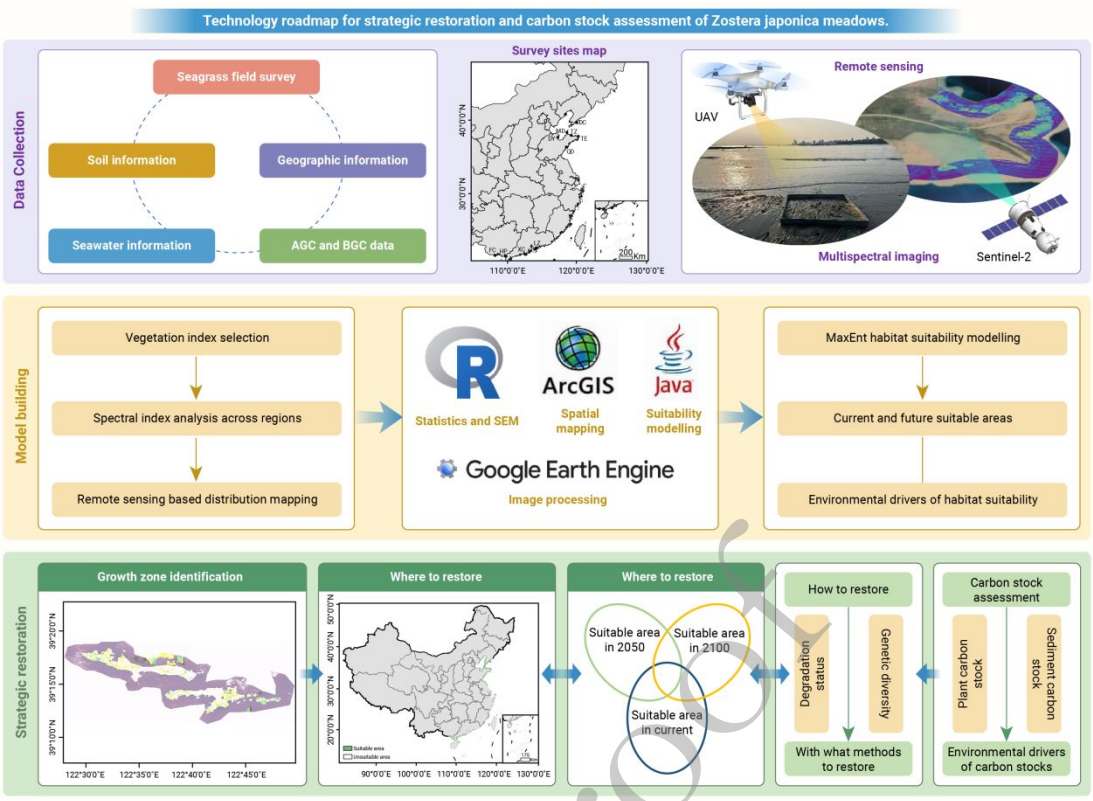

Figure 7. Technology roadmap for the strategic restoration of *Z. japonica* beds based on spatial modelling and carbon stock assessment The workflow integrates field data collection, remote sensing mapping, MaxEnt habitat suitability modelling, carbon stock assessment, and strategic restoration planning. Google Earth Engine, ArcGIS, Java based MaxEnt, and R were used for image processing, spatial mapping, habitat suitability prediction, and statistical analyses, respectively. Field derived carbon stock data were further used to support restoration planning and estimate the potential long term carbon benefits of future bed restoration.

DISCUSSION

The restoration of *Z. japonica* beds has the potential to enhance coastal carbon storage and contribute to China's carbon neutrality goals. By integrating habitat suitability modelling, remote sensing, field surveys, genetic information, and carbon stock assessments, this study provides a spatially explicit framework for determining where, when, and how restoration could be implemented along the Chinese coast.

We combined MaxEnt habitat suitability modelling with multitemporal remote sensing to identify potential priority areas for *Z. japonica* restoration. Under current and future climate scenarios, the Bohai Sea and Yellow Sea contained extensive areas of predicted suitable habitat, largely associated with favourable temperature, salinity, and hydrodynamic conditions. MaxEnt is widely used for species distribution modelling with presence-only data, and has been applied in marine species distribution and coastal habitat assessments,[34,35] including the identification of conservation and restoration priorities for seagrass ecosystems.[24] Nevertheless, predicted suitability represents the environmental potential for species occurrence rather than direct evidence of restoration success. Local substrate conditions, water quality, hydrodynamics, disturbance history, and propagule availability should therefore be evaluated before restoration is implemented.

Our temporal framework prioritizes areas predicted to remain suitable under current conditions and through the 2050s and 2100s as relatively stable core zones for restoration. Areas that are currently suitable but projected to become unsuitable should receive immediate conservation attention and may be appropriate only for short- to medium-term restoration where future risks can be managed. In contrast, areas projected to become suitable mainly by the 2100s should be regarded as potential adaptive reserves rather than immediate planting targets. This phased approach links present restoration opportunities with long-term environmental change and is consistent with restoration principles emphasizing appropriate timing, site selection, restoration scale, and adaptive management.[15,19,22,63]

Drawing on the literature synthesis and population genomic data, we developed a rule-based framework for selecting restoration methods according to bed degradation and genetic diversity[15]. Southern populations exhibited higher genetic diversity than northern populations, whereas northern China contained a larger extent of habitat projected to remain suitable under

future conditions. This spatial mismatch highlights the importance of considering both environmental suitability and evolutionary information in restoration planning. Southern populations represent important genetic resources and may provide candidate donor material for future assisted gene flow, but only after careful assessment of local adaptation, donor-bed impacts, genetic compatibility, and ecological risk. Northern regions, by contrast, provide extensive potential restoration space but may require greater attention to the conservation of locally adapted genetic resources. More generally, spatial differences between genetic diversity, population connectivity, and projected environmental suitability may arise from historical demographic processes, ocean-current-mediated dispersal, and climate-driven shifts in suitable habitat.[65,68-70]

This mismatch further highlights the importance of integrating evolutionary information with environmental projections. High-diversity southern populations represent valuable genetic resources that should be prioritized for conservation, because genetic variation can influence ecosystem resistance, recovery capacity, and long-term population persistence.[62,67,70] These populations may also inform future assisted gene flow, but the transfer of restoration material should proceed only after careful evaluation of local adaptation, donor availability, genetic compatibility, donor-population impacts, and ecological risk.[70-72] In contrast, northern regions provide extensive predicted suitable habitat for restoration. The framework distinguishes among seed-based restoration, shoot transplantation, combined approaches, and protection or natural recovery. Seed-based restoration may be appropriate where bed structure remains partly intact and suitable seed sources are available, provided that seeds are collected from environmentally compatible donor populations and impacts on donor beds are minimized[63,72]. Shoot transplantation may accelerate structural recovery in severely degraded beds when suitable donor material is available and disturbance pressures have been reduced.[15,63,73] A combined approach may be appropriate where both genetic diversity and bed area have declined substantially, although the relative contribution of seeds and transplanted shoots should be adjusted according to site conditions and donor-material availability.[63,73] Where genetic diversity remains high and area reduction is limited, protection, natural recovery, and continued monitoring should generally be prioritized.[15,16,64]

These recommendations should be treated as initial management options rather than fixed prescriptions because restoration outcomes also depend on sediment conditions, hydrodynamics, water quality, donor availability, restoration scale, and the causes of degradation. This approach aligns with restoration frameworks developed for seagrass and other coastal ecosystems, which emphasize context-dependent restoration based on environmental and biological conditions.[15,63,73] Previous studies have shown that restoration outcomes can be improved when methods are tailored to site conditions, including local environmental quality, historical population trends, restoration scale, and genetic variation.[21,62,63,72] Integrating these factors allows restoration planning to identify appropriate interventions and overcome limitations associated with reliance on a single method. Future work will benefit from combining genomic data with assessments of future vulnerability. Genome-level approaches can identify candidate adaptive genetic variation and improve the evaluation of population responses to environmental stress.[69-72] Integrating these approaches will improve the scientific basis of restoration planning and support the development of long-term strategies for *Z. japonica* conservation and recovery along the Chinese coast.

Carbon stocks in *Z. japonica* beds varied substantially among regions, with the highest values recorded at several sites in the Bohai Sea. Structural equation modelling was used to examine the environmental variables associated with these carbon stocks and indicated that different carbon pools were related to partly distinct environmental pathways. Aboveground carbon stock was associated with both water-column conditions and hydrodynamic variables, whereas belowground carbon stock was more closely associated with sediment physicochemical properties. Temperature may influence carbon stocks indirectly by altering oxygen availability and sediment chemical conditions, whereas hydrodynamic conditions may affect sediment stability, particle deposition, and organic matter retention[74,75]. However, the relatively high proportion of nonsignificant pathways in the sediment carbon model also suggests that additional factors, such as sediment grain size, sedimentation rate, organic matter sources, and historical carbon deposition, may contribute to sediment carbon accumulation[76]. Understanding these factors is important for developing restoration and management strategies that enhance coastal carbon storage and contribute to broader carbon-neutrality objectives[1,31,77,78].

Consistent with studies of mangrove carbon stocks, our results also emphasize the importance

of sediment conditions and temperature-related environmental processes in regulating coastal blue carbon storage.[59] However, the carbon benefits of restoration cannot be inferred from bed area alone. The projected suitable habitat represents a potential restoration opportunity space rather than a direct estimate of realized restoration area, and the associated carbon estimate represents potential carbon stock under the stated assumptions rather than guaranteed additional sequestration. Site-specific measurements of sediment properties, carbon stocks, and carbon accumulation rates will therefore be required to evaluate the realized carbon benefits of *Z. japonica* restoration.

Beyond carbon storage, restored seagrass beds can support biodiversity, improve water quality, stabilize sediments, and increase coastal resilience.[61,79,80] These co-benefits strengthen the rationale for incorporating seagrass restoration into broader coastal management and climate-mitigation strategies. Experiences from large-scale restoration programmes indicate that restoration success is improved by integrating spatial planning, context-specific method selection, appropriate restoration scale, and long-term monitoring.[15,63] Our framework extends these principles by linking habitat suitability, future environmental change, genetic information, restoration methods, and potential carbon benefits within a unified planning framework (Figure 7). However, field validation remains essential for translating projected habitat suitability and potential carbon benefits into successful restoration and long-term bed persistence.

Conclusion

The strategic restoration of *Z. japonica* beds offers a promising pathway for enhancing coastal carbon storage and supporting China's carbon neutrality goals. By integrating spatial modelling, field observations, genetic information, and carbon stock assessments, this study provides a practical framework for identifying priority restoration areas, selecting appropriate restoration methods, and evaluating potential ecological and carbon benefits. The framework emphasizes the importance of matching restoration timing and methods to local environmental conditions and population characteristics. Although our surveys covered most of the known distribution regions of *Z. japonica* in China, baseline information remains incomplete. Expanding long-term seagrass monitoring and carbon stock datasets will enable more robust assessments of restoration feasibility and the ecological and carbon benefits of seagrass beds.

References

[1] Liu Z., Deng Z., He G., et al. (2022). Challenges and opportunities for carbon neutrality in China. *Nat. Rev. Earth Environ.* **3**:141-155. DOI:10.1038/s43017-021-00244-x

[2] Houghton R. A. (2007). Balancing the global carbon budget. *Annu. Rev. Earth Planet. Sci.* **35**:313-347. DOI:10.1146/annurev.earth.35.031306.140057

[3] Luisetti T. (2021). Some countries donate blue carbon. *Nat. Clim. Change* **11**:647-648. DOI:10.1038/s41558-021-01103-9

[4] Duarte C. M., Agusti S., Barbier E., et al. (2020). Rebuilding marine life. *Nature* **580**:39-51. DOI:10.1038/s41586-020-2146-7

[5] Lu N., Tian H., Fu B., et al. (2022). Biophysical and economic constraints on China's natural climate solutions. *Nat. Clim. Change* **12**:847-853. DOI:10.1038/s41558-022-01432-3

[6] Lu F., Hu H., Sun W., et al. (2018). Effects of national ecological restoration projects on carbon sequestration in China from 2001 to 2010. *Proc. Natl. Acad. Sci. USA* **115**:4039-4044. DOI:10.1073/pnas.1700294115

[7] Yu Z., Ciais P., Piao S., et al. (2022). Forest expansion dominates China's land carbon sink since 1980. *Nat. Commun.* **13**:5374. DOI:10.1038/s41467-022-32961-2

[8] Piao S., He Y., Wang X., et al. (2022). Estimation of China's terrestrial ecosystem carbon sink: Methods, progress and prospects. *Sci. China Earth Sci.* **65**:641-651. DOI:10.1007/s11430-021-9892-6

[9] Nelleman C., Corcoran E., Duarte C. M., et al. (2008). Blue carbon: The role of healthy oceans in binding carbon (UNEP/FAO/UNESCO/IUCN/CSIC), pp:1-78. DOI:10.1590/S0100-06832008000200014.

[10] Macreadie P. I., Costa M. D. P., Atwood T. B., et al. (2021). Blue carbon as a natural climate solution. *Nat. Rev. Earth Environ.* **2**:826-839. DOI:10.1038/s43017-021-00224-1

[11] Falkowski P. G., Barber R. T. and Smetacek V. V. (1998). Biogeochemical controls and feedbacks on ocean primary production. *Science* **281**:200-207. DOI:10.1126/science.281.5374.200

[12] Duarte C. M. (1995). Submerged aquatic vegetation in relation to different nutrient regimes. *Ophelia* **41**:87-112. DOI:10.1080/00785236.1995.10422039

[13] Chefaoui R. M., Duarte C. M. and Serrao E. A. (2018). Dramatic loss of seagrass habitat under projected climate change in the Mediterranean Sea. *Global Change Biol.* **24**:4919-4928. DOI:10.1111/gcb.14401

[14] Duarte C. M., Kennedy H., Marbà N., et al. (2013). Assessing the capacity of seagrass meadows for carbon burial: Current limitations and future strategies. *Ocean Coast. Manage.* **83**:32-38. DOI:10.1016/j.ocecoaman.2011.09.001

[15] Orth R. J., Lefcheck J. S., McGlathery K. S., et al. (2020). Restoration of seagrass habitat leads to rapid recovery of coastal ecosystem services. *Sci. Adv.* **6**:eabc6434. DOI:10.1126/sciadv.abc6434

[16] Unsworth R. K. F., Cullen-Unsworth L. C., Jones B. L. H., et al. (2022). The planetary role of seagrass conservation. *Science* **377**:609-613. DOI:10.1126/science.abq6923

[17] Liu C., Liu G., Casazza M., et al. (2022). Current status and potential assessment of China's ocean carbon sinks. *Environ. Sci. Technol.* **56**:6584-6595. DOI:10.1021/acs.est.1c08106

[18] Zhou Q. Q., Ke Y. H., Wang X. Y., et al. (2022). Developing seagrass index for long term monitoring of seagrass bed: A case study in Yellow River Delta, China. *ISPRS J. Photogramm. Remote Sens.* **194**:286-301. DOI:10.1016/j.isprsjprs.2022.10.011

[19] Fourqurean J. W., Duarte C. M., Kennedy H., et al. (2012). Seagrass ecosystems as a globally significant carbon stock. *Nat. Geosci.* **5**:505-509. DOI:10.1038/ngeo1477

[20] Dunic J. C., Brown C. J., Connolly R. M., et al. (2021). Long-term declines and recovery of meadow area across the world's seagrass bioregions. *Global Change Biol.* **27**:4096-4109. DOI:10.1111/gcb.15684

[21] Orth R. J., Moore K. A., Marion S. R., et al. (2012). Seed addition facilitates eelgrass recovery in a coastal bay system. *Mar. Ecol. Prog. Ser.* **448**:177-195. DOI:10.3354/meps09522

[22] Waycott M., Duarte C. M., Carruthers T. J., et al. (2009). Accelerating loss of seagrasses across the globe threatens coastal ecosystems. *Proc. Natl. Acad. Sci. USA* **106**:12377-12381. DOI:10.1073/pnas.0905620106

[23] Huang Y.-H., Lee C.-L., Chung C.-Y., et al. (2015). Carbon budgets of multispecies seagrass beds at Dongsha Island in the South China Sea. *Mar. Environ. Res.* **106**:92-102. DOI:10.1016/j.marenvres.2015.03.004

[24] Hu W. J., Zhang D. A., Chen B., et al. (2021). Mapping the seagrass conservation and restoration priorities: Coupling habitat suitability and anthropogenic pressures. *Ecol. Indic.* **129**:107960. DOI:10.1016/j.ecolind.2021.107960

[25] Zhang X., Li Y. L., Kaldy J. E., et al. (2024). Population genetic patterns across the native and invasive range of a widely distributed seagrass: Phylogeographic structure, invasive history and conservation implications. *Divers. Distrib.* **30**:1-18. DOI:10.1111/ddi.13803

[26] Zhang X., Lin H., Song X., et al. (2019). A unique meadow of the marine angiosperm *Zostera japonica*, covering a large area in the turbid intertidal Yellow River Delta, China. *Sci. Total Environ.* **686**:118-130. DOI:10.1016/j.scitotenv.2019.05.320

[27] Huang X. P., Huang L. M., Li Y. H., et al. (2006). Main seagrass beds and threats to their habitats in the coastal sea of South China. *Chin. Sci. Bull.* **51**:136-142. DOI:10.1007/s11434-006-9136-5

[28] Yue S., Zhou Y., Xu S., et al. (2021). Can the non-native salt marsh halophyte Spartina alterniflora threaten native seagrass (*Zostera japonica*) habitats? a case study in the Yellow River Delta, China. *Front. Plant Sci.* **12**:643425. DOI:10.3389/fpls.2021.643425

[29] Hodoki Y., Ohbayashi K., Tanaka N., et al. (2013). Evaluation of Genetic Diversity in (Aschers. et Graebn.) for Seagrass Conservation in Brackish Lower Reaches of the Hii River System, Japan. *Estuaries Coasts* **36**:127-134. DOI:10.1007/s12237-012-9564-1

[30] Lee S., Ma S., Lim Y., et al. (2004). Genetic diversity and its implications in the conservation of endangered in Korea. *J. Plant Biol.* **47**:275-281. DOI:10.1007/Bf03030519

[31] Hepburn C., Qi Y., Stern N., et al. (2021). Towards carbon neutrality and China's 14th Five-Year Plan: Clean energy transition, sustainable urban development, and investment priorities. *Environ. Sci. Ecotechnol.* **8**:100130. DOI:10.1016/j.ese.2021.100130

[32] Short F. T. and Coles R. G. (2001). Global seagrass research methods (Elsevier), pp:1-473. DOI:10.1016/B978-0-444-50891-1.X5000-2.

[33] Hossain M. S., Bujang J. S., Zakaria M. H., et al. (2015). The application of remote sensing to seagrass ecosystems: an overview and future research prospects. *Int. J. Remote Sens.* **36**:61-114. DOI:10.1080/01431161.2014.990649

[34] Phillips S. J., Anderson R. P. and Schapire R. E. (2006). Maximum entropy modeling of species geographic distributions. *Ecol. Modell.* **190**:231-259. DOI:10.1016/j.ecolmodel.2005.03.026

[35] Elith J., Phillips S. J., Hastie T., et al. (2011). A statistical explanation of MaxEnt for ecologists. *Divers. Distrib.* **17**:43-57. DOI:10.1111/j.1472-4642.2010.00725.x

[36] Dormann C. F., Elith J., Bacher S., et al. (2013). Collinearity: a review of methods to deal with it and a simulation study evaluating their performance. *Ecography* **36**:27-46. DOI:10.1111/j.1600-0587.2012.07348.x

[37] Liang H., Wang L., Wang S., et al. (2023). Remote sensing detection of seagrass distribution in a marine lagoon (Swan Lake), China. *Opt. Express* **31**:27677-27695. DOI:10.1364/OE.498901

[38] Tucker C. J. (1979). Red and photographic infrared linear combinations for monitoring vegetation. *Remote Sens. Environ.* **8**:127-150. DOI:10.1016/0034-4257(79)90013-0

[39] Xu H. Q. (2006). Modification of normalised difference water index (NDWI) to enhance open water features in remotely sensed imagery. *Int. J. Remote Sens.* **27**:3025-3033. DOI:10.1080/01431160600589179

[40] Healey S. P., Cohen W. B., Yang Z. Q., et al. (2005). Comparison of tasseled cap-based landsat data structures for use in forest disturbance detection. *Remote Sens. Environ.* **97**:301-310. DOI:10.1016/j.rse.2005.05.009

[41] Somers B. and Asner G. P. (2013). Multi-temporal hyperspectral mixture analysis and feature selection for invasive species mapping in rainforests. *Remote Sens. Environ.* **136**:14-27. DOI:10.1016/j.rse.2013.04.006

[42] Muscarella R., Galante P. J., Soley-Guardia M., et al. (2014). ENMeval: An R package for conducting spatially independent evaluations and estimating optimal model complexity for MAXENT ecological niche models. *Methods Ecol. Evol.* **5**:1198-1205. DOI:10.1111/2041-210x.12261

[43] Brown J. L., Bennett J. R. and French C. M. (2017). SDMtoolbox 2.0: the next generation Python-based GIS toolkit for landscape genetic, biogeographic and species distribution model analyses. *PeerJ* **5**:e4095. DOI:10.7717/peerj.4095

[44] Wood S. N. (2017). Generalized additive models: an introduction with R (chapman and hall/CRC), pp:1-447. DOI:10.1201/9781315370279.

[45] Zuur A. F., Ieno E. N., Walker N. J., et al. (2009). Mixed effects models and extensions in ecology with R (Springer), pp:938–939. DOI:10.1111/j.1467-985X.2010.00663_9.x.

[46] Wood S. N. (2011). Fast stable restricted maximum likelihood and marginal likelihood estimation of semiparametric generalized linear models. *Journal of the Royal Statistical Society Series B-Statistical Methodology* **73**:3-36. DOI:10.1111/j.1467-9868.2010.00749.x

[47] Saunders M. I., Leon J., Phinn S. R., et al. (2013). Coastal retreat and improved water quality mitigate losses of seagrass from sea level rise. *Glob Chang Biol* **19**:2569-2583. DOI:10.1111/gcb.12218

[48] Stocker T. F., Qin D., Plattner G.-K., et al. (2014). IPCC, 2013: climate change 2013: the physical science basis. Contribution of working group I to the fifth assessment report of the intergovernmental panel on climate change (Cambridge University Press), pp:117-1308. DOI:10.1017/CBO9781107415324.

[49] Pörtner H.-O., Roberts D. C., Masson-Delmotte V., et al. (2019). The ocean and cryosphere in a changing climate. *IPCC special report on the ocean and cryosphere in a changing climate* **1155**:10-1017. DOI:10.1017/9781009157964

[50] Giribabu D., Hari R., Sharma J., et al. (2024). Performance assessment of GEBCO_2023 gridded bathymetric data in selected shallow waters of Indian ocean using the seafloor from ICESat-2 photons. *Mar. Geophys. Res.* **45**:1. DOI:10.1007/s11001-023-09534-z

[51] Nicholls R. J. and Cazenave A. (2010). Sea-level rise and its impact on coastal zones. *Science* **328**:1517-1520. DOI:10.1126/science.1185782

[52] Duarte C. M. (1991). Seagrass Depth Limits. *Aquat. Bot.* **40**:363-377. DOI:10.1016/0304-3770(91)90081-F

[53] Duarte C. M., Marbà N., Krause-Jensen D., et al. (2007). Testing the predictive power of seagrass depth limit models. *Estuaries Coasts* **30**:652-656. DOI:10.1007/Bf02841962

[54] Capistrant-Fossa K. A. and Dunton K. H. (2024). Rapid sea level rise causes loss of seagrass meadows. *Commun. Earth Environ.* **5**:87. DOI:10.1038/s43247-024-01236-7

[55] Lajeunesse M. J. (2015). Bias and correction for the log response ratio in ecological meta-analysis. *Ecology* **96**:2056-2063. DOI:10.1890/14-2402.1

[56] Assis J., Tyberghein L., Bosch S., et al. (2018). Bio-ORACLE v2. 0: Extending marine data layers for bioclimatic modelling. *Global Ecol. Biogeogr.* **27**:277-284. DOI:10.1111/geb.12693

[57] Tyberghein L., Verbruggen H., Pauly K., et al. (2012). Bio-ORACLE: a global environmental dataset for marine species distribution modelling. *Global Ecol. Biogeogr.* **21**:272-281. DOI:10.1111/J.1466-8238.2011.00656.X

[58] Wu N., Qu Y., Guse B., et al. (2018). Hydrological and environmental variables outperform spatial factors in structuring species, trait composition, and beta diversity of pelagic algae. *Ecol. Evol.* **8**:2947-2961. DOI:10.1002/ece3.3903

[59] Meng Y. C., Gou R. K., Bai J. K., et al. (2022). Spatial patterns and driving factors of carbon stocks in mangrove forests on Hainan Island, China. *Global Ecol. Biogeogr.* **31**:1692-1706. DOI:10.1111/geb.13549

[60] Rahmawati S., Hernawan U. E., McMahon K., et al. (2019). Blue carbon in seagrass ecosystem: guideline for the assessment of carbon stock and sequestration in Southeast Asia (UGM PRESS), pp:1-112.

[61] Saunders M. I., Doropoulos C., Bayraktarov E., et al. (2020). Bright Spots in Coastal Marine Ecosystem Restoration. *Curr. Biol.* **30**:R1500-R1510. DOI:10.1016/j.cub.2020.10.056

[62] Hughes A. R. and Stachowicz J. J. (2004). Genetic diversity enhances the resistance of a seagrass ecosystem to disturbance. *Proc. Natl. Acad. Sci. USA* **101**:8998-9002. DOI:10.1073/pnas.0402642101

[63] van Katwijk M. M., Thorhaug A., Marbà N., et al. (2016). Global analysis of seagrass restoration: the importance of large-scale planting. *J. Appl. Ecol.* **53**:567-578. DOI:10.1111/1365-2664.12562

[64] Duarte C. M., Apostolaki E. T., Serrano O., et al. (2025). Conserving seagrass ecosystems to meet global biodiversity and climate goals. *Nat. Rev. Biodivers.* **1**:150-165. DOI:10.1038/s44358-025-00028-x

[65] Yu L., Khachaturyan M., Matschiner M., et al. (2023). Ocean current patterns drive the worldwide colonization of eelgrass (*Zostera marina*). *Nat. Plants* **9**:1207-1220. DOI:10.1038/s41477-023-01464-3

[66] Reusch T. B. H. (2006). Does disturbance enhance genotypic diversity in clonal organisms? A field test in the marine angiosperm *Zostera marina*. *Mol. Ecol.* **15**:277-286. DOI:10.1111/j.1365-294X.2005.02779.x

[67] Jahnke M., Olsen J. L. and Procaccini G. (2015). A meta-analysis reveals a positive correlation between genetic diversity metrics and environmental status in the long-lived seagrass *Posidonia oceanica*. *Mol. Ecol.* **24**:2336-2348. DOI:10.3390/biology10111089

[68] Atwater D. Z., Ervine C. and Barney J. N. (2018). Climatic niche shifts are common in introduced plants. *Nat. Ecol. Evol.* **2**:34-43. DOI:10.1038/s41559-017-0396-z

[69] Jahnke M., Gullström M., Larsson J., et al. (2019). Population genetic structure and connectivity of the seagrass in the Western Indian Ocean is influenced by predominant ocean currents. *Ecol. Evol.* **9**:8953-8964. DOI:10.1002/ece3.5420

[70] Procaccini G., Olsen J. L. and Reusch T. B. H. (2007). Contribution of genetics and genomics to seagrass biology and conservation. *J. Exp. Mar. Biol. Ecol.* **350**:234-259. DOI:10.1016/j.jembe.2007.05.035

[71] van Oosterhout C., Supple M. A., Morales H. E., et al. (2025). Genome engineering in biodiversity conservation and restoration. *Nat. Rev. Biodivers.* **1**:543-555. DOI:10.1038/s44358-025-00065-6

[72] Thorogood R., Mustonen V., Aleixo A., et al. (2023). Understanding and applying biological resilience, from genes to ecosystems. *npj Biodivers.* **2**:16. DOI:10.1038/s44185-023-00022-6

[73] Pansini A., Berlino M., Mangano M. C., et al. (2025). Meta-analysis reveals the effectiveness and best practices for the iconic Mediterranean seagrass restoration. *Sci. Total Environ.* **976**:179325. DOI:10.1016/j.scitotenv.2025.179325

[74] Samper-Villarreal J., Lovelock C. E., Saunders M. I., et al. (2016). Organic carbon in seagrass sediments is influenced by seagrass canopy complexity, turbidity, wave height, and water depth. *Limnol. Oceanogr.* **61**:938-952. DOI:10.1002/lno.10262

[75] Röhr M. E., Holmer M., Baum J. K., et al. (2018). Blue carbon storage capacity of temperate eelgrass (*Zostera marina*) meadows. *Global Biogeochem. Cycles* **32**:1457-1475. DOI:10.1029/2018GB005941

[76] Krause J. R., Cameron C., Arias-Ortiz A., et al. (2025). Global seagrass carbon stock variability and emissions from seagrass loss. *Nat. Commun.* **16**:3798. DOI:10.1038/s41467-025-59204-4

[77] Zhu J.-J. and Yan B. (2022). Blue carbon sink function and carbon neutrality potential of mangroves (Elsevier), pp:153438. DOI:10.1016/j.scitotenv.2022.153438.

[78] Zhang D., Zhao Y. and Wu J. (2023). Assessment of carbon balance attribution and carbon storage potential in China's terrestrial ecosystem. *Resour. Conserv. Recycl.* **189**:106748. DOI:10.1016/j.resconrec.2022.106748

[79] Lovelock C. E. and Reef R. (2020). Variable Impacts of Climate Change on Blue Carbon. *One Earth* **3**:195-211. DOI:10.1016/j.oneear.2020.07.010

[80] Wang F., Sanders C. J., Santos I. R., et al. (2021). Global blue carbon accumulation in tidal wetlands increases with climate change. *Natl. Sci. Rev.* **8**:nwaa296. DOI:10.1093/nsr/nwaa296

FUNDING AND ACKNOWLEDGMENTS

This research was funded by the National Natural Science Foundation of China (42206117), the Natural Science Foundation of Shandong Province (ZR2024QD017), the NSFC-Shandong Joint Fund (U1806213), and the National Key R&D Program of China (2019YFD0901204). The funders had no role in study design, data collection and analysis, decision to publish, or preparation of the manuscript.

AUTHOR CONTRIBUTIONS

H. W. contributed to the conceptualization, methodology, software, formal analysis, and writing (original draft) of the manuscript. J. C., and X. T. contributed to the conceptualization, methodology, funding acquisition, supervision, and review & editing of the manuscript. X. L., Y. Z., J. X., S. X., and L. L. contributed to the conceptualization and review & editing of the manuscript. All authors contributed to the manuscript and approved the final version.

DECLARATION OF INTERESTS

The authors declare that there are no conflicts of interest.

DATA AND CODE AVAILABILITY

The data that support the findings of this study are available from the corresponding author upon reasonable request